

NASA CR-152186

(NASA-CR-152186) AN ANALYSIS OF
PROP-FAN/AIRFRAME AERODYNAMIC INTEGRATION
Final Report (Boeing Commercial Airplane
Co., Seattle) 74 p HC A04/MF A01 CSCL 01A

N84-19281

Unclas

G3/02 11928

An Analysis of Prop-Fan/Airframe Aerodynamic Integration

**The Boeing Commercial Airplane Company
P.O. Box 3707
Seattle, Washington 98124**

**Prepared for
Ames Research Center
under contract NAS2-9104**



NASA

**National Aeronautics and
Space Administration**

October 1978



| | | | | | |
|--|--|---|--|---|--|
| 1. Report No. NASA CR-152186 | | 2. Government Accession No. | | 3. Recipient's Catalog No. | |
| 4. Title and Subtitle FINAL REPORT— An Analysis of Prop-Fan/Airframe Aerodynamic Integration | | | | 5. Report Date October 1978 | |
| | | | | 6. Performing Organization Code B-7200 | |
| 7. Author(s) M.L. Bector, C.W. Clay, C.F. Watson | | | | 8. Performing Organization Report No. D6-47113 | |
| | | | | 10. Work Unit No. | |
| 9. Performing Organization Name and Address Boeing Commercial Airplane Company P.O. Box 3707 Seattle, Washington 98124 | | | | 11. Contract or Grant No. NAS2-9104 | |
| | | | | 13. Type of Report and Period Covered Final Report October 1978 | |
| 12. Sponsoring Agency Name and Address National Aeronautics and Space Administration Ames Research Center Moffet Field, California 94035 | | | | 14. Sponsoring Agency Code FVS | |
| | | | | | |
| 15. Supplementary Notes Technical Monitor: Louis J. Williams NASA Ames Research Center Moffet Field, California 94035 | | | | | |
| 16. Abstract This study addresses an approach to aerodynamic integration of turbo-props and airframes, with emphasis placed upon wing-mounted installations. Potential flow analytical techniques were employed to study aerodynamic integration of the prop-fan propulsion concept with advanced, subsonic, commercial transport airframes. Three basic configurations were defined and analyzed: <ul style="list-style-type: none"> ● Wing-mounted prop-fan at a cruise Mach number of 0.8 ● Wing-mounted prop-fan in a low-speed configuration ● Aft-mounted prop-fan at a cruise Mach number of 0.8 | | | | | |
| 17. Key Words (Suggested by Author(s)) potential-flow analysis prop-fan slipstream prop-fan swirl | | | | 18. Distribution Statement UNLIMITED | |
| 19. Security Classif. (of this report) Unclassified | | 20. Security Classif. (of this page) Unclassified | | 22. Price* | |
| | | | | 21. No. of Pages — | |

CONTENTS

| | Page |
|--|------|
| 1.0 SUMMARY | 1 |
| 1.1 General | 1 |
| 1.2 Conclusions | 1 |
| 1.3 Recommendations | 4 |
| 2.0 INTRODUCTION | 6 |
| 2.1 Background | 6 |
| 2.2 Study Objective and Scope | 7 |
| 3.0 ABBREVIATIONS AND SYMBOLS | 8 |
| 4.0 ANALYSIS AND DESIGN METHODS | 10 |
| 4.1 Computer Program A 230 Description | 10 |
| 4.2 Analysis Using Slipstream and Pre- and Post-Processors | 10 |
| 4.3 Computer Program A 236 Description | 12 |
| 4.4 Design Method | 13 |
| 5.0 WING-MOUNTED PROP-FAN—CRUISE | 17 |
| 5.1 Configuration and Flight Conditions | 17 |
| 5.2 Slipstream Characteristics | 20 |
| 5.3 Pressure Coefficient Data | 21 |
| 5.4 Wing Isobars | 26 |
| 5.5 Force Data | 28 |
| 5.6 Propeller Thrust Recovery Assessment | 30 |
| 5.7 Assessment | 33 |
| 6.0 WING-MOUNTED PROP-FAN—LOW SPEED | 34 |
| 6.1 Geometrical Definition | 34 |
| 6.2 Design Procedure | 37 |
| 6.3 Slipstream Characteristics | 39 |
| 6.4 Pressure Coefficient Data | 40 |
| 6.5 Force Data | 40 |
| 6.6 Drag and Thrust Recovery | 44 |
| 6.7 Effect of One-Engine Failure | 44 |
| 6.8 Assessment | 46 |
| 7.0 AFT-MOUNTED PROP-FAN | 47 |
| 7.1 Configuration and Flight Conditions | 47 |
| 7.2 Slipstream Characteristics | 49 |
| 7.3 Pressure Distribution and Span Loading | 49 |
| 7.4 Drag and Thrust Recovery | 54 |
| 7.5 Assessment | 55 |
| 8.0 REFERENCES | 56 |
| APPENDIX A BASELINE AND MODIFIED WING GEOMETRY | A1 |

FIGURES

| No. | | Page |
|-------------|--|------|
| SECTION 1.0 | | |
| 1 | Summary of Study Approach and Results | 2 |
| 2 | Typical Modification Concept for Prop-Fan Cruise Wing | 5 |
| SECTION 4.0 | | |
| 3 | Technique for Modeling Prop Slipstream | 11 |
| 4 | Test Case—Flow Over Stub Wing: Strip 2 | 12 |
| 5 | Prop-Fan Wing Design Technique | 14 |
| 6 | Cruise Wing Geometry | 15 |
| 7 | Cruise Wing Twist Distribution | 16 |
| 8 | Cruise Wing Thickness Distribution | 16 |
| SECTION 5.0 | | |
| 9 | Baseline Wing Body Model | 17 |
| 10 | Baseline Wing Body/Nacelle Model | 18 |
| 11 | Paneling of Modified Cruise Wing | 19 |
| 12 | Modified Cruise Wing | 19 |
| 13 | Radial Distribution of Swirl and Total Pressure in Prop Slipstream | 20 |
| 14 | Effect of Slipstream on Chordwise Pressure Distribution: Strip 3 | 22 |
| 15 | Effect of Slipstream on Chordwise Pressure Distribution: Strip 4 | 22 |
| 16 | Effect of Slipstream on Chordwise Pressure Distribution: Strip 5 | 23 |
| 17 | Effect of Slipstream on Chordwise Pressure Distribution: Strip 6 | 23 |
| 18 | Wing Pressure Profiles: Strip 3 | 24 |
| 19 | Wing Pressure Profiles: Strip 4 | 24 |
| 20 | Wing Pressure Profiles: Strip 5 | 25 |
| 21 | Wing Pressure Profiles: Strip 6 | 25 |
| 22 | Upper Surface Wing Isobars—Clear Wing | 26 |
| 23 | Upper Surface Wing Isobars—Baseline Wing + Nacelle | 27 |
| 24 | Upper Surface Wing Isobars—Baseline Wing + Nacelle + Slipstream | 27 |
| 25 | Upper Surface Wing Isobars—Modified Wing + Nacelle + Slipstream | 28 |
| 26 | Cruise Wing Lift Curves | 29 |
| 27 | Effect of Slipstream on Span Loading | 29 |
| 28 | Wing Spanwise Load Distribution | 30 |
| 29 | Spanwise Distribution of C_{pMIN} | 31 |
| 30 | Wing Drags Incremented from Clean Wing | 32 |

| No. | | Page |
|-----|--|------|
|-----|--|------|

SECTION 6.0

| | | |
|----|--|----|
| 31 | Leading- and Trailing-Edge Flaps for Low-Speed Configuration | 34 |
| 32 | Krueger Flap Definition | 35 |
| 33 | Paneling Scheme—Low-Speed Configuration | 36 |
| 34 | Krueger Wing—Low-Speed Configuration | 36 |
| 35 | Krueger Flap Deflection Schedule | 37 |
| 36 | Low-Speed Wing Pressure Profiles: Strip 3 | 38 |
| 37 | Low-Speed Wing Pressure Profiles: Strip 6 | 38 |
| 38 | Radial Distribution of Swirl and Total Pressure in Prop Slipstream | 39 |
| 39 | Radial Distribution of Axial Velocity Increment in Prop Slipstream | 40 |
| 40 | Low-Speed Wing Pressure Profiles with Slipstream: Strip 3 | 41 |
| 41 | Low-Speed Wing Pressure Profiles with Slipstream: Strip 4 | 41 |
| 42 | Low-Speed Wing Pressure Profiles with Slipstream: Strip 5 | 42 |
| 43 | Low-Speed Wing Pressure Profiles with Slipstream: Strip 6 | 42 |
| 44 | Krueger Wing—Low-Speed Configuration Lift Curve | 43 |
| 45 | Krueger Wing—Low-Speed Configuration Spanwise Load Distribution | 43 |
| 46 | Krueger Wing—Low-Speed Configuration Induced Drag Due to Slipstream | 44 |
| 47 | Krueger Wing—Low-Speed Configuration Rolling Moment Coefficient | 45 |
| 48 | Rolling Moment Due to Engine-Out Comparison with Preliminary Estimates | 45 |

SECTION 7.0

| | | |
|----|---|----|
| 49 | Paneling of Aft-Mounted Prop-Fan | 47 |
| 50 | Aft-Mounted Prop-Fan Isometric Projection | 48 |
| 51 | Aft-Mounted Prop-Fan Cross Sectional Area Distribution | 48 |
| 52 | Aft-Mounted Prop-Fan Side-of-Fody Pressure Profile | 49 |
| 53 | Aft-Mounted Prop-Fan Strut Pressure Profiles: Strip 1 | 50 |
| 54 | Aft-Mounted Prop-Fan Strut Pressure Profiles: Strip 2 | 51 |
| 55 | Aft-Mounted Prop-Fan Strut Pressure Profiles: Strip 3 | 51 |
| 56 | Aft-Mounted Prop-Fan Vertical Tail Pressure Profiles: Strip 1 | 52 |
| 57 | Aft-Mounted Prop-Fan Vertical Tail Pressure Profiles: Strip 2 | 52 |
| 58 | Aft-Mounted Prop-Fan Vertical Tail Pressure Profiles: Strip 3 | 53 |
| 59 | Aft-Mounted Prop-Fan Vertical Tail Pressure Profiles: Strip 4 | 53 |
| 60 | Aft-Mounted Prop-Fan Effect of Slipstream on Strut Loading | 54 |
| 61 | Aft-Mounted Prop-Fan Effect of Slipstream on Induced Drag | 55 |

APPENDIX A

| | | |
|-----|--------------------------|----|
| A-1 | Wing Planform Dimensions | A1 |
|-----|--------------------------|----|

1.0 SUMMARY

1.1 GENERAL

Previous NASA/industry advanced-turboprop-propeller and prop-fan studies and wind tunnel tests indicate that point design, installed propulsive efficiencies on the order of 80% at Mach 0.8 are achievable; and that a net reduction of 18% in TSFC could be expected over a comparable, bypass-ratio-six, turbofan-powered airplane. In the absence of any associated penalties, this reduction in TSFC (18%) would result in a net fuel saving of approximately 25% for a twin-engine, 180-passenger, Mach 0.8, commercial transport designed for 3300-km (1800-nmi) range. However, the weight and drag of the prop-fan-powered airplanes were judged to be larger than those of the turbo-fan-powered airplanes. When these penalties were assessed in one study (ref 1), the fuel savings of 25% for the 3300-km (1800-nmi) design range were reduced to 9.7% for the wing-mounted prop-fan and 5.8% for the aft-mounted prop-fan airplanes. This earlier study recommended additional analysis and design to add realism to these preliminary assessments.

This study, implemented in response to one of these recommendations, addresses an approach to the aerodynamic integration of turbo-props and airframes. Both the wing-mounted and aft-mounted prop-fan installations were considered, but emphasis was placed upon the wing-mounted installation as it represented the most difficult task.

Potential flow techniques were employed to study the aerodynamic integration of the prop-fan propulsion concept with the airframe of advanced subsonic commercial transports. Three basic configurations were defined and analyzed:

- A wing-mounted prop-fan at a cruise Mach number of 0.8
- A wing-mounted prop-fan in a low-speed configuration
- An aft-mounted prop-fan at cruise Mach number of 0.8

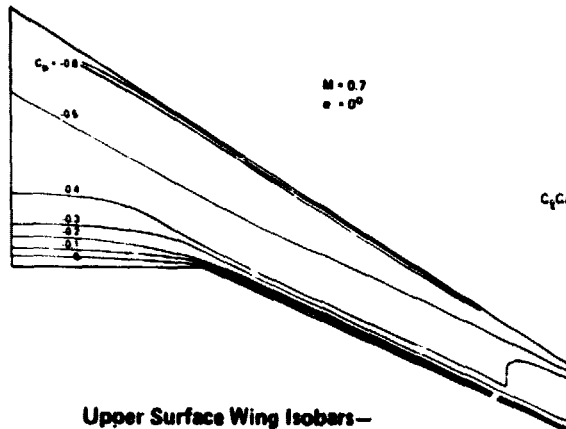
In each case, the propeller slipstream was modeled and its interaction with the configuration calculated.

To minimize aerodynamic interference penalties, the cruise wing of the wing-mounted configuration was redesigned to reproduce or approximate the clean-wing pressure distribution after inclusion of nacelle and slipstream effects.

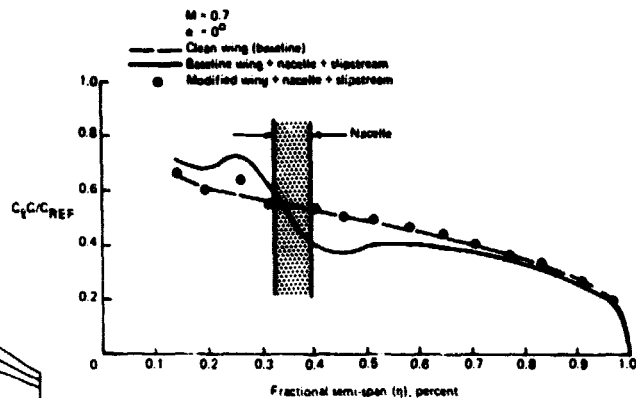
1.2 CONCLUSIONS

This study has demonstrated the feasibility of using potential flow analysis techniques to calculate prop-fan airplane aerodynamics. The study objective of minimizing propeller slipstream effects upon a wing was accomplished (fig. 1). However, the resulting wing was structurally unsatisfactory because of an arbitrary ground rule to hold the leading edge constant, with the remaining wing geometry contoured to reduce or eliminate prop slipstream effects. The resulting wing with sheared front and rear spars would be impractical due to excessive weight penalties, particularly when other solutions would be available with addi-

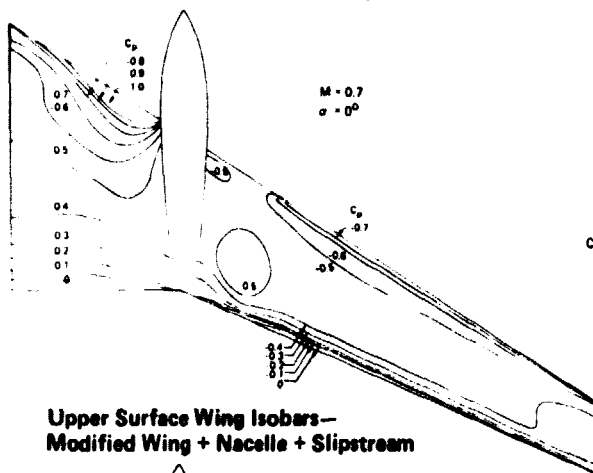
Upper Surface Wing Isobars—
Clean Wing



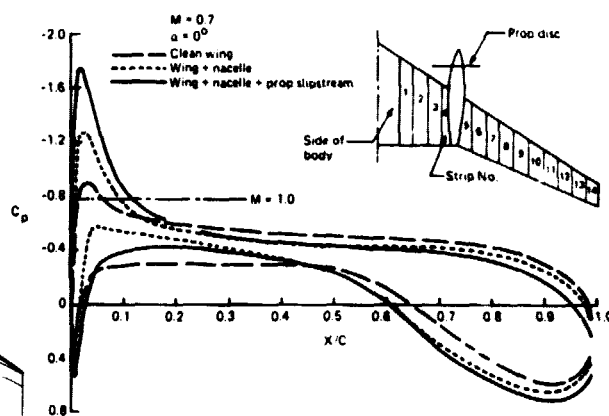
Wing Spanwise Load Distribution



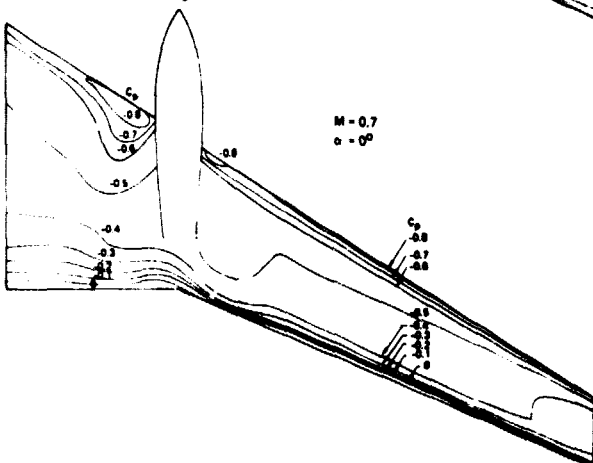
Upper Surface Wing Isobars—
Baseline Wing + Nacelle + Slipstream



Wing Pressure Profiles: Strip 4



Upper Surface Wing Isobars—
Modified Wing + Nacelle + Slipstream



Wing Pressure Profiles: Strip 5

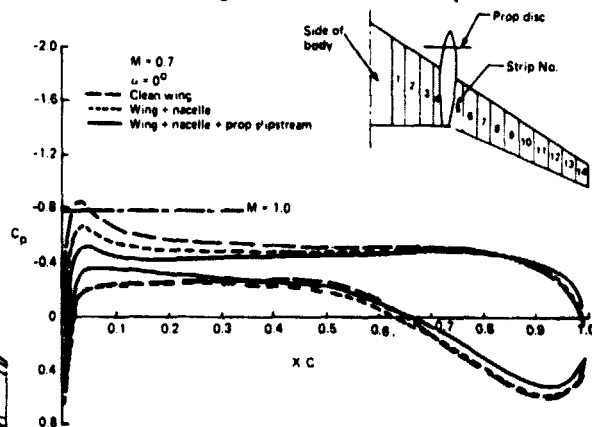


Figure 1. Summary of Study Approach and Results

tional analysis and/or wind tunnel testing. Therefore, wind tunnel testing of the configuration developed by this study is not recommended. Additional studies of alternate means to achieve the same or better aerodynamic results for a practical wing design are needed, and wind tunnel testing should then be done to validate the resulting wing design.

Additional conclusions resulting from this study are discussed in the following paragraphs.

1.2.1 WING-MOUNTED PROP-FAN—HIGHSPEED

- Predicated on the assumption of isentropic flow over the inboard wing, the baseline wing has the potential for recovering up to 50% of the thrust lost due to swirl by de-rotating the slipstream. However, the upwash from the propeller results in high pressure peaks on the upper surface of the inboard wing, a condition that renders the wing susceptible to shock waves, flow separation, high drag, and buffet. This condition could more than offset the potential thrust recovery.
- The wing, modified for minimum cruise drag, generally accomplishes the objective of neutralizing the adverse effects of the slipstream, but in so doing fails to de-rotate the slipstream. The profile drag penalties are mostly eliminated; however, the potential thrust recovery gains are also eliminated.
- The approach taken results in a modified wing that has large variations in twist and thickness and is considered structurally undesirable due to potential manufacturing cost and weight penalties. Alternate approaches for modifying the wing and/or nacelle are recommended for further study.

1.2.2 WING-MOUNTED PROP-FAN—LOW SPEED

- The chordwise velocity increase in the slipstream is the predominant effect at low speed, and is more important than the effect of swirl.
- Large increments in chordwise velocity result in overloading the wing both inboard and outboard of the nacelle.
- A high-lift system designed for achieving high power-off C_{LMAX} does de-rotate the slipstream to some extent and results in partial thrust recovery.
- When considering all-engine slipstream effects, the high-lift condition drag polar is improved because of the large increase in C_L combined with thrust recovery.
- Rolling moment caused by one engine being inoperative is much less than the estimates for the Reference 1 study and does not appear to be a major concern.

1.2.3 AFT-MOUNTED PROP-FAN

- The aft-mounted prop-fan configuration is aerodynamically similar to a comparable turbofan configuration.

- The prop slipstream effects extend beyond the strut to the body and vertical tail and influence the longitudinal cross section area distribution.
- Partial ($\cong 10\%$) thrust recovery resulting from the straightening effect of the strut on the slipstream appears as an increment in strut C_L , rather than a decrement in drag. The opposing tendencies of the wing downwash and the propeller swirl influence the flow about the leading edge of the strut and in turn, the thrust recovery vector.
- Overall, the prop slipstream has little effect on the aerodynamics of the airplane for aftmounted engines as compared to wing-mounted engines.

1.3 RECOMMENDATIONS

This study was directed at applying analytical techniques to minimize propeller slipstream/ airplane aerodynamic interference effects and to maximize overall aircraft aerodynamic efficiency during cruise. Potential flow analysis techniques to calculate prop-fan airplane aerodynamics were applied. Additional studies of alternate methods for achieving the same or better results with a more practical wing design are required. Therefore, the following efforts are recommended to ensure a balanced, logical development of prop-fan technology; and ultimately, a convincing evaluation of the economic and energy saving potential for prop-fan propulsion systems.

1.3.1 PROP-FAN/AIRFRAME AERODYNAMIC INTEGRATION

- Develop a cruise wing design that incorporates changes to the planform and leading/ trailing edges, but that essentially maintains the structural wing box. This may include changes in local wing sweep, leading- and trailing-edge camber, wing aspect ratio, thickness ratio, and nacelle contouring.
- Determine the influence of the wing on wing propeller environment and aft-mounted propfan installations.

1.3.2 NOISE RADIATION AND ATTENUATION

- These recommendations result from the Reference 1 study.
- Develop a data base and theoretical methods for predicting noise radiation from prop-fans.
- Develop a light-weight structure to attenuate noise at the prop-fan blade passing frequencies.

1.3.3 PROP-FAN MISSIONS AND APPLICATION

- Determine the optimum range and Mach number for a prop-fan airplane.
- Conduct a fully integrated study that includes all technical elements of airplane design.

As indicated, the cruise wing design should incorporate changes to the planform. For example, leading-edge extensions on both sides of the nacelle could effectively reduce the local thickness ratio without reducing the physical wing thickness. This leading-edge extension permits incorporation of local leading-edge camber without distorting the wing structural box. The large suction peaks caused by the swirling slipstream inboard of the nacelle could be mitigated by merely drooping the extended leading-edge. Conversely, the wing leading-edge could be upcambered on the outboard side to compensate for the loss of load on that side. This concept is shown in Figure 2.

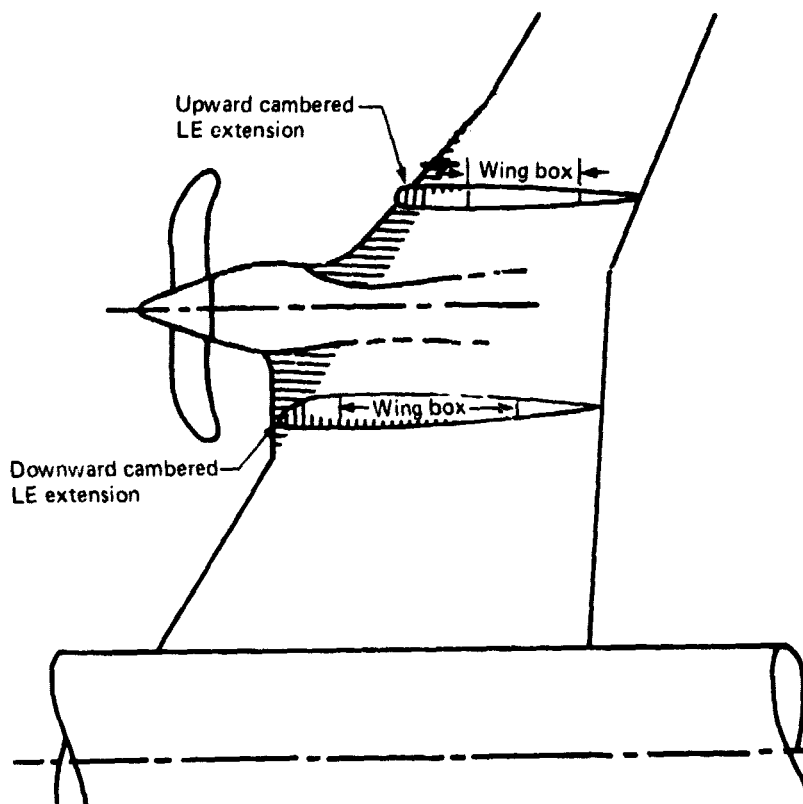


Figure 2. Typical Modification Concept for Prop-Fan Cruise Wing

2.0 INTRODUCTION

2.1 BACKGROUND

Elementary considerations of momentum and energy lead to the conclusion that, in the absence of compensating losses, propulsive efficiency is improved by accelerating more fluid by a smaller velocity increment. Introduction of the high-bypass-ratio turbofan engine stimulated a new generation of transport aircraft by using this principle to reduce fuel consumption without substantially sacrificing the simplicity, reliability, and low maintenance costs that have come to be expected by the airlines since reciprocating engines were replaced by turbojets.

The increase in the relative cost of fuel following the 1973 Arab oil embargo, along with national concern over the need of fuel conservation, have prompted Government and industry to examine possibilities for further reducing aircraft fuel consumption.

A 1976 NASA-sponsored study (ref 1) concluded that modest gains in efficiency could be achieved by pushing turbofan technology further through the application of geared fans, higher overall pressure ratios, and higher turbine inlet temperatures. The same study also noted that the propeller offered more dramatic gains than advanced turbofans if it could be adapted to the Mach 0.75+ cruise speed favored by airframe technology and expected by the traveling public.

The high propulsive efficiency of propellers is difficult to maintain at cruise speeds above Mach 0.7 because:

- The helical-tip Mach number becomes supersonic, and the outer section of the blade incurs increased drag, leading to increased noise and the associated penalties,
- or,
- The rotational speed must be reduced to the point where excessive slipstream swirl necessitates the added weight and complexity of dual rotation.

In 1975, the Hamilton Standard Division of United Technologies Corporation proposed the prop-fan concept. This concept is one in which a slightly supersonic outer blade speed is accepted, and alleviation of increased drag and noise is accomplished by the use of thin and swept-back blade sections. Also, to keep the diameter reasonable while absorbing the very high power required for high-speed transport designs, eight to ten broad blades are used.

Wind tunnel tests conducted by Hamilton Standard and the NASA Lewis Research Center indicate a point-design installed propulsive efficiency of 80% at Mach 0.8 cruise is achievable, and a net reduction of 18% in TSFC over a comparable technology bypass-ratio-six turbofan may be expected.

Study results reported in Reference 1 indicate that this 18% advantage in cruise TSFC for a twin-engine, Mach 0.8 commercial transport designed for 3300-km (1800-nmi) range with

180 passengers could result in a net fuel savings of approximately 25% if there were not compensating penalties. However, both the installation weight and drag penalties of the prop-fan-powered airplanes were judged to be larger than those of the turbo-fan.

When these penalties are assessed, the estimated fuel savings are reduced to 9.7% for the wing-mounted prop-fan airplane and 5.8% for the aft-mounted prop-fan.

Early analysis and design work are necessary to add realism to these assessments and to help guide decisions regarding the development of prop-fan technology.

2.2 STUDY OBJECTIVE AND SCOPE

The objective of the current study is to apply analytical techniques to the problem of the wing and aft-body installation, thus minimizing propeller slipstream/airplane interference, to maximize overall aircraft aerodynamic efficiency in cruise, and to define appropriate high-lift devices for takeoff and landings.

2.2.1 TASK I—WING-MOUNTED PROP-FAN—HIGH SPEED

A "clean" wing of appropriate geometry is defined and analyzed (using a 3-D potential-flow computer program, Boeing A 230) to provide a baseline pressure distribution. The nacelle and slipstream then are added, and the resulting distorted isobar pattern examined to identify problem areas associated with pressure peaks, adverse pressure gradients, and local loss of effective sweepback. Design changes are defined to alleviate these problems, and a revised wing-nacelle geometry analyzed to provide new pressure distribution data for validation of the proposed changes. A wing model for high-speed wing tunnel testing is defined and thrust recovery due to slipstream de-rotation estimated.

2.2.2 TASK II—WING-MOUNTED PROP-FAN—LOW SPEED

Leading- and trailing-edge flap geometry and the fan flow field is examined at takeoff and landing approach flight conditions. Pressures and streamline patterns at the leading edge (with and without slipstream) are computed, and leading-edge devices required to mitigate pressure peaks and to provide reasonable protection from flow separation are defined and analyzed. Probable power-off behavior and requirements for automatic retraction or angle adjustment in case of engine failure are estimated and thrust recovery due to slipstream de-rotation is calculated.

2.2.3 TASK III—AFT—MOUNTED PROP-FAN

Aerodynamic integration of aft-mounted engines poses a completely different set of problems. Most of the requirements constraining the wing do not apply to a strut having only the function of supporting the propulsion pod (and possibly to develop some thrust by removing slipstream swirl). On the other hand, the drag of the aft-body may be sensitive to disturbances caused by the nacelle and propeller because of the thick boundary layer and adverse pressure gradient to be expected there. Potential flow methods are used to compute pressure distributions and streamline paths.

3.0 ABBREVIATIONS AND SYMBOLS

| | |
|------------------------------------|---|
| A | Cross sectional area |
| b_{REF} | Reference span |
| C | Chord |
| C_D | Drag coefficient |
| C_{D_i} | Induced drag coefficient |
| C_{D_p} | Profile drag coefficient |
| C_k | Krueger flap chord |
| C_ℓ | Lift coefficient per unit span |
| C_L | Lift coefficient |
| C_{L_{MAX}} | Maximum lift coefficient |
| C_{MX} | Rolling moment coefficient |
| C_p | Pressure coefficient |
| C_{p_{MIN}} | Minimum pressure coefficient |
| C_{REF} | Reference chord |
| D | Propeller diameter |
| G | Geometry |
| G_F | Error-free initial geometry |
| G₀ | Clean-wing initial geometry |
| LE | Leading edge |
| M | Local Mach number |
| MAC | Mean aerodynamic chord |
| M_∞ | Freestream Mach number |
| n | Unit normal |
| nmi | Nautical mile |
| p(r) | Static pressure at radius r |
| p_∞ | Static pressure at infinity |
| P(r) | Total pressure at radius r |
| P₀ | Total pressure at infinity |
| q | Dynamic head |
| r | Radial distance |
| R | Propeller radius |
| S | Arc length |
| S/C | Arc length from leading edge/chord |
| SHP | Shaft horsepower |

| | |
|--------------------------------|--|
| T | Thrust |
| TE | Trailing edge |
| t/c | Thickness ratio |
| TSFC | Thrust specific fuel consumption |
| | |
| U_{∞} | Freestream velocity |
| | |
| V | Local velocity |
| V_n | Normal velocity component |
| V_{PROP} | Slipstream perturbation velocity |
| V_t | Tangential velocity component |
| V_x | Axial velocity |
| | |
| w/U | Uniform cross-flow |
| W | Vertical component of velocity vector |
| WBL | Wing buttock line |
| WL | Water line |
| | |
| X,Y,Z | Cartesian coordinates |
| | |
| α | Angle-of-attack |
| δ | Swirl angle |
| δ_F | Trailing-edge flap deflection |
| δ_K | Krueger flap deflection |
| Δ | Incremental quantity |
| η | Fractional semispan |
| θ | Wing twist |
| γ | Ratio of specific heats for air |

4.0 ANALYSIS AND DESIGN METHODS

Three-dimensional potential flow techniques have been in use for many years for analysis and design of complex aerodynamic configurations. These techniques have been found to be adequate even though local patches of supersonic flow and shock waves at high subsonic Mach numbers are not simulated. Consistent with current design practices, this analysis was conducted at Mach 0.7.

4.1 COMPUTER PROGRAM A 230 DESCRIPTION

The Boeing-developed computer program A 230 (ref 2) is a general boundary-value problem solver that uses source and doublet panels distributed on the configuration boundary surfaces and internally. The flow field over the configuration is determined by a computational routine, which calculates the strengths of the sources and doublets that produce a flow field satisfying the boundary conditions. Each boundary condition statement consists of the following specifications:

- Spatial coordinates of the boundary point
- Direction cosines of a unit vector
- The desired velocity component along the unit vector

For a general impermeable surface, the boundary point is positioned at the panel centroid, with the unit vector directed normal to the panel. The condition of zero velocity along the normal vector produces a flow that is parallel to the surface. This type of boundary condition is provided automatically by the program and requires no input from the user. However, if a nonzero velocity component is specified along the unit normal vector, problems such as controlling the inflow distribution into a simulated fan face may be formulated. This option has been exercised in the present study to represent the interaction of the slipstream with the configuration without actually generating the swirling flow behind the propeller.

4.2 ANALYSIS USING SLIPSTREAM AND PRE- AND POST-PROCESSORS

The methodology for inclusion of the prop slipstream in the three-dimensional, potential-flow analysis model is presented in this section. The swirling flow behind the propeller disc, impinging on the surface of the configuration is simulated mathematically through a restatement of the boundary conditions at those boundary points that are washed by the wake. The obtained solution is corrected to ensure satisfaction of the tangency condition at all points in the presence of the slipstream.

The boundary conditions underlying the potential flow problem are described schematically in Figure 3. The slipstream perturbation velocity (V_{PROP}) is resolved into a normal (V_n) and tangential (V_t) component to the local panel. The boundary condition at the panel center is expressed as:

$$V \cdot n = -V_n$$

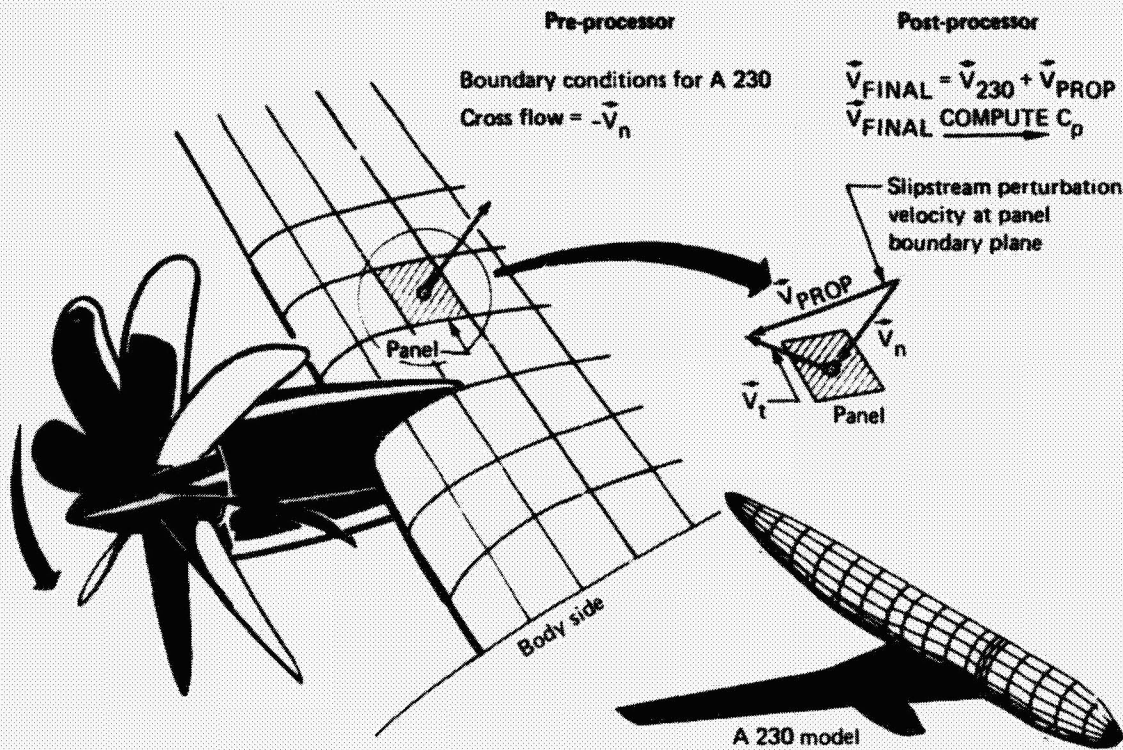


Figure 3. Technique for Modeling Prop Slipstream

The requirement that there be a normal flow through the surface of magnitude $-\vec{V}_n$ is equivalent to requiring the local singularity strength to oppose \vec{V}_{PROP} , had the latter been generated by an appropriate distribution of singularities in the flow field. Post-solution addition of \vec{V}_{PROP} to the local velocity vector ensures satisfaction of the tangency condition and yields the effect of the slipstream on the configuration.

A pre- and post-processor computer program has been developed to handle the boundary value problem described above. In the pre-processor section, the slipstream velocity vector \vec{V}_{PROP} is generated from swirl angle and total pressure data aft of the propeller (see derivation in Section 5.0). This vector (\vec{V}_{PROP}) is then resolved normal to the configuration panels within reach of the wake. The normal velocity ($-\vec{V}_n$) is generated and entered (as the boundary condition) into potential flow program A 230. A solution is obtained and the post-processor then is called upon to:

1. Regenerate the slipstream velocity vector \vec{V}_{PROP} at all affected boundary points
2. Vectorially add \vec{V}_{PROP} to the velocity vector arising from the potential flow solution
3. Recompute pressure coefficient, C_p
4. Integrate the pressures for forces and moments on a column-by-column basis

This technique described above can be used to superimpose any velocity field on a boundary value problem. An example is given in Figure 4 for the flow over a stub wing at an angle of attack, $\alpha = 5^\circ$. The solution obtained superimposes a uniform cross-flow of magnitude $w/U = \tan \alpha$ to the configuration at $\alpha = 0^\circ$. The excellent agreement with the exact solution at $\alpha = 5^\circ$ supports applicability of the method.

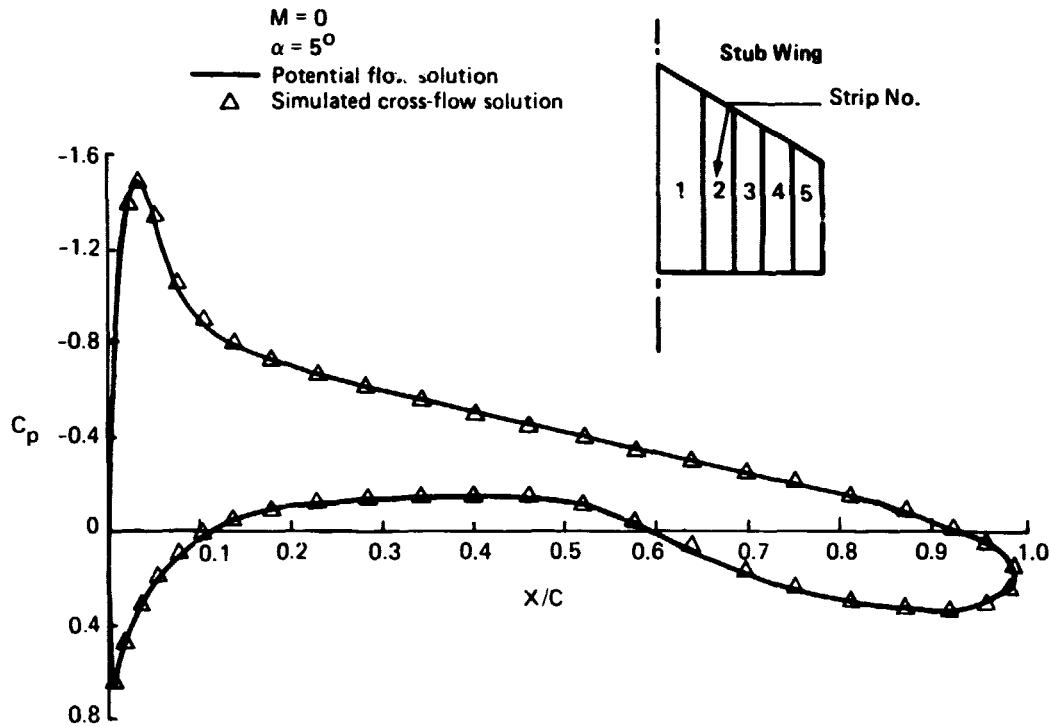


Figure 4. Test Case—Flow Over Stub Wing: Strip 2

4.3 DESCRIPTION OF COMPUTER PROGRAM A 236

The Boeing A 236 computer program (ref 3) is a design-analysis-optimization program, which has been used in the present study to redesign the baseline wing of the wing-mounted prop-fan. In the design mode, A 236 calculates the wing geometry required to support a specified pressure distribution. To achieve design capabilities, a number of limitations were

imposed upon A 236, as compared with the more general program, A 230. The variations between these two programs are:

| A 230 | A 236 |
|---|---|
| 1. Analysis only | Analysis, design, and optimization |
| 2. Accepts general configurations of any shape | Accepts wing/body only |
| 3. Exact boundary conditions (applied on surface) | Linearized wing boundary conditions (applied on wing design plane, exact boundary conditions on body) |
| 4. Lifting surfaces treated as a whole | Wing split into camber and thickness |
| 5. Paneling external to program | Automatic paneling provided |

Features of A 236 include:

- It handles wing/body configurations only. The wing may be designed in the presence of the body, but nacelle and slipstream are excluded.
- Linearized boundary conditions are applied on the wing design plane, eliminating the need to estimate the initial geometry when designing the wing.
- Wing camber and thickness are treated separately and their effects are superimposed. This is a necessary limitation of the linear theory.
- Since only wing/body configurations are admissible into A 236, automatic paneling is provided. The wing is considered flat and is paneled over its planform.

4.4 DESIGN METHOD

The problem of redesigning the baseline wing of the wing-mounted prop-fan for favorable interaction with the slipstream was as follows:

“Find the wing geometry which, in the presence of the nacelle and slipstream will support the pressure distribution of the clean wing”. Because the nacelle and slipstream could not be modeled on the design program A 236, a scheme employing both programs A 230 and A 236 was devised (fig. 5). The clean wing-body configuration was analyzed on A 236, resulting in the pressure distribution, C_{pI} (only one wing section is used for illustration in the figure). The increment C_p of the nacelle-slipstream over the clean wing, calculated by A 230, was then subtracted from C_{pI} to produce C_{pII} , thus:

$$C_{pII} = C_{pI} - \Delta C_p$$

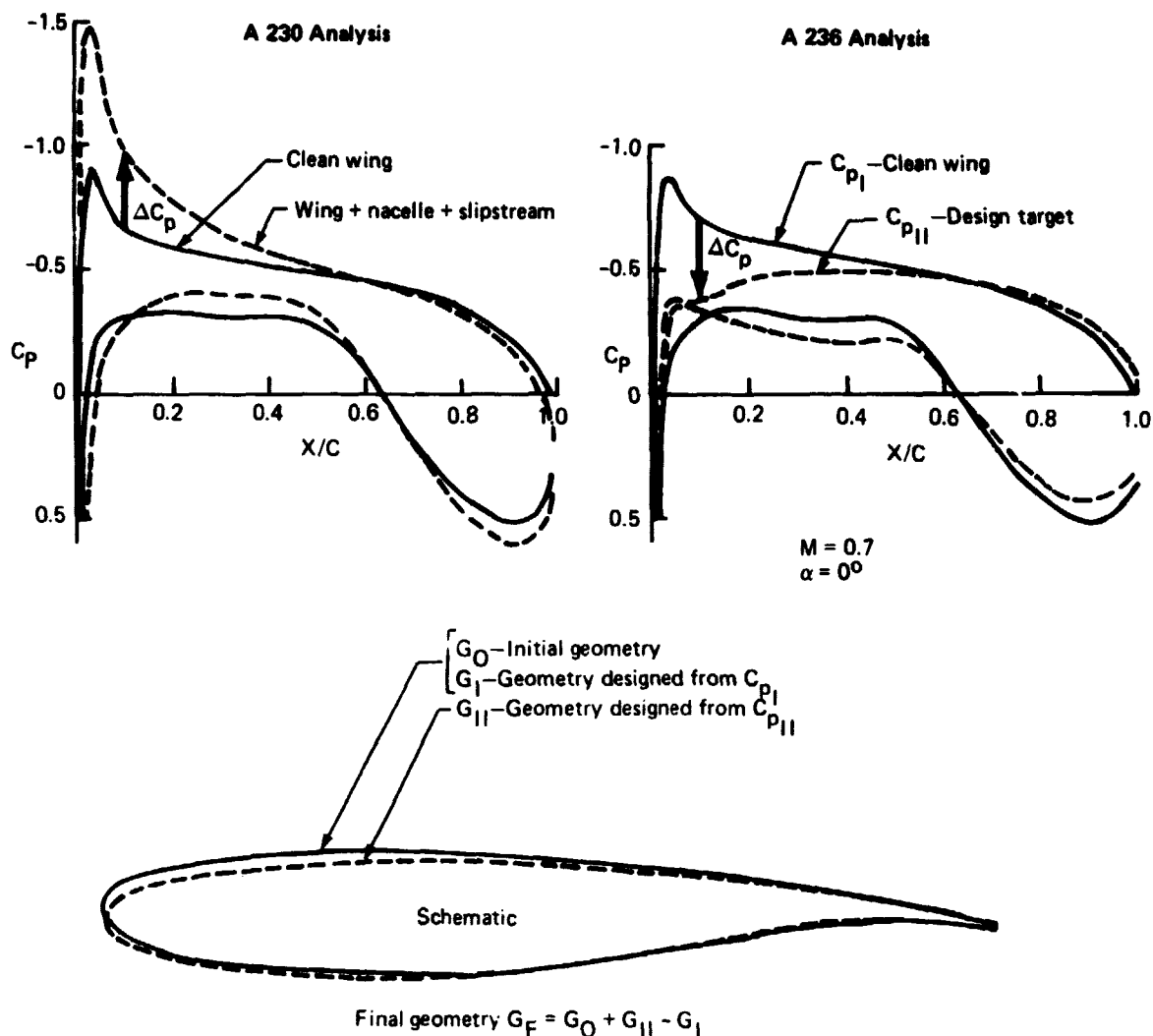


Figure 5. Prop-Fan Wing Design Technique

In an attempt to eliminate errors inherent in the solution of the design problem, two design runs were executed on A 236; one for C_{pI} and another for C_{pII} . The resulting wing geometries are symbolically denoted G_I and G_{II} , respectively in the figure. The final wing geometry was then calculated from:

$$G_F = G_0 + G_{II} - G_I$$

where G_0 is the initial geometry of the clean wing. $G_I - G_0$ represents the error attributable to the lack of reversibility in the analysis-design-analysis cycle on A 236. By subtracting it from G_{II} , an error-free final geometry (G_F) is obtained.

Figure 6 shows a comparison of baseline and redesigned wing sections on the two sides of the nacelle. Large changes in twist, thickness, and airfoil shape are evident as a result of the design exercise. Figure 7 defines the twist distribution of the baseline and modified wings. A twist increment of approximately $+6^\circ$ outboard and -5° inboard of the nacelle appears to be almost equal and opposite to the swirl angles at cruise stated in Section 5.0. The wing thickness distribution of the baseline and modified wings is shown in Figure 8. As a result of this design exercise, the maximum wing thickness ratio has been reduced by 18% inboard and by 10% outboard of the nacelle.

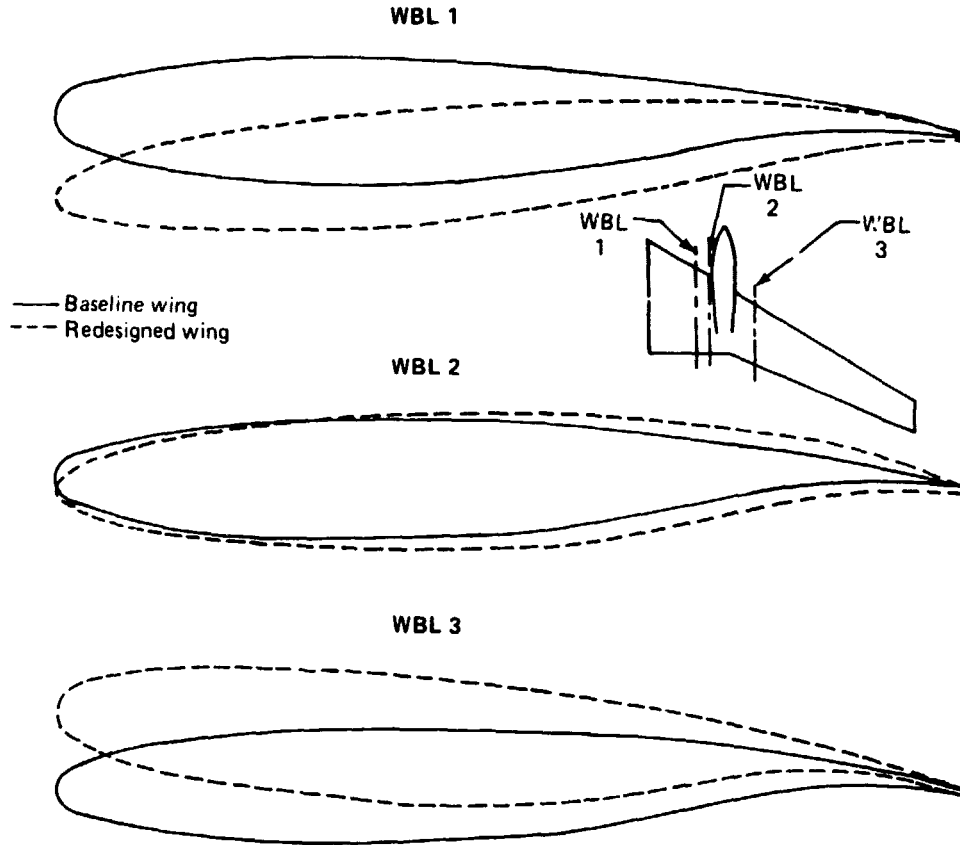


Figure 6. Cruise Wing Geometry

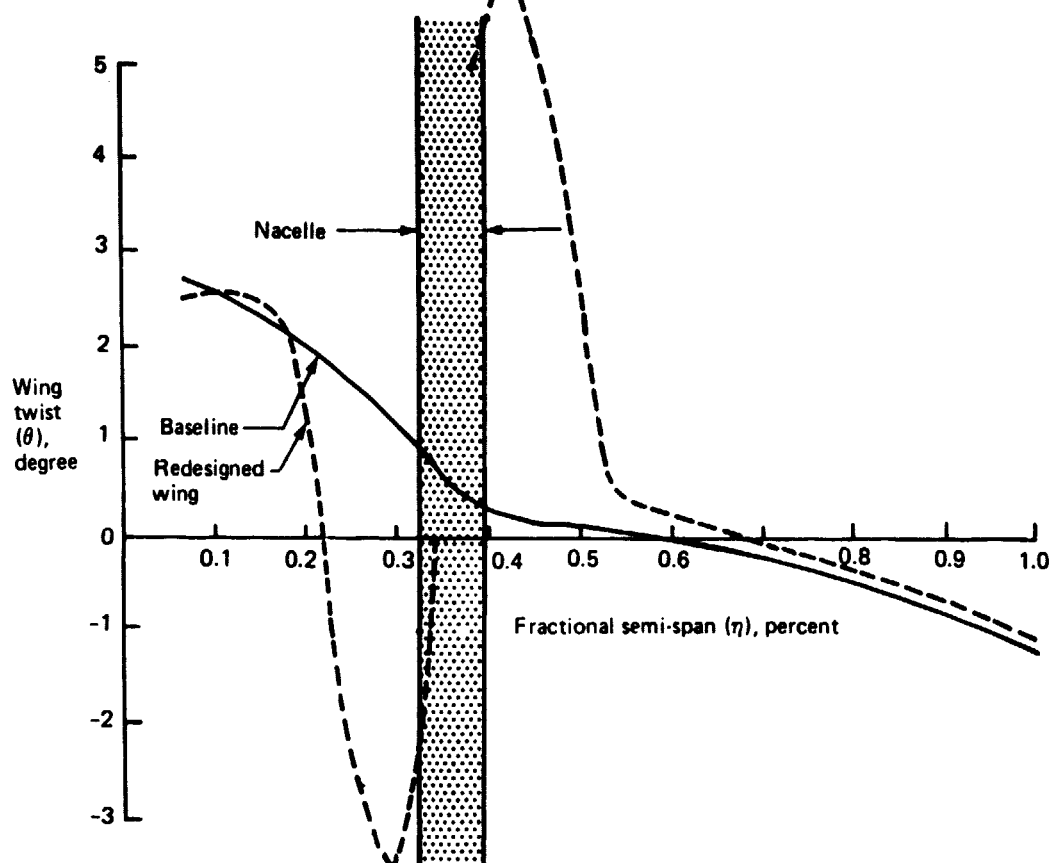


Figure 7. Cruise Wing Twist Distribution

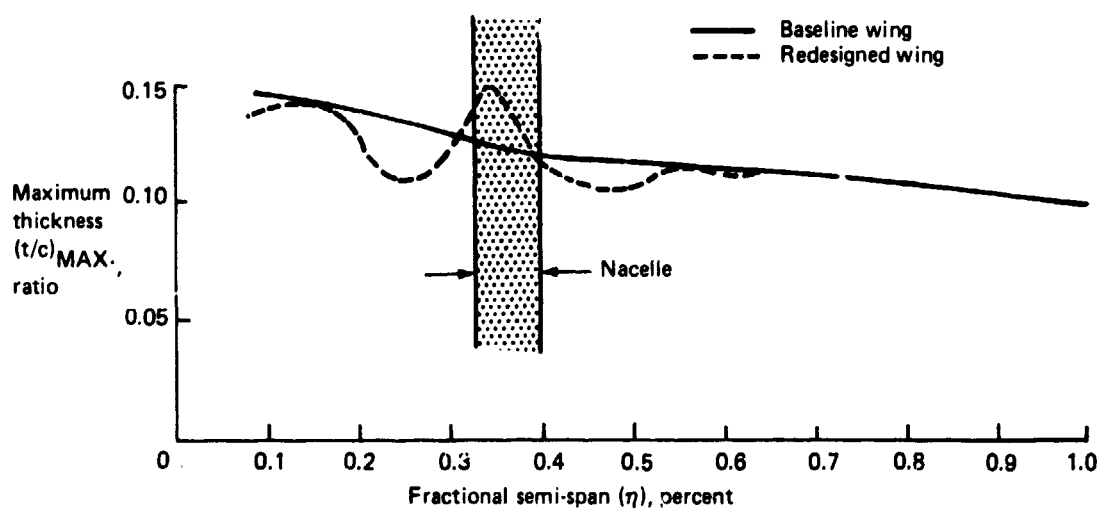


Figure 8. Cruise Wing Thickness Distribution

5.0 WING-MOUNTED PROP-FAN—CRUISE

5.1 CONFIGURATION AND FLIGHT CONDITIONS

Potential-flow analysis of the wing-mounted prop-fan in a cruise configuration is presented in this section. The analysis was carried out on the Boeing A 230 general potential flow computer system (Section 4.0) at values of α from -3° to $+3^\circ$, and at 0.7 freestream Mach number. Several configurations comprising wing, body, nacelle and slipstream were modeled and analyzed in a systematic buildup toward achieving a broad understanding of the phenomena involved. The baseline wing employed in the study was essentially that of a twin-turbofan airplane meeting similar requirements and available from previous Boeing studies. This wing was subsequently redesigned, using the method described in Section 4.0, with the objective of achieving the clean wing pressure distribution in the presence of the nacelle and slipstream. Figures 9 and 10 show the paneling arrangement for the clean wing and the

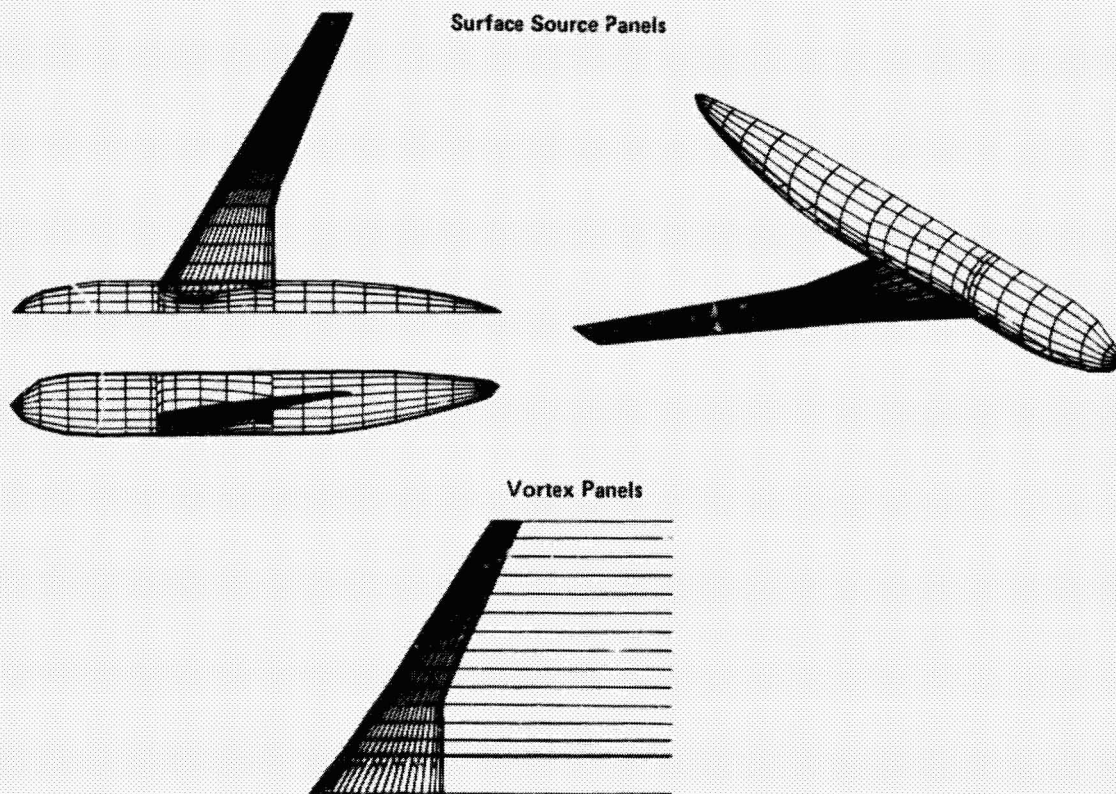


Figure 9. Baseline Wing Body Model

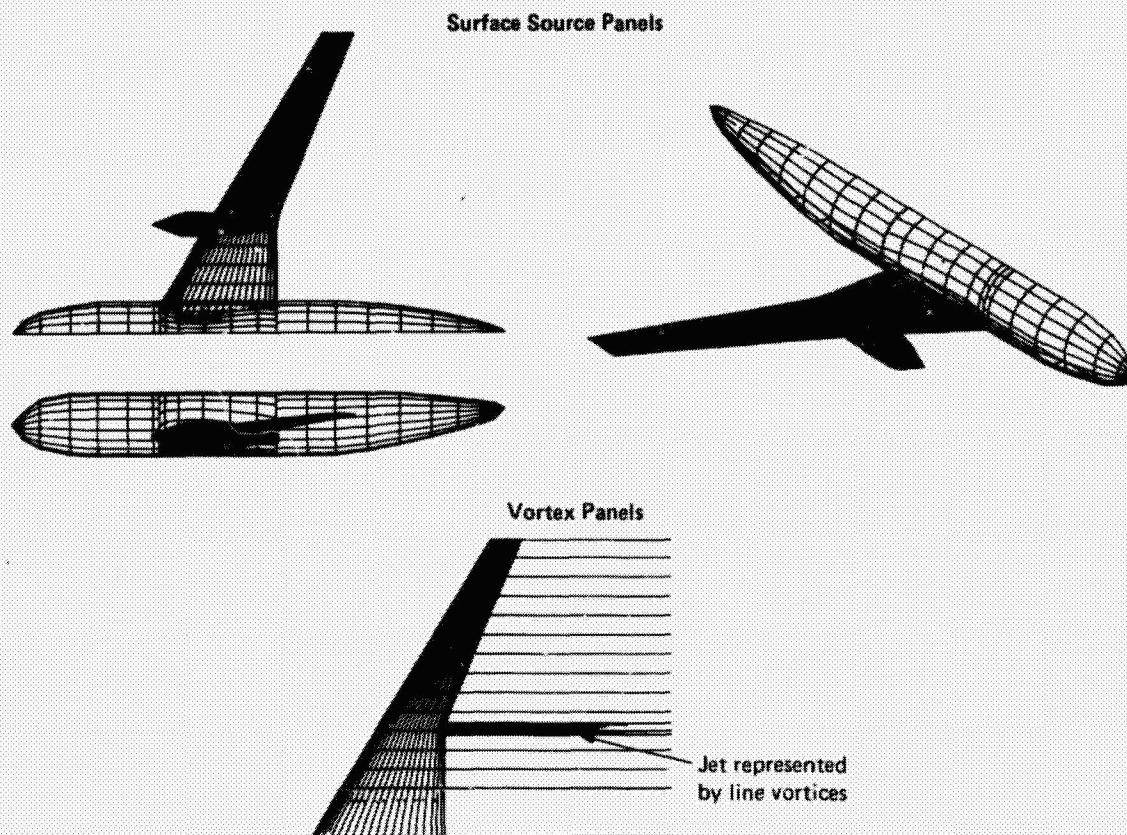


Figure 10. Baseline Wing Body/Nacelle Model

wing plus nacelle, respectively, as defined for potential flow analysis. In each case, the wing has been subdivided into 14 strips having 48 source panels each. The modified wing-nacelle-body configuration is shown in Figures 11 and 12. Definition of the baseline and modified wings is given in Appendix A. Sharp discontinuities in twist and thickness across the nacelle make this wing structurally undesirable. For this reason, although wind tunnel testing to validate the theory and to assess the extent to which the design objectives were achieved could be conducted, they are not recommended for this wing geometry. Instead, further research to define a more realistic wing geometry is recommended.

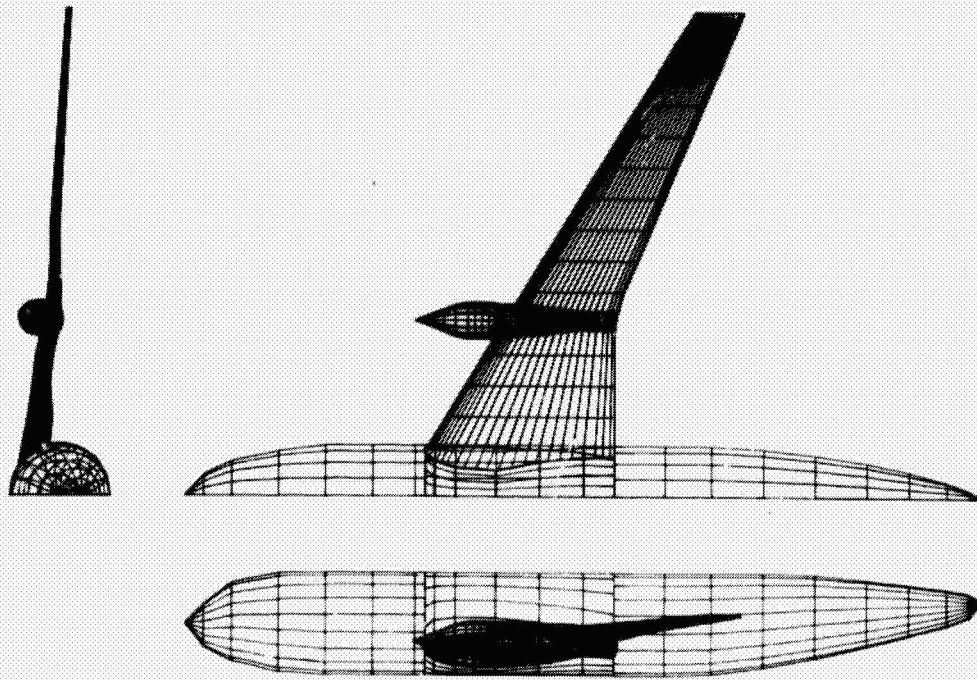


Figure 11. Paneling of Modified Cruise Wing

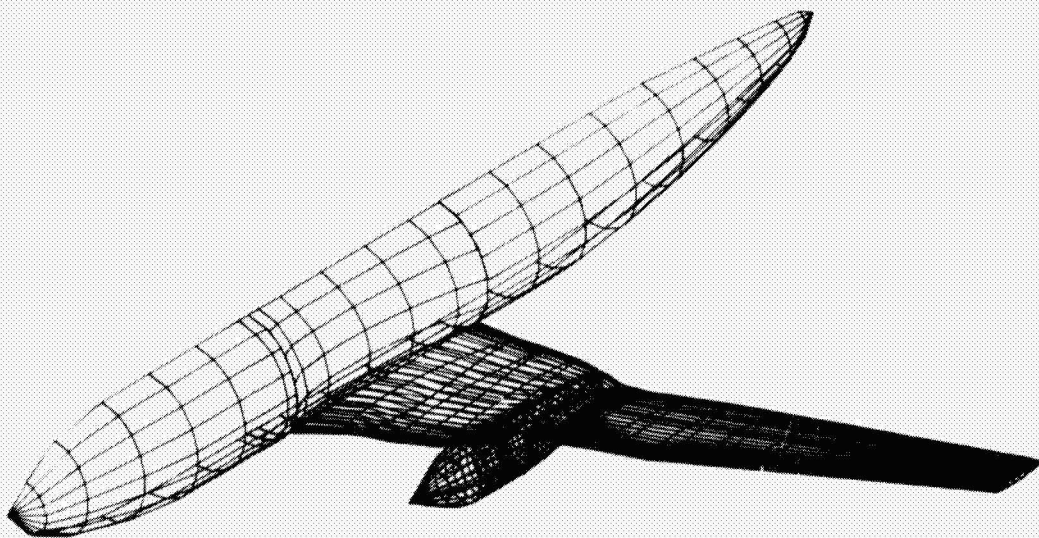


Figure 12. Modified Cruise Wing

5.2 SLIPSTREAM CHARACTERISTICS

Figure 13 presents a comparison of the measured and calculated total pressure ratios and swirl angles along the blade radius as stated by Hamilton Standard in reference 4. The measured data, taken one blade chord behind the propeller, indicated that the root sections were overloaded and the top portions were underloaded compared to the design objectives. Because further refinements were contemplated by Hamilton Standard to achieve the design objectives, the theoretical distribution was selected for inclusion in the potential flow model.

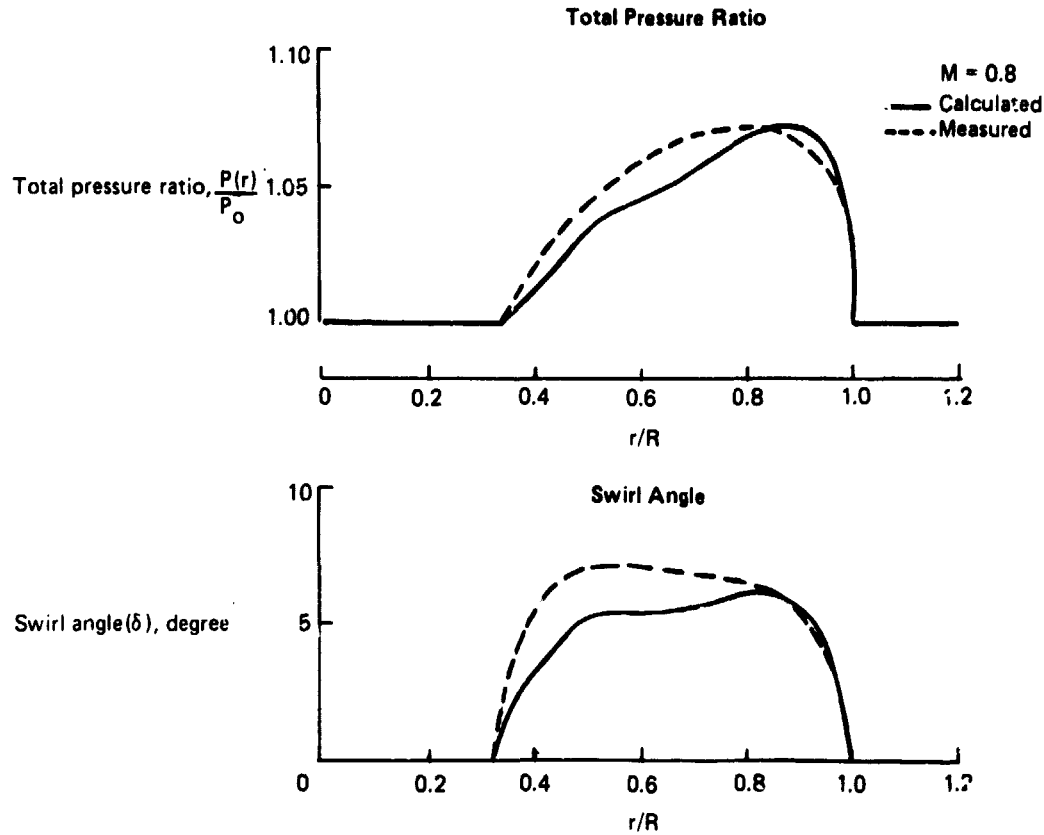


Figure 13. Radial Distribution of Swirl and Total Pressure in Prop Slipstream

The magnitude of the velocity vector $V(r)$ in the propeller slipstream is isentropically related to the total pressure ratio $P(r)/P_0$ as follows:

$$\frac{V(r)}{U_\infty} = \frac{1}{M_\infty} \left[\left(\frac{P(r)}{P_0} \right)^{\frac{\gamma-1}{\gamma}} \left(\frac{2}{\gamma-1} + M_\infty^2 \right) - \frac{2}{\gamma-1} \right]^{1/2}$$

with the assumption that the local static pressure is constant: $p(r) = p$

The axial velocity component, V_x/U_∞ is determined from $V(r)$ and the swirl angle $\delta(r)$ thus,

$$\frac{V_x}{U_\infty} = \frac{V(r)}{U_\infty} \cos \delta(r)$$

The pressure coefficient is calculated from:

$$C_p = \frac{\left[1 + \frac{\gamma-1}{2} M_\infty^2 \left(1 + \frac{V(r)^2}{U_\infty^2} \right) \right] \frac{\gamma}{\gamma-1} - 1}{\frac{\gamma}{2} M_\infty^2} + \frac{\Delta P(r)}{q}$$

where q is the dynamic head and $\Delta P(r)/a$ is a correction term to account for the change in total head across the propeller disc. It is given by:

$$\frac{\Delta P(r)}{q} = \left(\frac{P(r)}{P_0} - 1 \right) \frac{\left[1 + \frac{\gamma-1}{2} M_\infty^2 \right] \frac{\gamma}{\gamma-1}}{\frac{\gamma}{2} M_\infty^2}$$

The above formulation has been used for all potential flow calculations in the present document.

5.3 PRESSURE COEFFICIENT DATA

Pressure profiles for the baseline wing on the two sides of the nacelle are shown in Figures 14 through 17. On the inboard side (strips 3 and 4), the effect of the nacelle is to increase the superelevations on both upper and lower surfaces. This is equivalent to an increased-thickness effect. The propeller slipstream induces a local upwash which further aggravates the upper surface pressure peaks. Local Mach numbers of up to 1.5, corresponding to a freestream Mach number of 0.7, have been calculated. It is thus postulated that severe penalties in drag may be incurred as a result of shock formation on the inboard wing. On the outboard side of the nacelle (strips 4 and 5), both the nacelle and the slipstream contribute to unloading the local wing sections. The nacelle produces a diminished-thickness effect, whereas the swirl reduces the effective local incidence.

Pressure profiles for the modified wing are compared with the baseline profiles in Figures 18 through 21. These figures indicate that, to a large extent, the design objective of achieving the clean wing pressure distribution has been attained. The design procedure (outlined in Section 4.0) necessitated changes in the wing twist, thickness, and airfoil shape and was limited to a single design cycle.

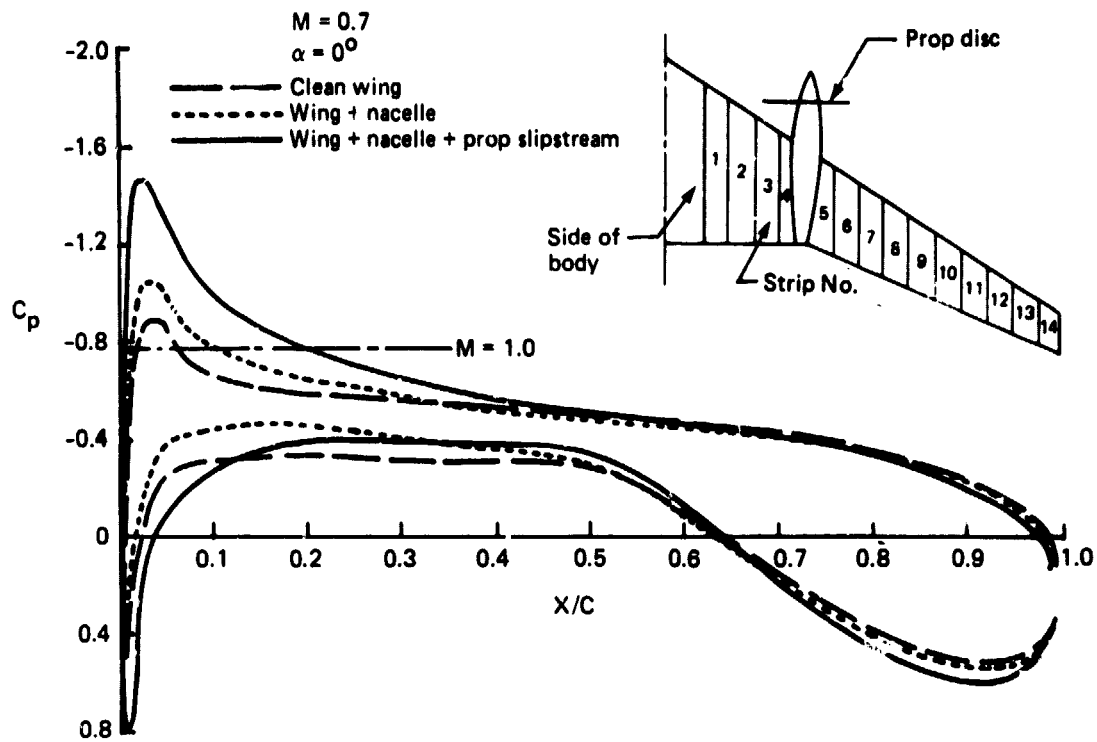


Figure 14. Effect of Slipstream on Chordwise Pressure Distribution: Strip 3

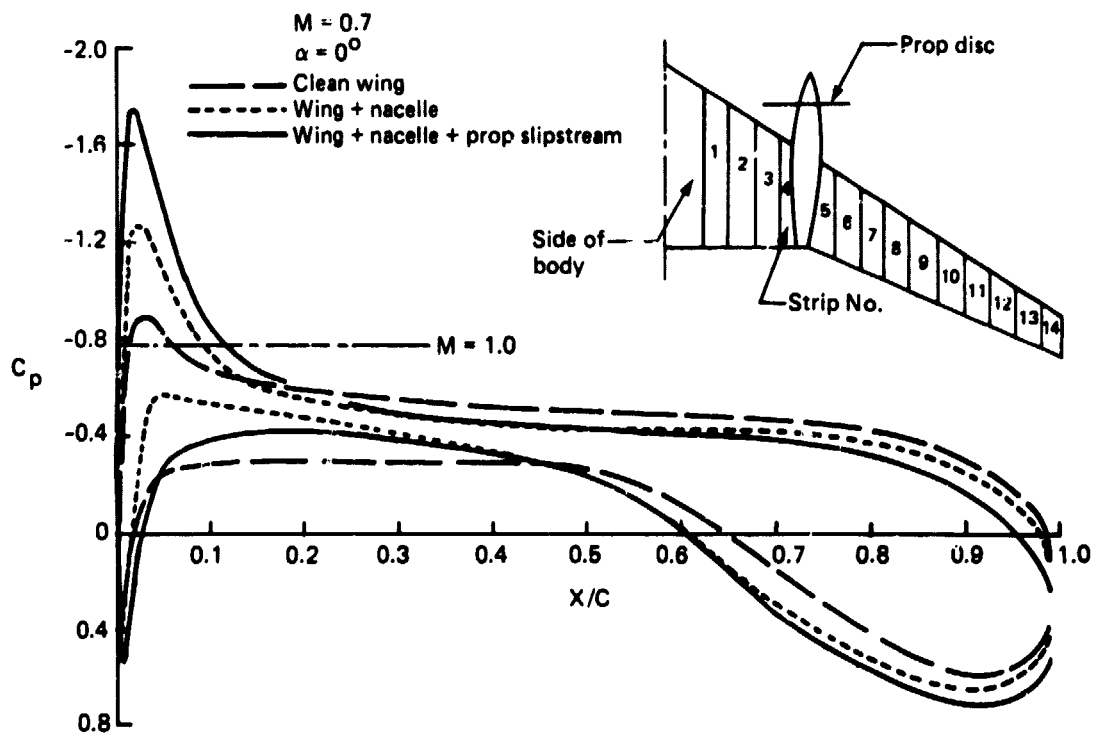


Figure 15. Effect of Slipstream on Chordwise Pressure Distribution: Strip 4

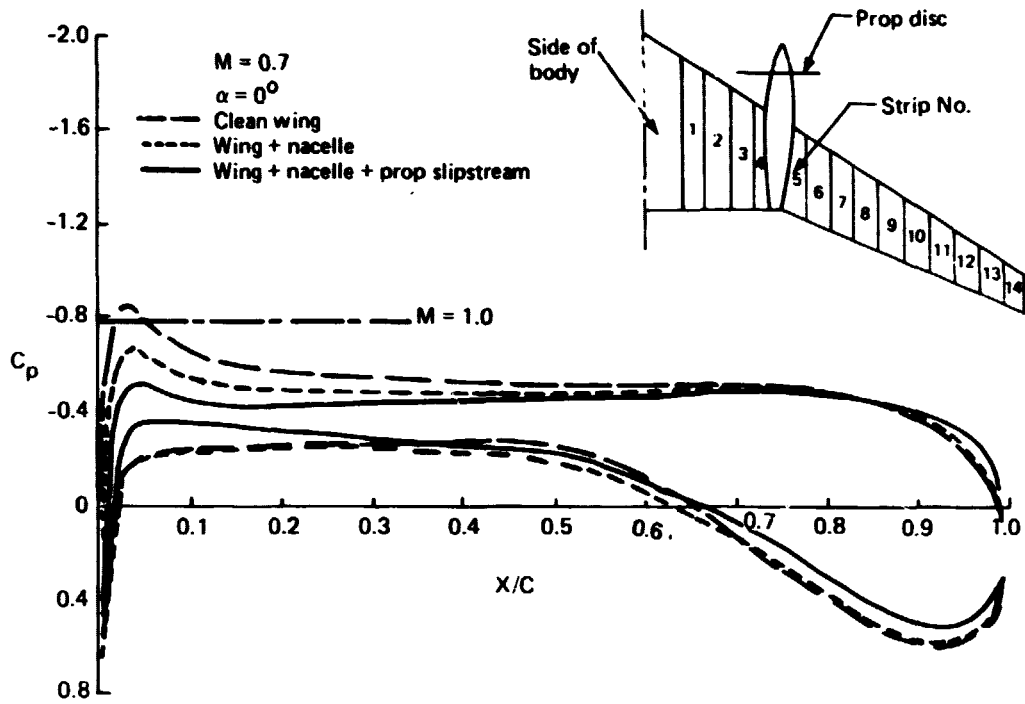


Figure 16. Effect of Slipstream on Chordwise Pressure Distribution: Strip 5

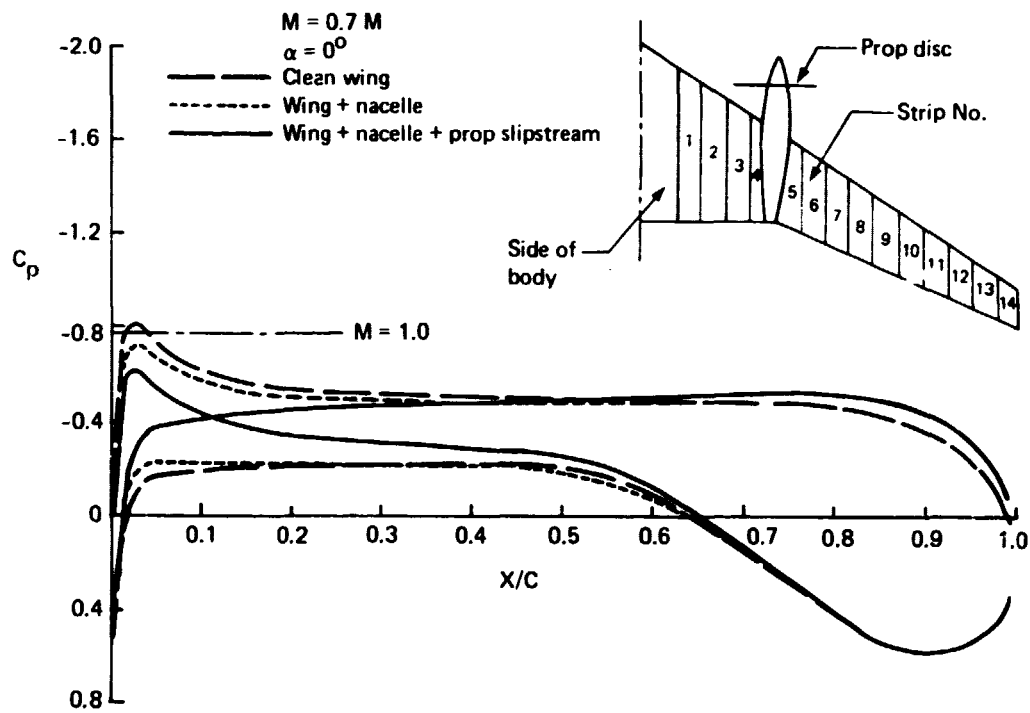


Figure 17. Effect of Slipstream on Chordwise Pressure Distribution: Strip 6

ORIGINAL PAGE IS
OF POOR QUALITY

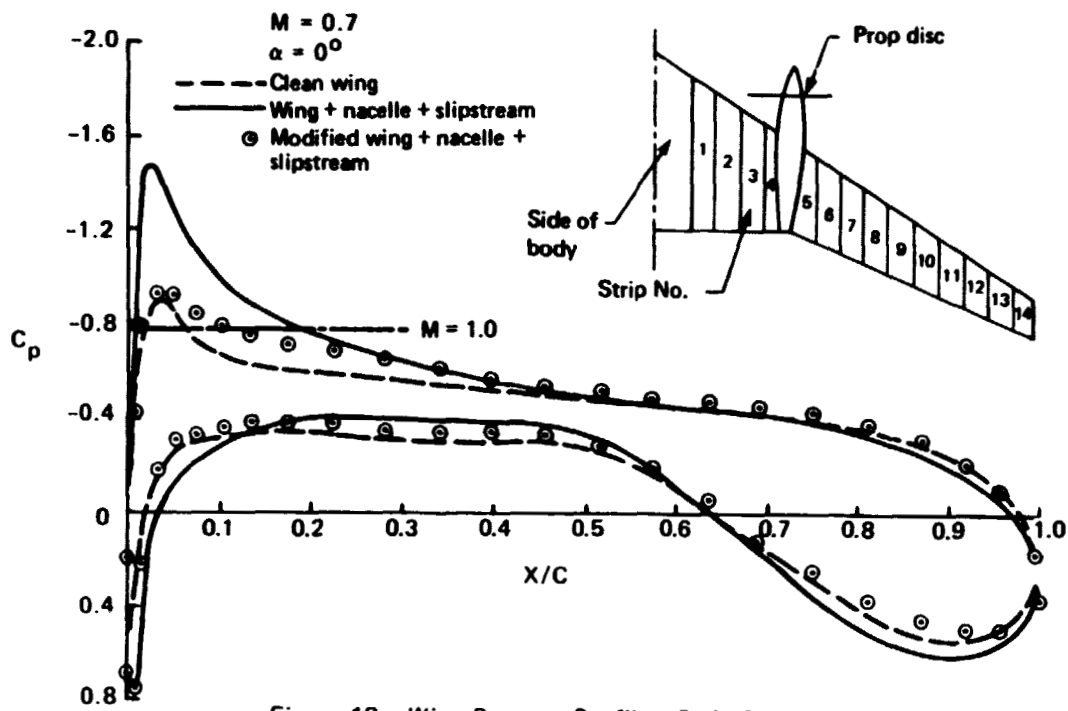


Figure 18. Wing Pressure Profiles: Strip 3

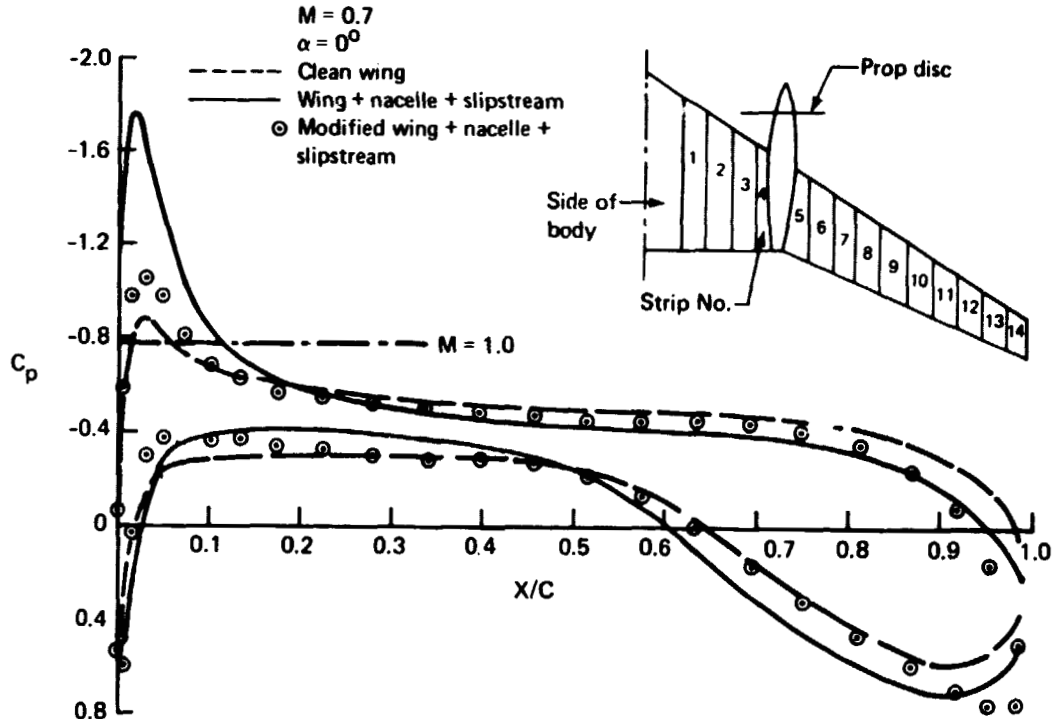


Figure 19. Wing Pressure Profiles: Strip 4

ORIGINAL PAGE IS
OF POOR QUALITY

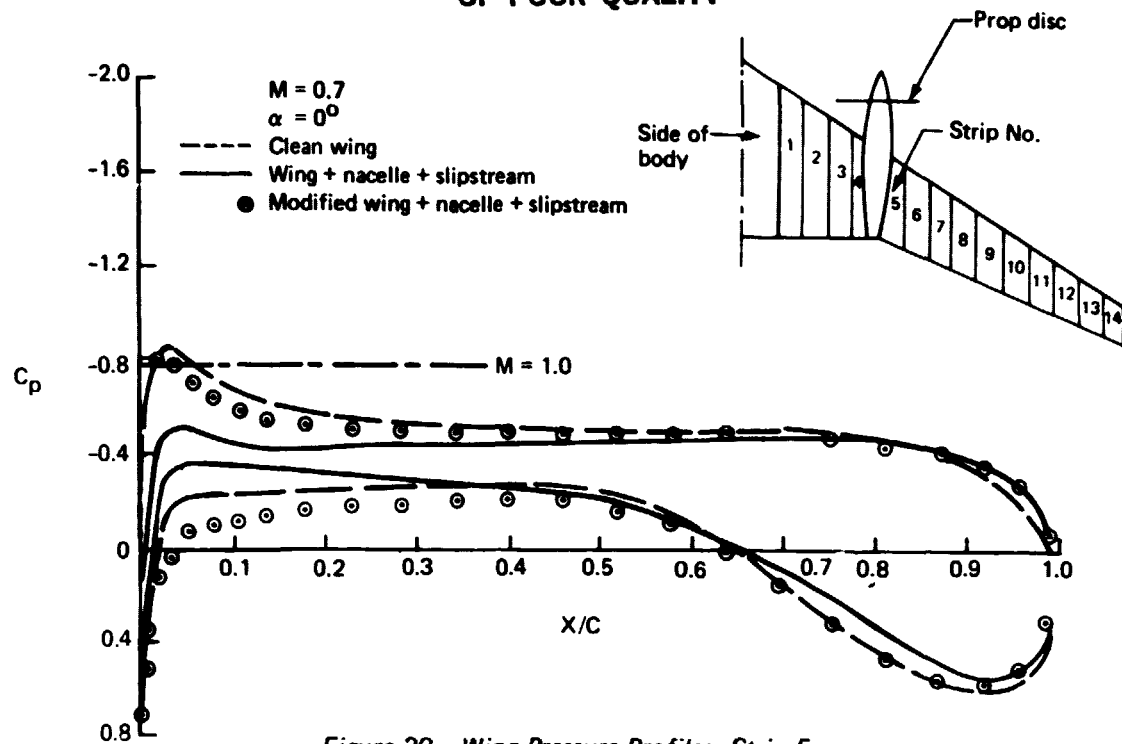


Figure 20. Wing Pressure Profiles: Strip 5

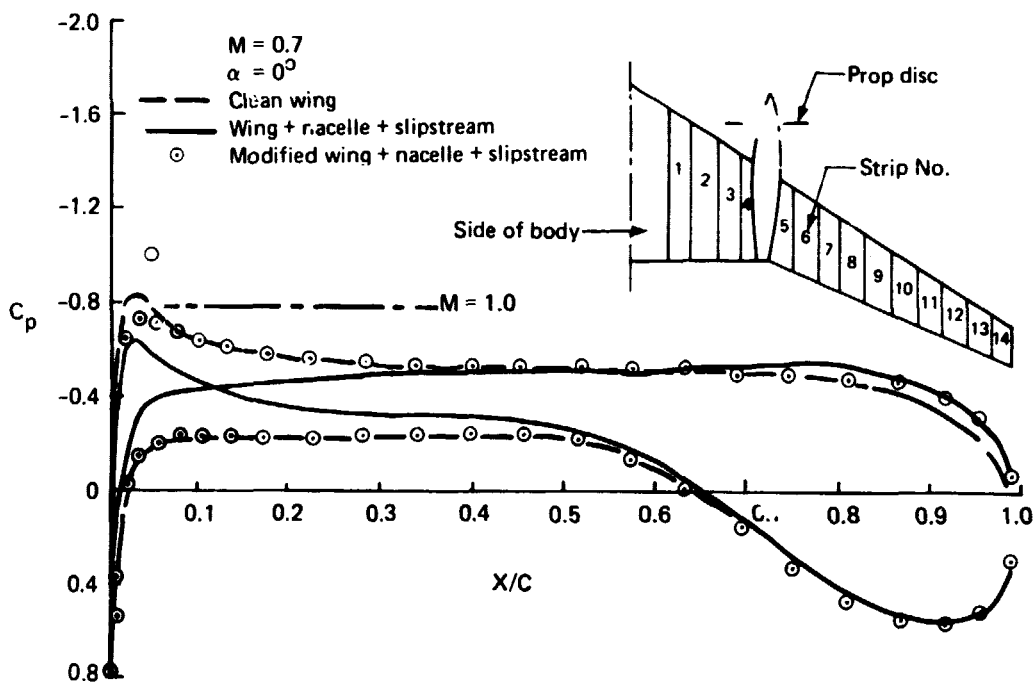


Figure 21. Wing Pressure Profiles: Strip 6

5.4 WING ISOBARS

Wing upper surface isobars for the baseline and modified wings are presented in Figures 22 through 25. The effect of the nacelle alone (fig. 23) is to disrupt the isobar pattern near the wing leading edge. Increased suction peaks inboard of the nacelle, which die out near the side of the body, appear as elongated puddles. The effect of the swirl (fig. 24) is to further increase the suction peaks inboard of the nacelle and to cause puddling of the isobars on the outboard side.

The modified wing (fig. 25) exhibits an outboard isobar pattern similar to that of the clean wing. Inboard, the isobar pattern reveals the presence of suction peaks higher than those of the clean wing that have not been fully mitigated through the design exercise.

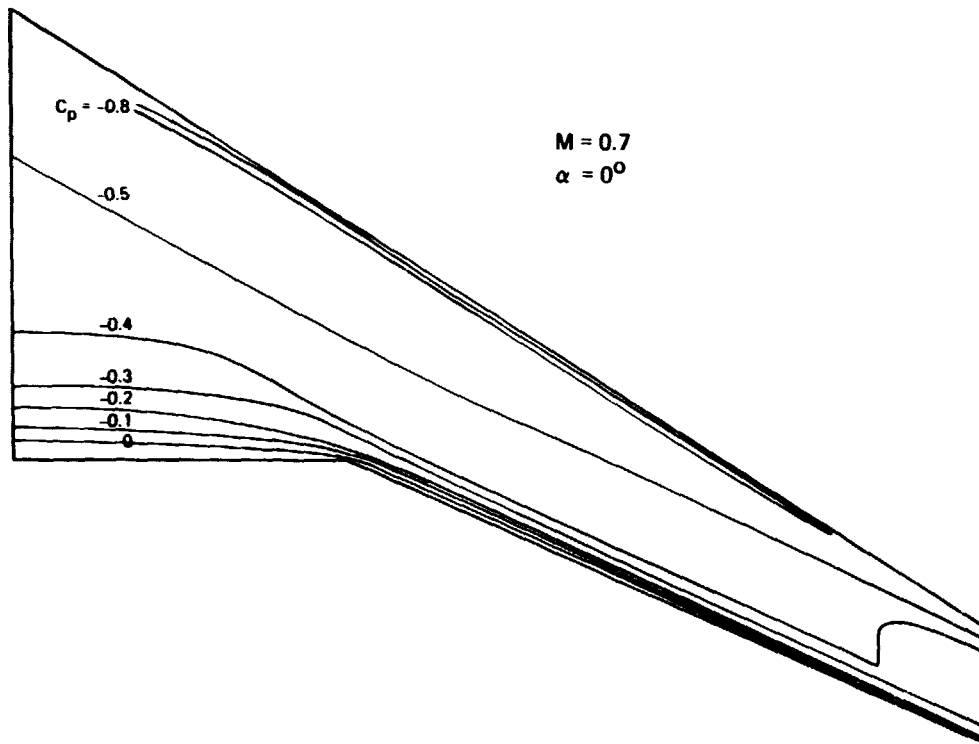


Figure 22. Upper Surface Wing Isobars—Clean Wing

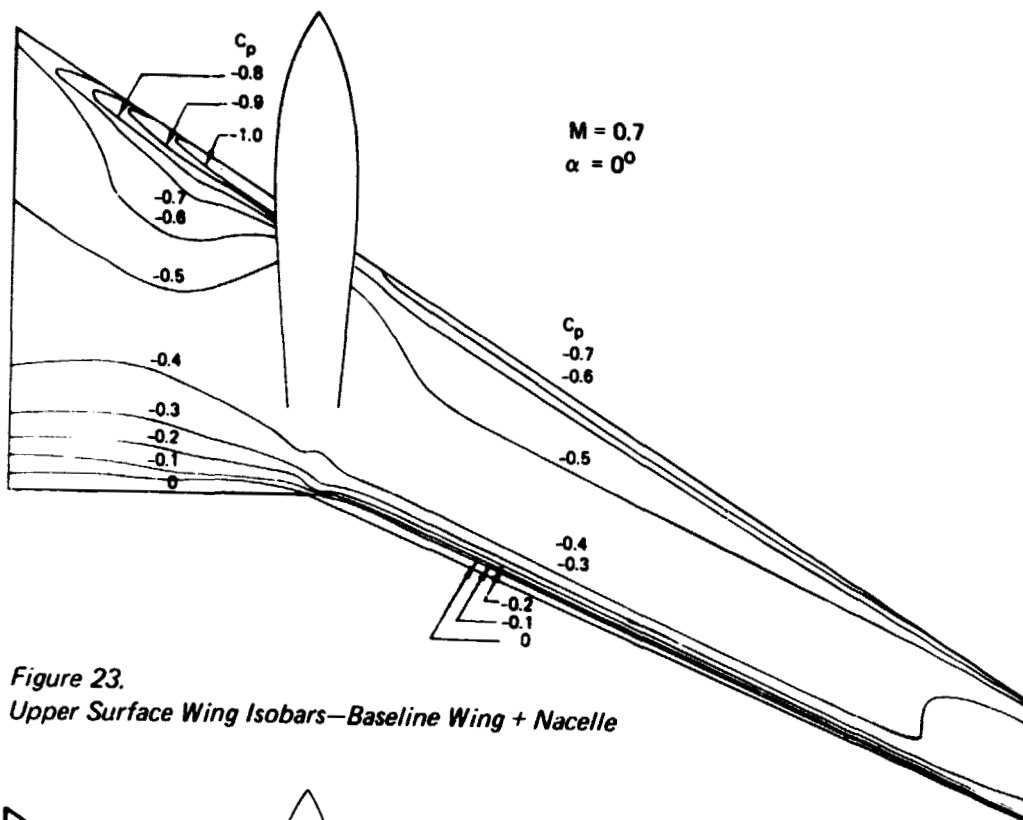


Figure 23.
Upper Surface Wing Isobars—Baseline Wing + Nacelle

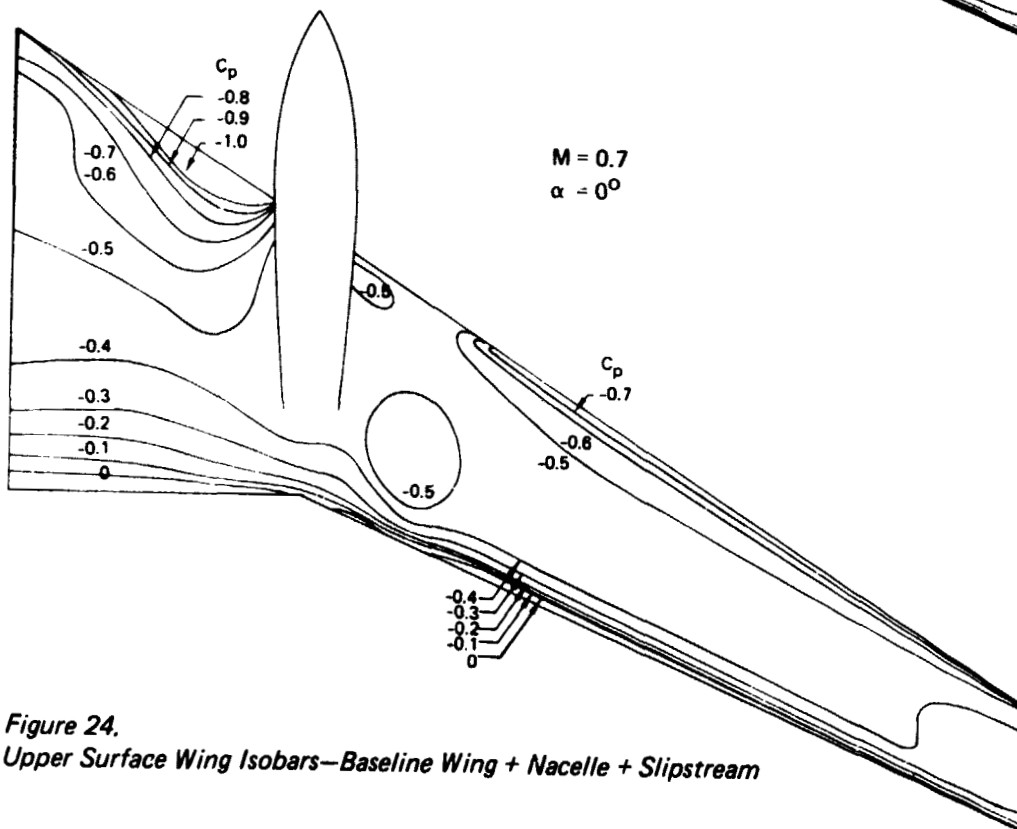


Figure 24.
Upper Surface Wing Isobars—Baseline Wing + Nacelle + Slipstream

ORIGINAL PAGE IS
OF POOR QUALITY

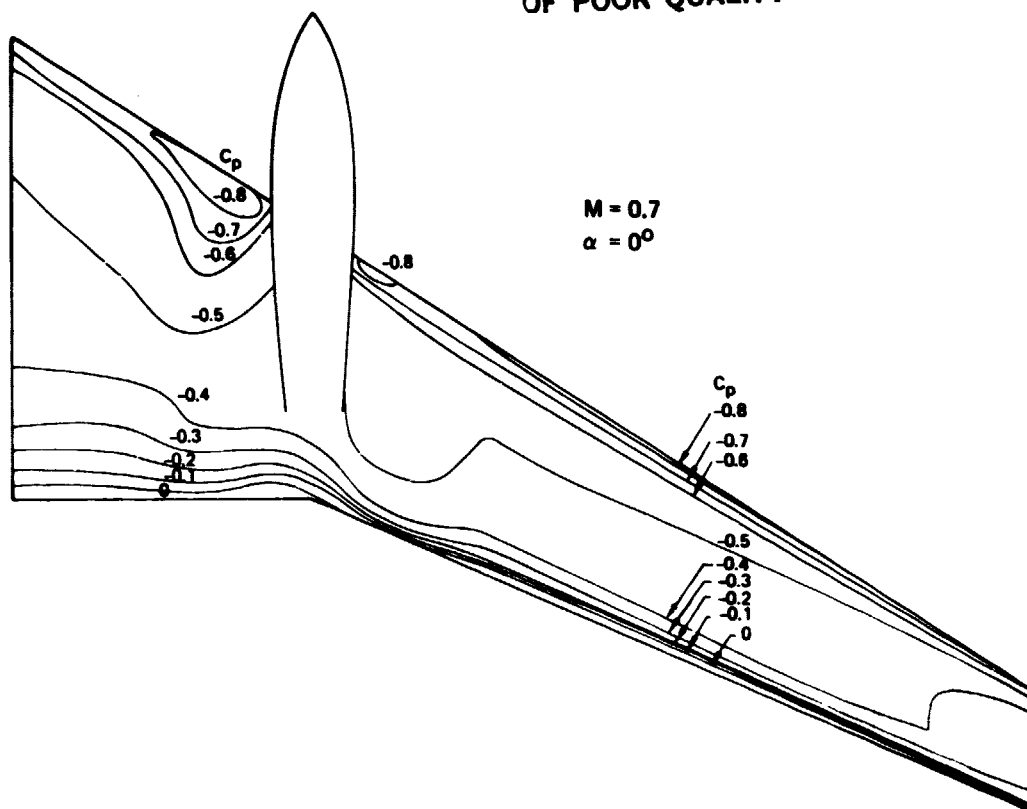


Figure 25. Upper Surface Wing Isobars—Modified Wing + Nacelle + Slipstream

5.5 FORCE DATA

C_L vs α curves for the cruise wing-body-nacelle configuration are shown in Figure 26. At $\alpha = 0^\circ$, the effect of the slipstream is to increase the total lift by approximately 5%. The slope of the lift curve is slightly lower for the modified wing relative to the baseline in the absence of slipstream effects. In all cases, a design C_L value of 0.5 is achieved at α close to 0° .

Wing spanwise load distributions are presented in Figures 27 and 28. Figure 27 shows the incremental effects of the nacelle and slipstream on the loading of the baseline wing. The asymmetry created by the prop slipstream is compatible with the pressure profiles of Figures 13 through 16. The wing, in this case, acts as a pair of stators tending to straighten the swirling flow behind the propeller and thus contribute to thrust recovery. Figure 28 gives the span load distribution for the modified wing which is in agreement with that of the clean wing, as set forth in the design objective.

Spanwise distribution of C_{pMIN} for the baseline and modified wing is presented in Figure 29 at $\alpha = 0^\circ$. Inboard of the nacelle, the baseline wing is highly critical because of upwash from the swirling slipstream. At 0.8 cruise Mach number, strong shock waves and, possibly,

ORIGINAL PAGE IS
OF POOR QUALITY

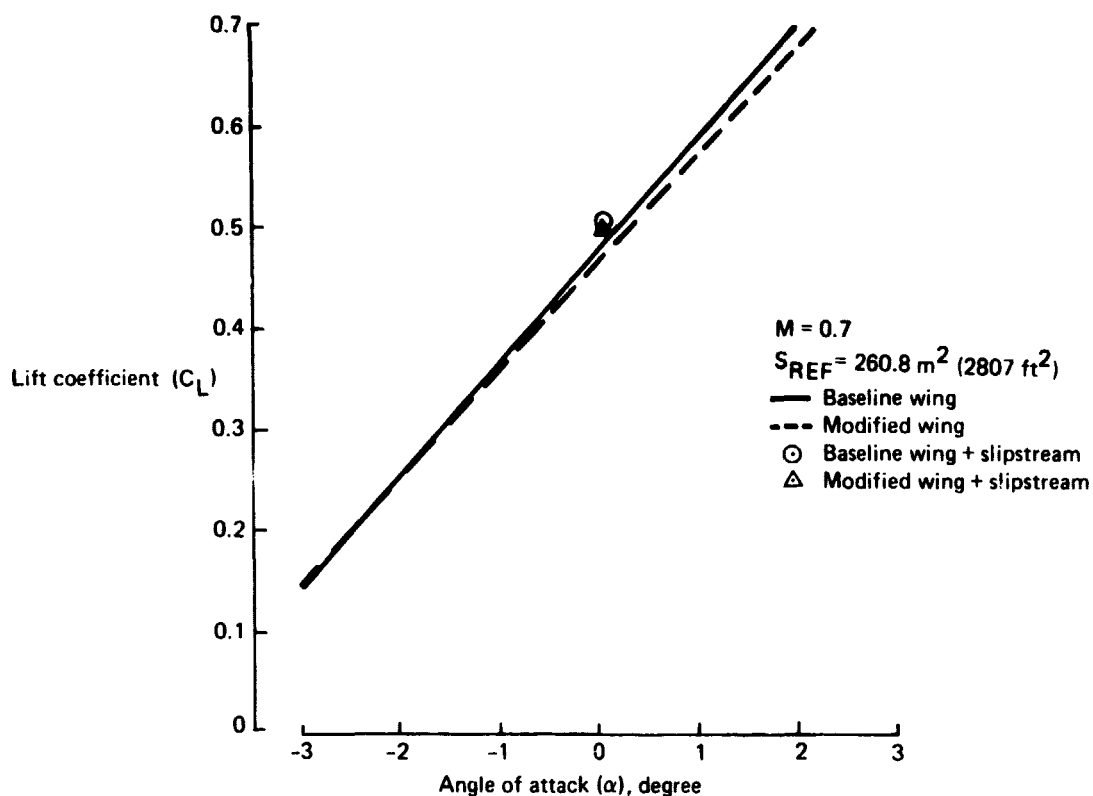


Figure 26. Cruise Wing Lift Curves

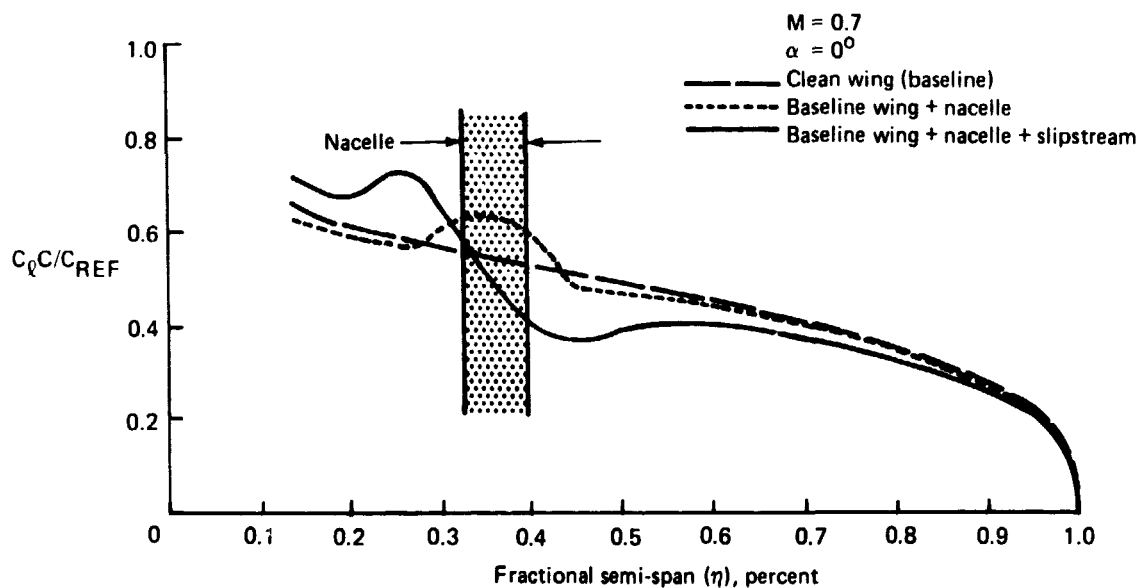


Figure 27. Effect of Slipstream on Span Loading

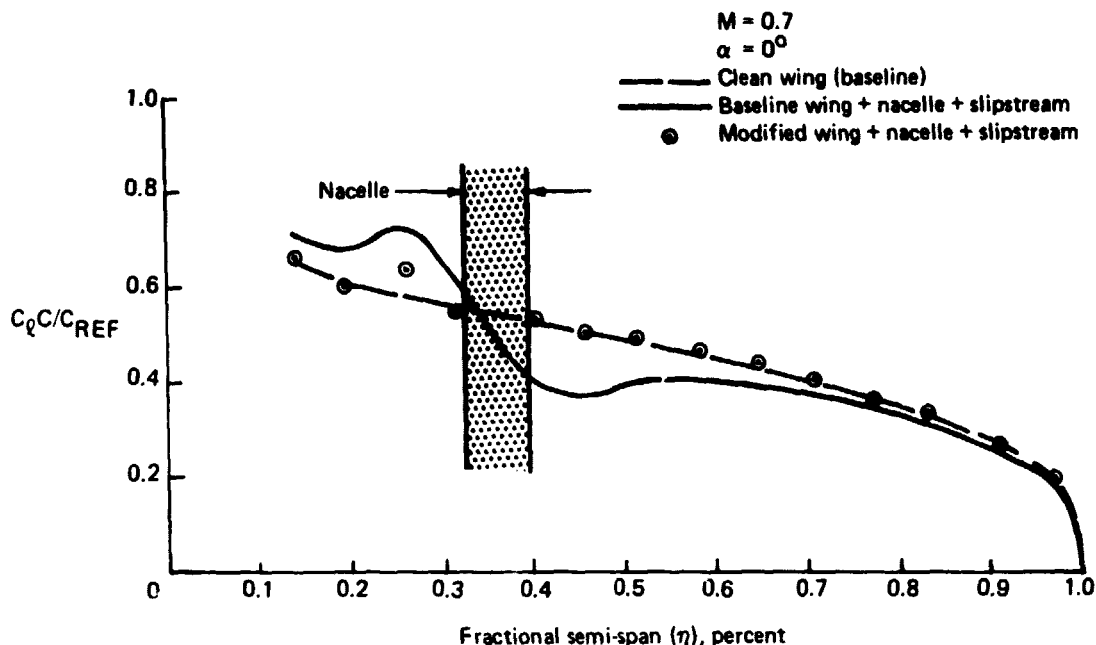


Figure 28. Wing Spanwise Load Distribution

shock-induced separation are likely to occur on the inboard baseline wing. Corresponding penalties in profile drag are difficult to assess without a full-scale wind tunnel test. However, these penalties are expected to outweigh gains accrued from propeller thrust recovery. The modified wing (fig. 29) exhibits substantially reduced pressure peaks, although still higher than those of the clean wing.

5.6 PROPELLER THRUST RECOVERY

Swirl velocities in the prop slipstream represent lost thrust and hence lower efficiency. In Reference 1, these losses were estimated at 8% during cruise and 13% at takeoff. The wing, acting as a large chord stator, may be expected to recover some of the lost thrust by de-rotating the slipstream. Physically, the slipstream induces a local angle-of-attack, which causes the lift vector to tilt forward, producing thrust.

In the present context, the thrust increment due to the slipstream has been obtained by integration of the surface pressure. Figure 30 gives a drag buildup for the baseline and the modified wing, each incremented from the clean wing. The increments in profile drag (C_{DP}) were postulated on the basis of the spanwise distribution of C_{pMIN} of Figure 29. Early shock formation could lead to an early break in the polar as suggested in Figure 30. Uncertainty factors for the increments in C_{DP} may be as high as 100%.

Vector ΔC_{Di} in Figure 30 represents the increment in induced drag between the wing plus nacelle and the clean wing. It was calculated by the induced drag program A 323 (ref. 5) and is strictly a function of the span load distribution. This vector is negligible for the baseline wing, but significant (4.5 drag counts) for the modified wing.

ORIGINAL PAGE IS
OF POOR QUALITY

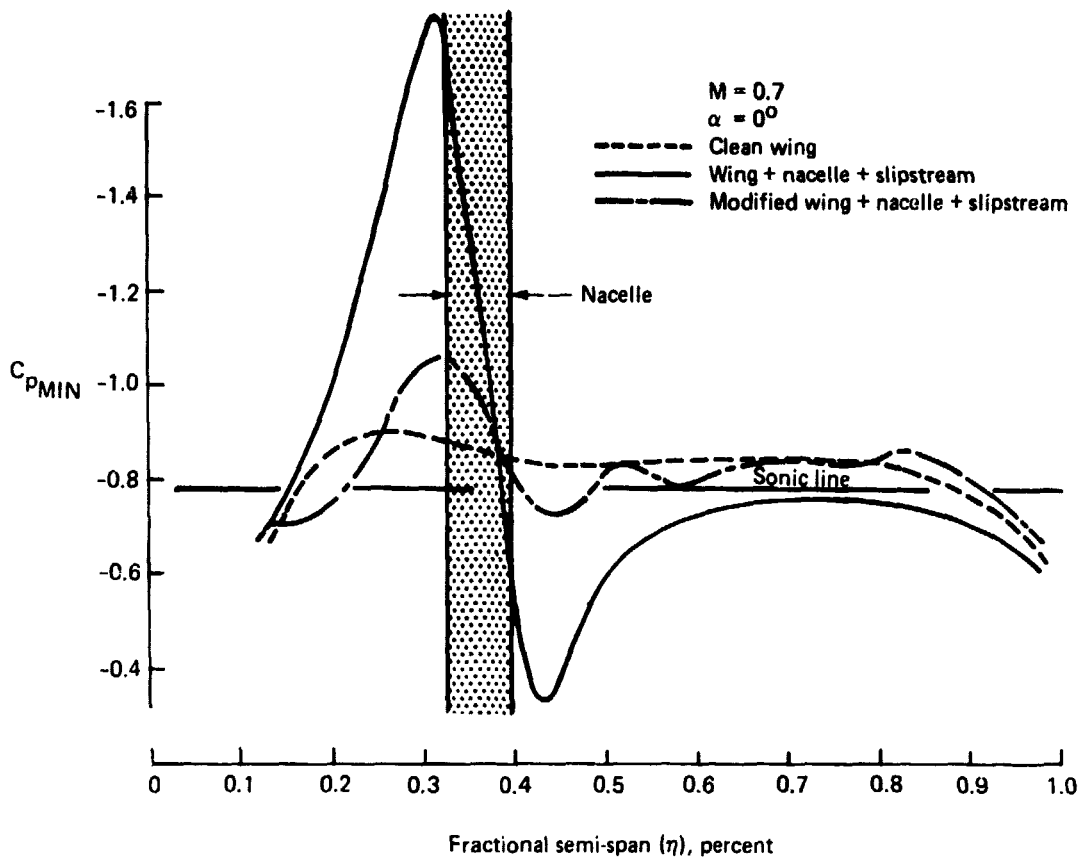


Figure 29. Spanwise Distribution of C_{pMIN}

The thrust recovery vector was calculated by potential flow program A 230 as the difference in integrated surface pressures between the configuration with and without swirl. For the modified wing this vector is composed of a ΔC_L of 0.026 and a ΔC_D of one drag count. It is considered inconsequential.

The baseline wing shows a thrust recovery vector equivalent to 11 counts of thrust. At Mach 0.8 and 10 700m (35 000 ft), this translates into 2.97 kN (668 lb) of thrust. The total thrust of the airplane may be estimated from the propeller power loading given by Reference 4:

$$\frac{SHP}{D^2} = 37.5 \text{ per engine}$$

Where SHP is shaft horsepower and $D = 5.97\text{m}$ (19.6 ft) is propeller diameter. At Mach 0.8 and 10 700m (35 000 ft), the total thrust, assuming a propeller efficiency of 0.8, is:

$$T = 72.427 \text{ kN (16 283 lb)}$$

ORIGINAL PAGE IS
OF POOR QUALITY

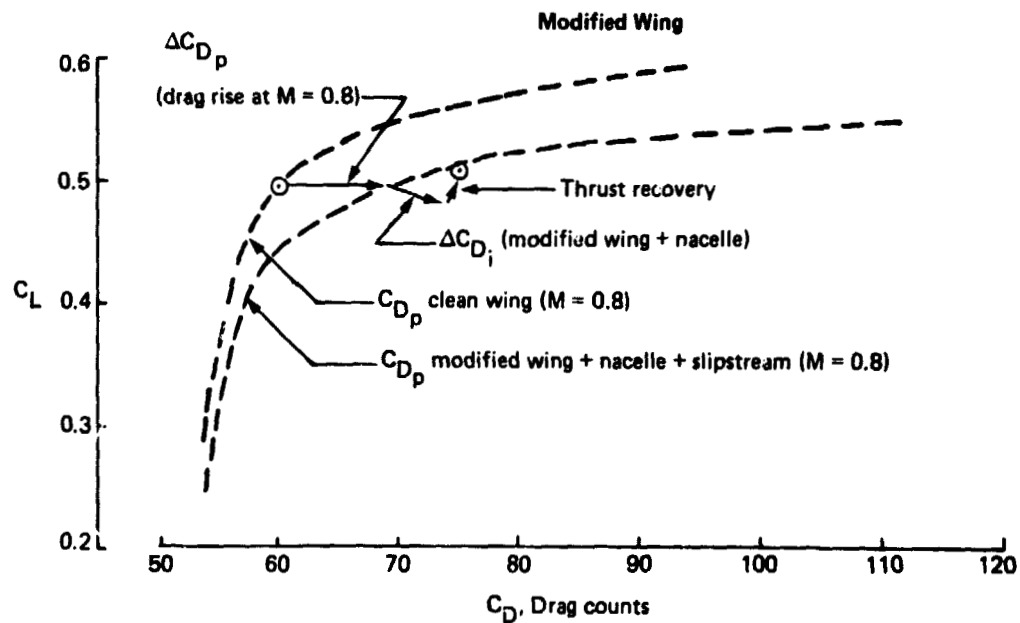
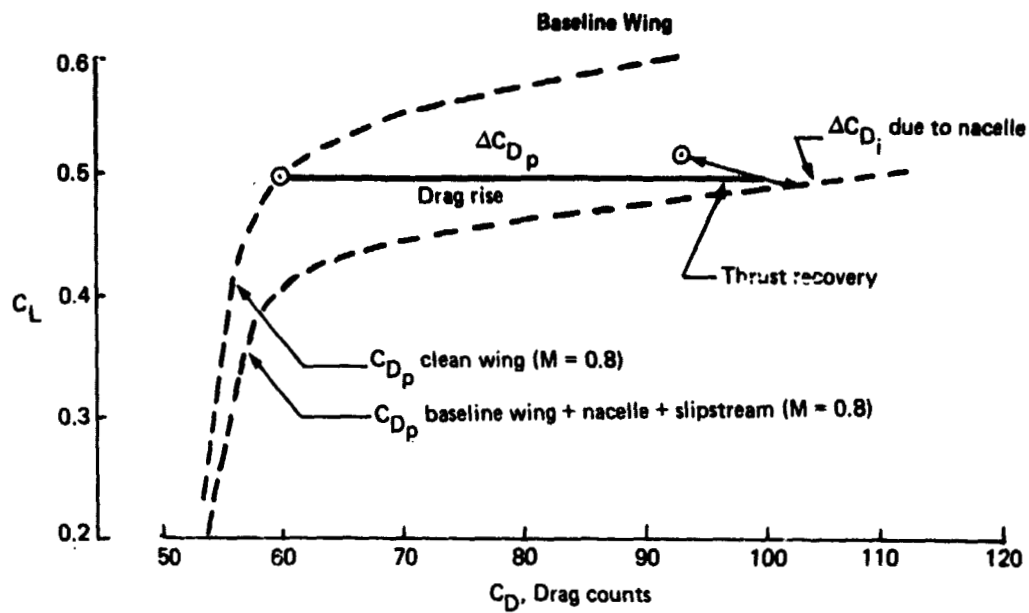


Figure 30. Wing Drags Incremented from Clean Wing

From the above, the recovered thrust for the baseline wing is 4.1% of the total, or approximately 50% of the estimated thrust lost due to swirl.

This estimate of thrust recovery is predicated on the ability of the baseline wing to sustain the calculated pressure profiles in shock and separation-free flow.

5.7 ASSESSMENT

The influence of the nacelle (without slipstream) on the baseline wing is significant as is indicated in Figures 14, 15, 24, and 27. The present study did not consider recontouring the nacelle. However, future study efforts should include this consideration, perhaps in combination with some thrust line toe-out to align it with the local flow.

The swirl produced by the wing-mounted prop-fan imparts a strong local upwash to the wing inboard of the nacelle and a downwash on the outboard side. Large leading edge suction pressures appearing on the inboard wing were found to produce a thrust force, equivalent to the momentum removed from the swirling slipstream through the straightening effect of the wing. The analysis further indicated that at high cruise Mach number ($M = 0.8$), isentropic flow could not be maintained on the inboard wing and that shock waves were likely to occur. If this occurs, the readjustment of pressure on the inboard wing would largely eliminate the calculated thrust increment and would further lead to sizeable penalties in profile drag. To alleviate the adverse effects of the nacelle and swirl on the wing, the latter was redesigned to neutralize these effects. The resulting wing is characterized by large variations in twist and thickness and shows little potential for thrust recovery. The trade between profile drag and thrust recovery must ultimately be determined through wind tunnel testing.

6.0 WING-MOUNTED PROP-FAN-LOW SPEED

Low-speed analysis of the takeoff configuration and flight condition was selected because the slipstream effects are much greater than in the landing approach condition.

6.1 GEOMETRICAL DEFINITION

Leading- and trailing-edge flap geometries have been defined for the modified cruise wing (described in sec. 5.0) to simulate the takeoff flight condition. Figure 31 depicts a stream-wise section of the flapped wing as defined for potential flow analysis. A trailing-edge flap of 22% chord, extending over the entire wing span was assumed. A flap deflection δ_F of 10° was selected for the takeoff condition and was achieved by rotating the trailing-edge about the 78% chord line.

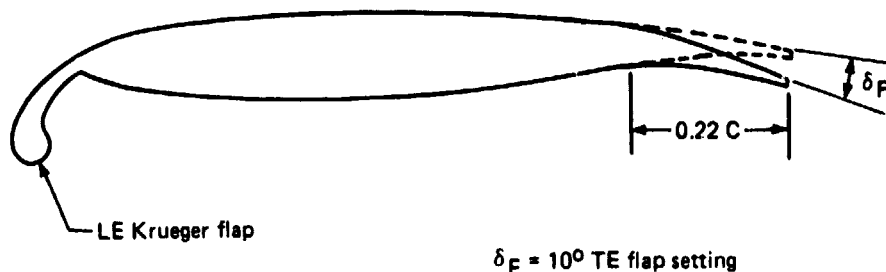


Figure 31. Leading- and Trailing-Edge Flaps for Low-Speed Configuration

The leading-edge Krueger flap geometry was defined as shown in Figure 32 and described below:

- Point A—A point of tangency on the wing upper surface at 2% chord from the leading-edge.
- Point B—Located at the intersection of the tangent from A and the wing chord line.
- The Krueger leading edge (point C) was determined by constructing from point B a line at an angle δ_K to the wing chord line and equal in length to the Krueger flap chord. The latter was fixed at 15% of the basic wing chord. The Krueger angle δ_K was initially selected equal to 63° . In a subsequent design cycle, it was varied between 50° and 55° spanwise, in an attempt to improve the flow pattern over the leading edge.

- The Krueger upper surface profile was extracted from an existing Boeing design and geometrically stretched to fit between points B and C while remaining tangent to line AB.
- The Krueger lower surface profile was faired in arbitrarily to complete the section definition. It does not significantly impact the performance of the wing.

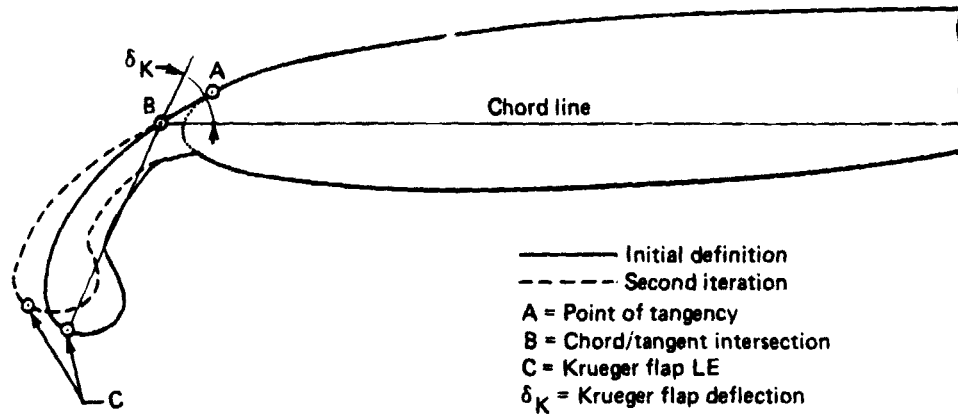


Figure 32. Krueger Flap Definition

The above procedure was fully automated for rapid generation of the entire wing, given a set of Krueger flap angles and chord ratios (C_K/C).

Paneling of the low-speed configuration for potential flow analysis is shown in Figures 33 and 34. Particular attention was required in modeling the wing-body intersection because of the Krueger flap dipping below the body. Bound vortices within the wing lifting system, located in the Krueger flap region, could not be extended to the body centerplane as is normally done. Instead, they were routed to a point aft of the Krueger, deflected to the plane of symmetry, then shed aft to infinity.

ORIGINAL PAGE 18
OF POOR QUALITY

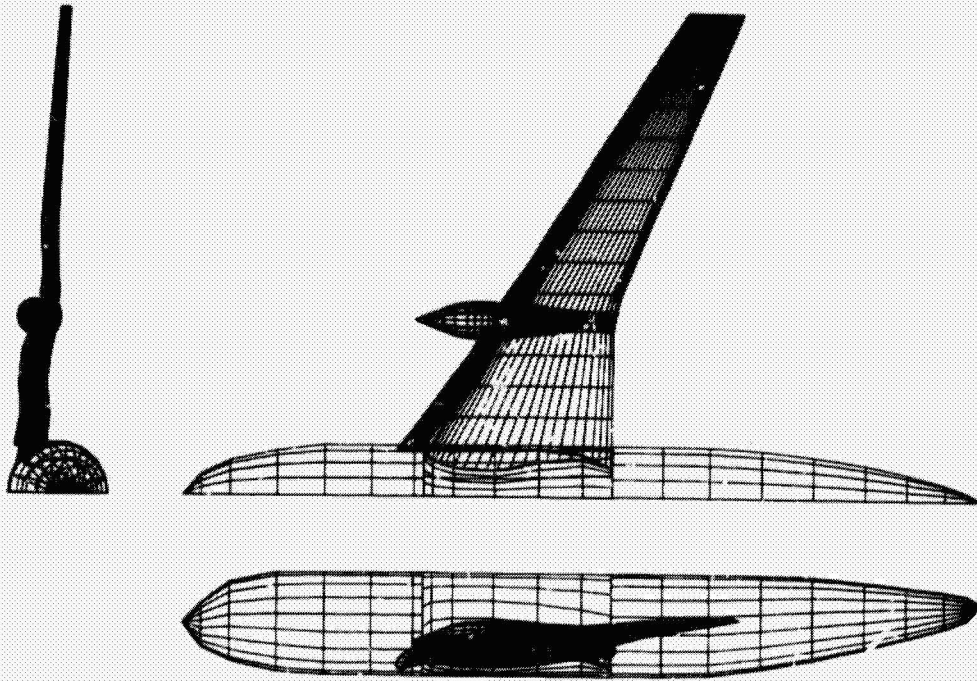


Figure 33. Paneling Scheme—Low-Speed Configuration

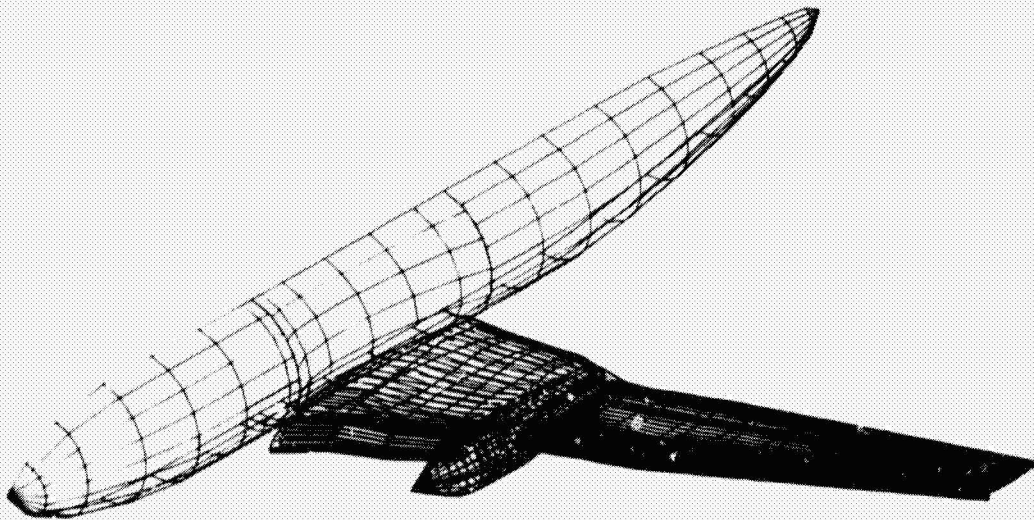


Figure 34. Krueger Wing—Low-Speed Configuration

6.2 DESIGN PROCEDURE

Initial definition of the low-speed configuration included a Krueger flap of constant deflection angle, $\delta_K = 63^\circ$ and chord ratio $C_K/C = 0.15$ (see fig. 32). This configuration was analyzed, less slipstream effects on potential flow program A 230. The results indicated a nonuniform stagnation pattern along the Krueger leading edge, partly because of the large variations in the wing twist distribution. In a second design cycle, the Krueger flap was redefined in accordance with the deflection schedule of Figure 35. A comparison of pressure profiles along strips 3 and 6 for the two design cases is given in Figures 36 and 37. The data are plotted versus arc length (S/C) from the Krueger flap leading edge. At $\alpha = 4^\circ$, the stagnation point is located on the upper side of the leading edge in both design cases. At higher angles-of-attack and/or increasing trailing-edge flap deflections (δ_F), the stagnation point is expected to move down past the leading edge toward a more favorable location corresponding to C_{LMAX} . Because of a more uniform distribution of the stagnation line along the wing leading edge, the second iteration design was selected for further analysis.

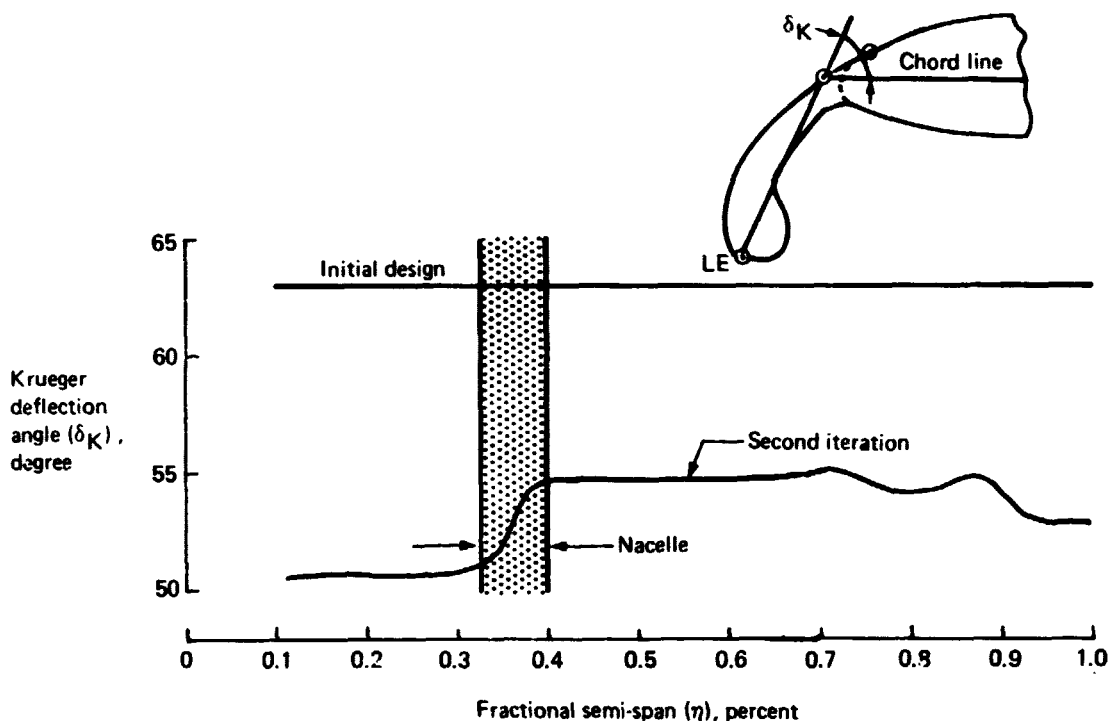


Figure 35. Krueger Flap Deflection Schedule

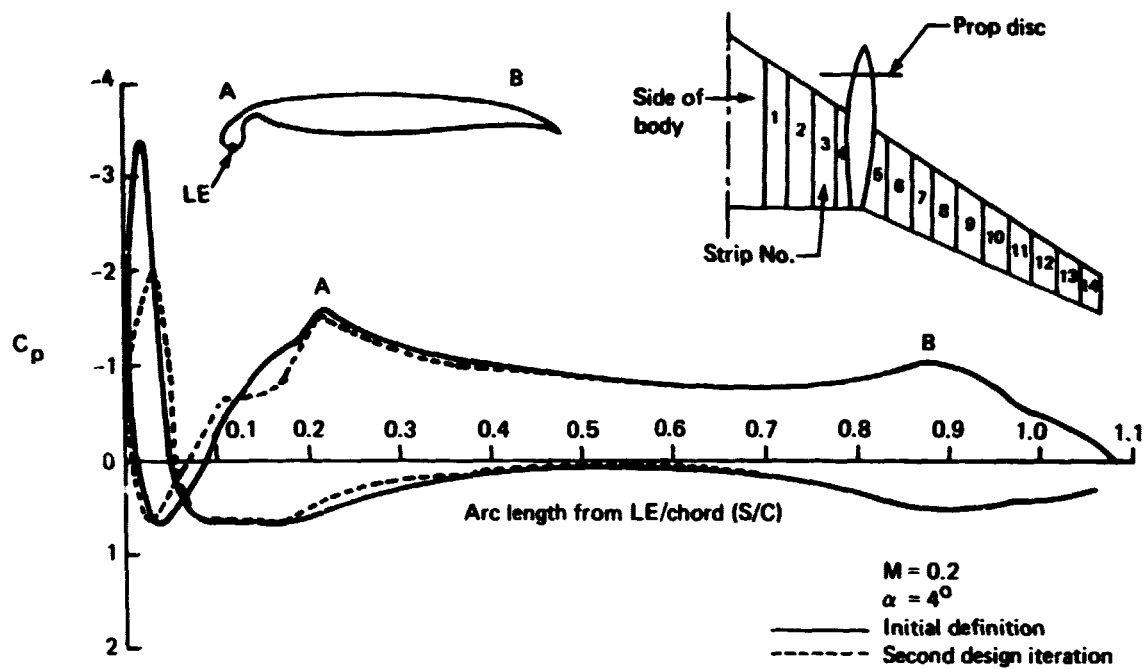


Figure 36. Low-Speed Wing Pressure Profiles: Strip 3

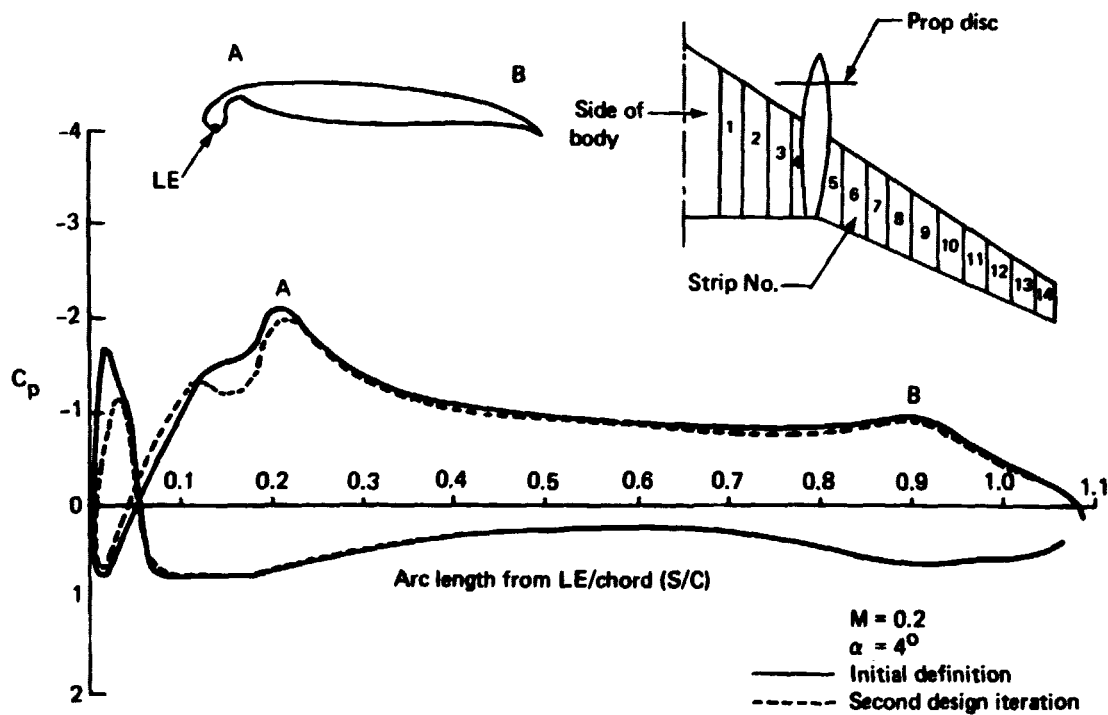


Figure 37. Low-Speed Wing Pressure Profiles: Strip 6

6.3 SLIPSTREAM CHARACTERISTICS

Radial distribution of total pressure ratio and swirl angle aft of the propeller for the cruise and takeoff conditions are given in Figure 38. The takeoff data at Mach 0.2 were obtained by Hamilton Standard through wind tunnel testing. Swirl angles of about 9 degrees are predicted, compared to 6 degrees at cruise. The incremental axial velocity ($\Delta V_x/U_\infty$) corresponding to the above data (calculated by the method described in sec. 5.0) is presented in Figure 39. These increments are very large during takeoff and have a significant impact on the wing aerodynamic characteristics.

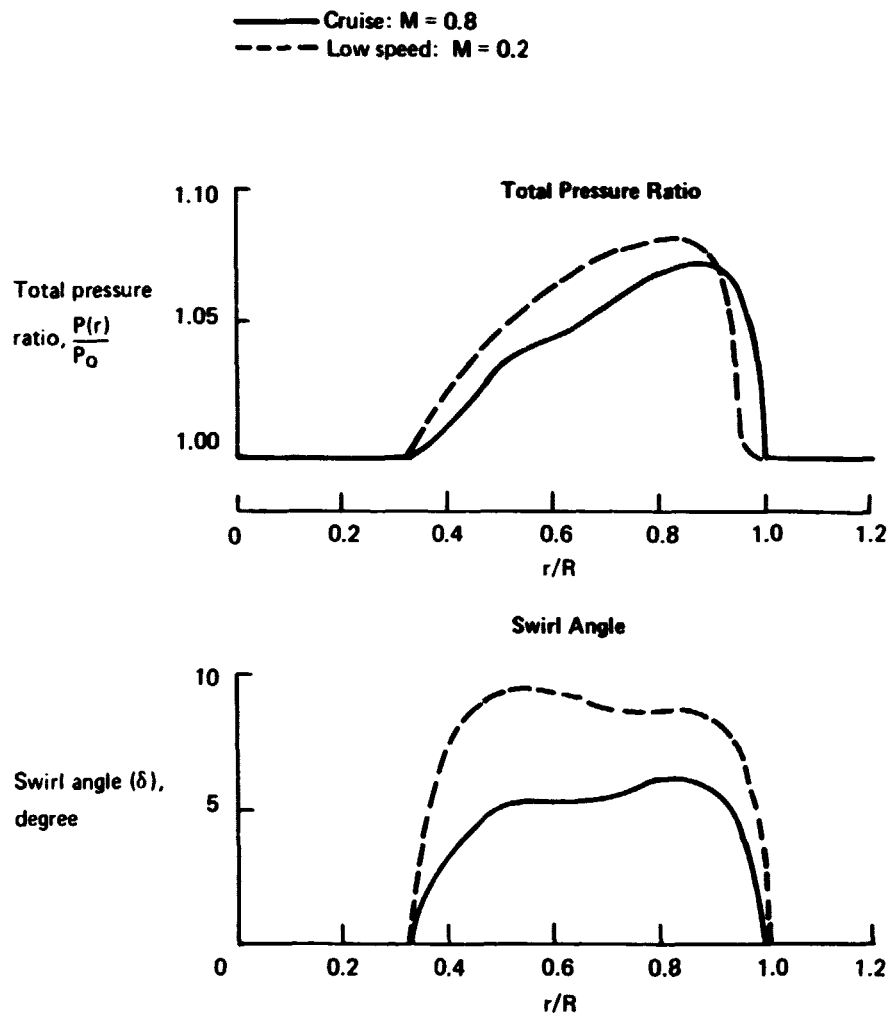


Figure 38. Radial Distribution of Swirl and Total Pressure in Prop Slipstream

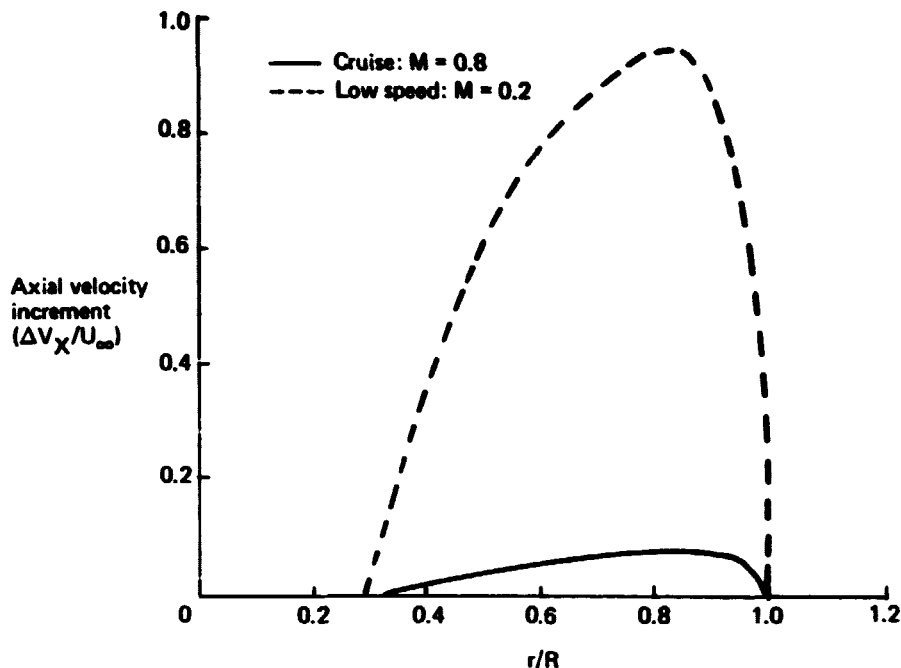


Figure 39. Radial Distribution of Axial Velocity Increment in Prop Slipstream

6.4 PRESSURE COEFFICIENT DATA

Pressure profiles for strips 3 through 6 at $\alpha = 4^\circ$, showing the effect of the propeller slipstream, are given in Figures 40 through 43. On the inboard side of the nacelle, the swirl angles and the increments in axial velocity have additive effects, resulting in high loading of the local wing sections. On the outboard side, these effects are subtractive with the axial velocity slightly more predominant. The net effect is an increase in load on the outboard, as well as the inboard wing. The effect of the slipstream on the wing as a whole is discussed further below.

6.5 FORCE DATA

The lift curve for the low-speed configuration is shown in Figure 44. At $\alpha = 4^\circ$, the effect of the slipstream is to increase C_L from 1.328 to 1.610, a 21% increase. Preliminary design estimates in Reference 1 give a climbout C_L value of 1.63 with a trailing-edge flap setting of 10° .

Figure 45 shows the effect of the slipstream on the wing-span load distribution. Local increases in the wing loading on both sides of the nacelle correspond to the pressure profiles of Figures 40 through 43.

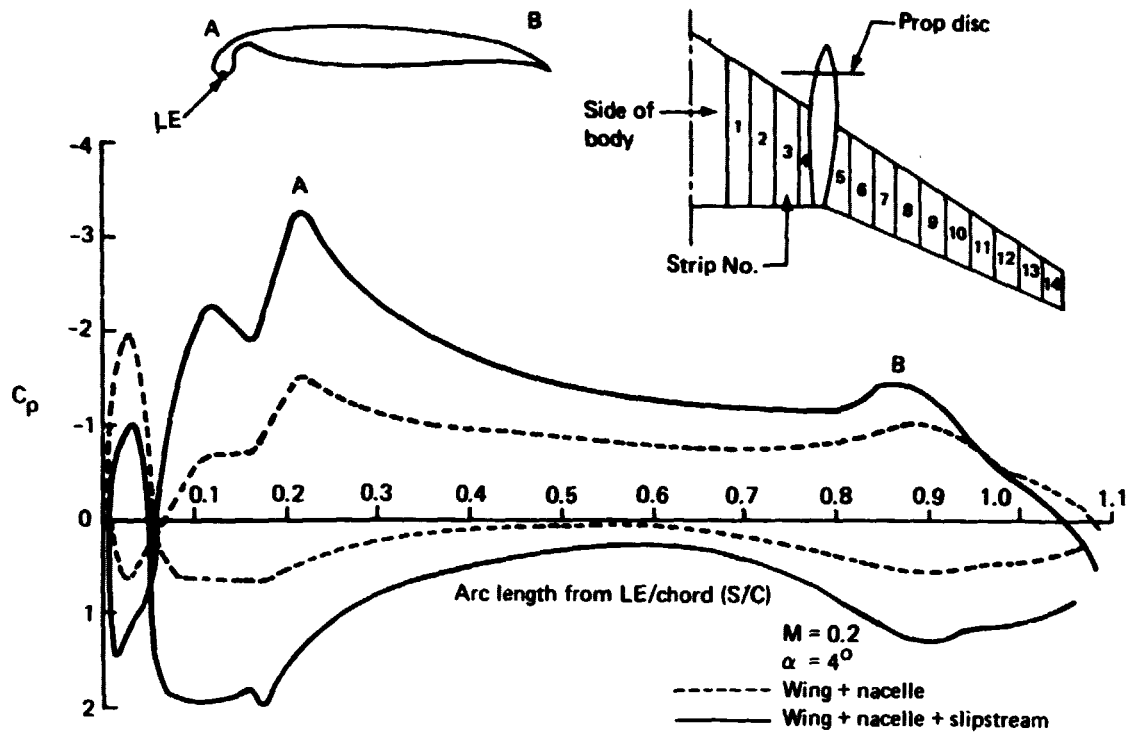


Figure 40. Low-Speed Wing Pressure Profiles with Slipstream: Strip 3

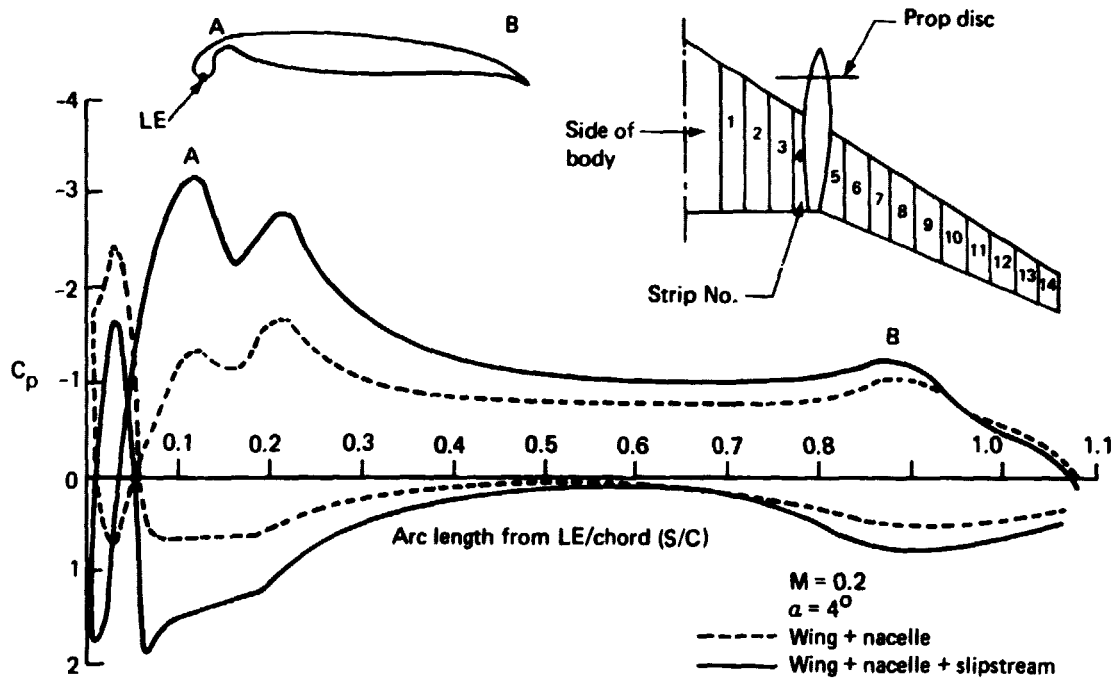


Figure 41. Low-Speed Wing Pressure Profiles with Slipstream: Strip 4

ORIGINAL PAGE IS
OF POOR QUALITY

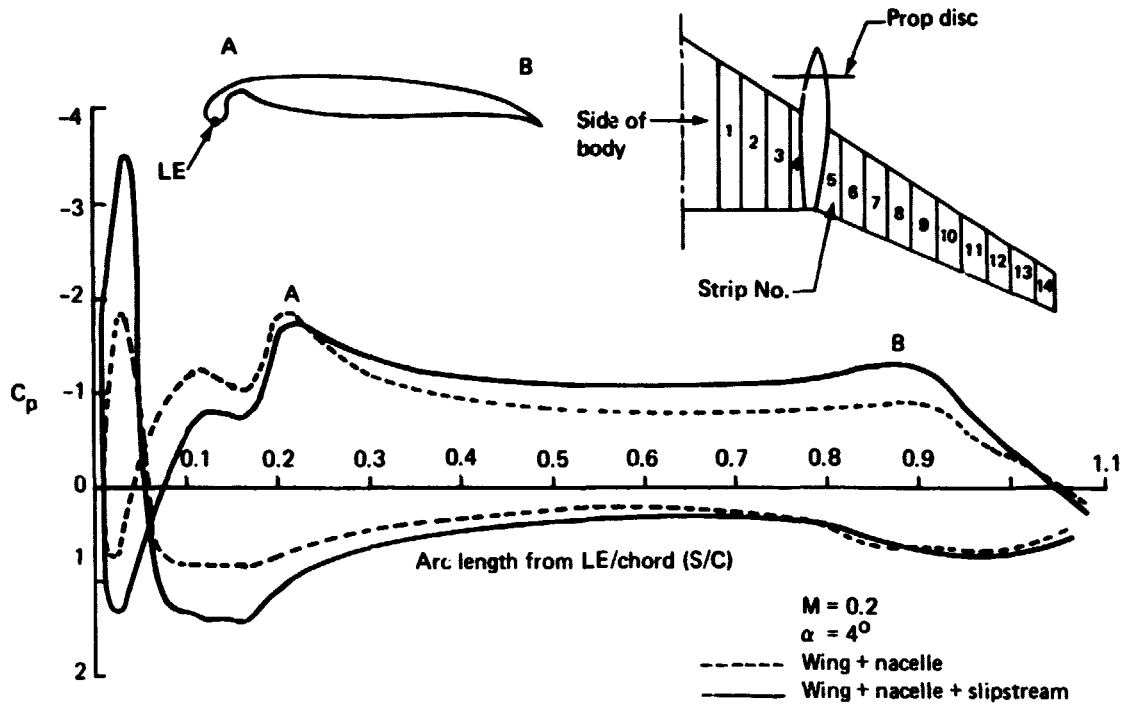


Figure 42. Low-Speed Wing Pressure Profiles with Slipstream: Strip 5

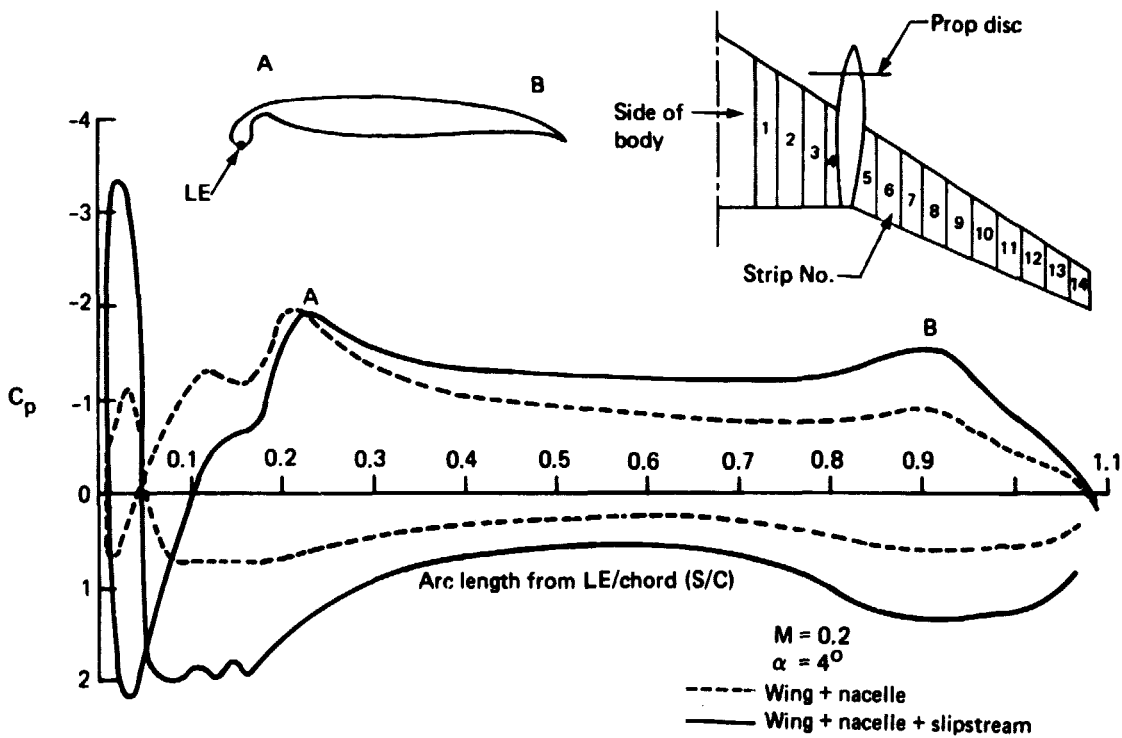


Figure 43. Low-Speed Wing Pressure Profiles with Slipstream: Strip 6

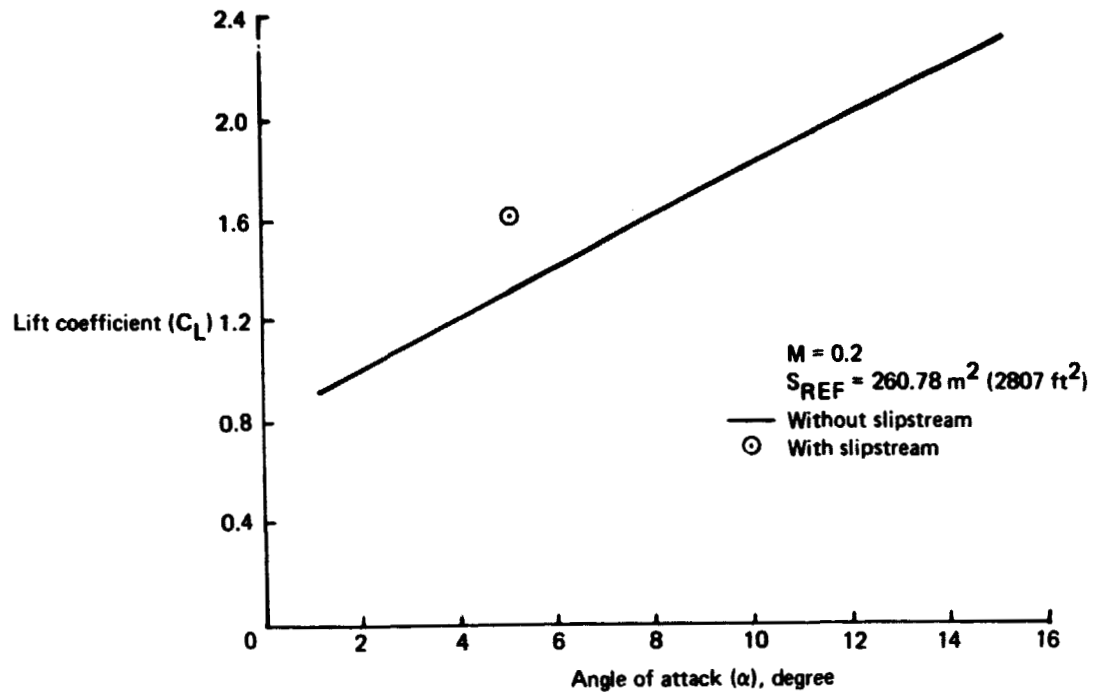


Figure 44. Krueger Wing—Low-Speed Configuration Lift Curve

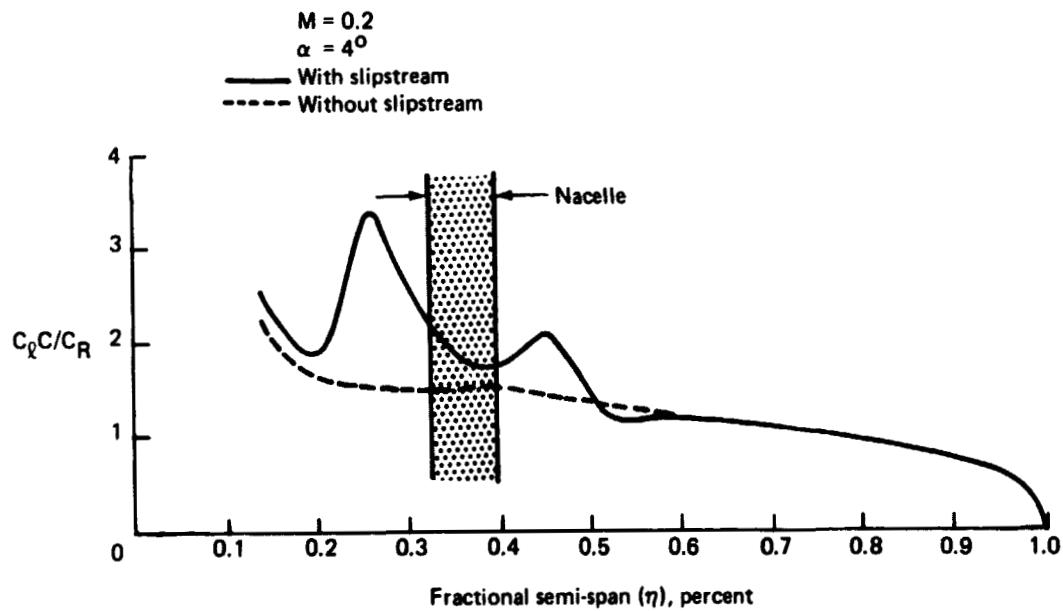


Figure 45. Krueger Wing—Low-Speed Configuration Spanwise Load Distribution

6.6 DRAG AND THRUST RECOVERY

Induced drag of the wing/body/nacelle configuration, calculated from the span load distribution of Figure 45, is shown in Figure 46. The effect of the slipstream (shown in fig. 46) was calculated as an increment in the integrated surface pressures over the configuration. This vector is largely composed of a C_L increment ($\Delta C_L = 0.282$) with 36 counts of drag reduction, which contributes to thrust recovery. If, however, the effect of the slipstream is to be considered at constant C_L , the thrust recovery could be as high as 350 counts, depending on the general shape of the polar.

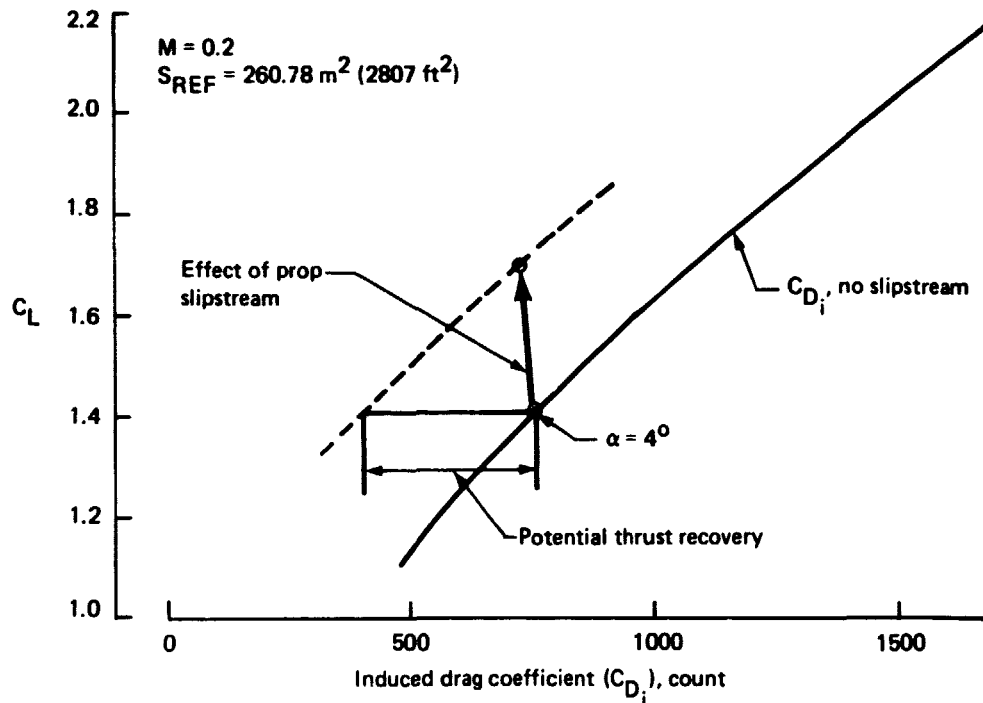


Figure 46. Krueger Wing—Low-Speed Configuration Induced Drag Due to Slipstream

6.7 EFFECT OF ONE-ENGINE FAILURE

In the case of a one-engine failure, the aerodynamic forces and moments attributed to the slipstream will act only on one side of the airplane, creating a general aerodynamic imbalance that must be trimmed.

Figure 47 depicts the rolling moment C_{MX} as a function of C_L for only one-half of the configuration. The effect of the slipstream, calculated by integration of the surface pressures, is shown on the figure as a vector composed of:

$$\begin{aligned}\Delta C_L &= 0.141 \\ \Delta C_{MX} &= 0.018\end{aligned}$$

This represents the engine-out increment of the prop-fan over the turbofan. It is substantially smaller than preliminary estimates for the Reference 1 study, as indicated in Figure 48.

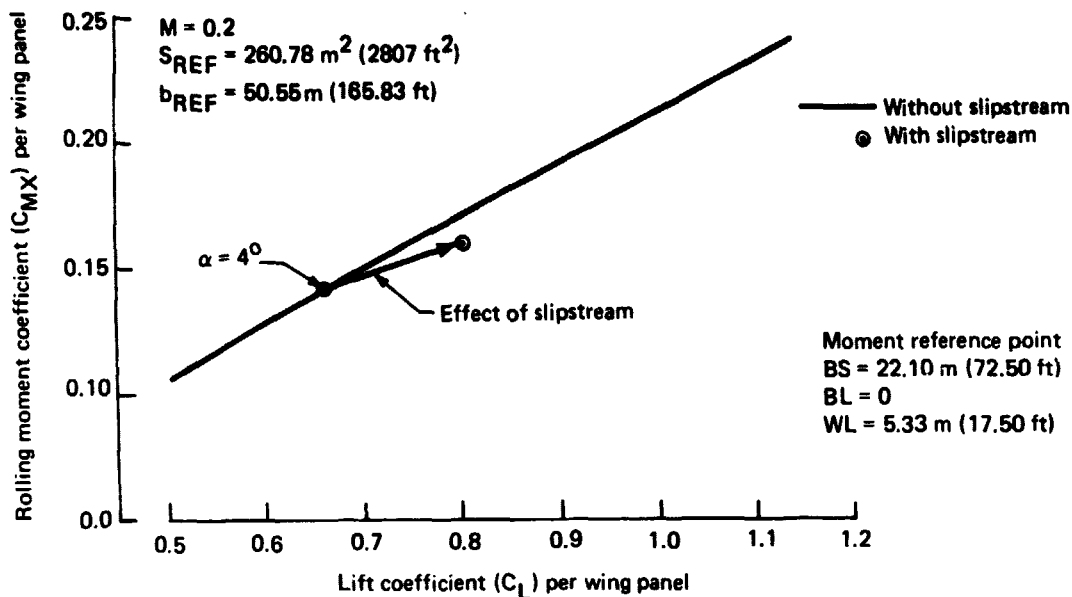


Figure 47. Krueger Wing—Low-Speed Configuration Rolling Moment Coefficient

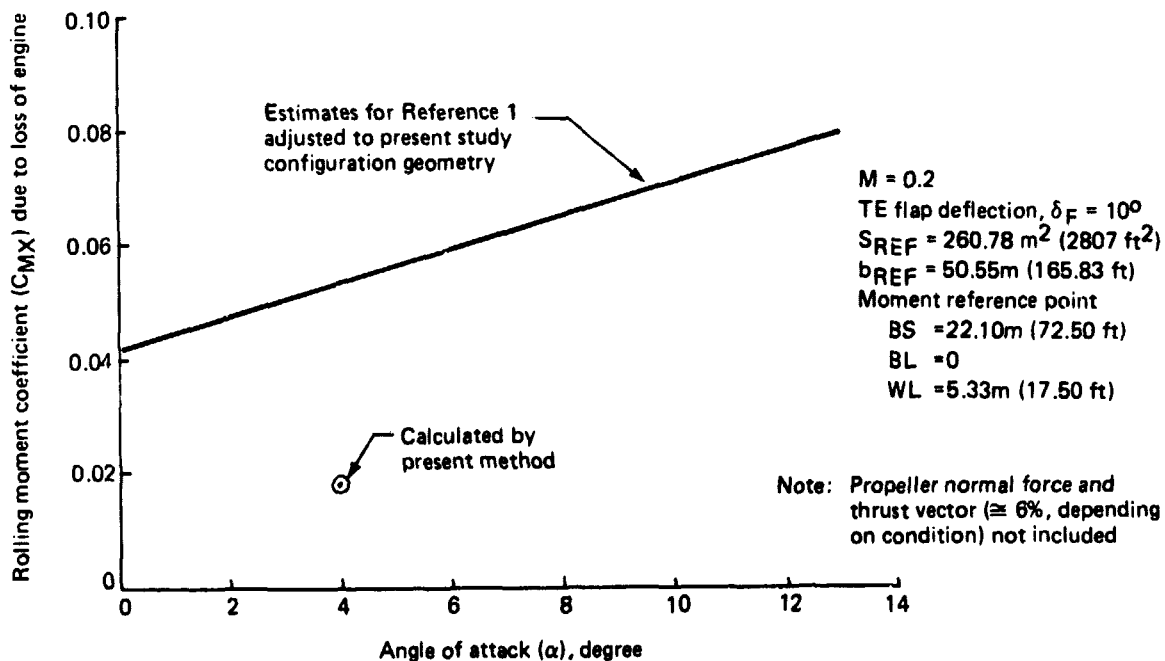


Figure 48. Rolling Moment Due to Engine-Out Comparison with Preliminary Estimates

6.8 ASSESSMENT

Leading- and trailing-edge flaps were defined for the modified cruise wing, and are suitable for both landing and takeoff. The flap definition was intended for potential flow analysis only, and would normally undergo extensive tailoring prior to hardware application. The analysis showed the nature and extent of the problems associated with the wing-slipstream interaction during takeoff; landing approach problems would be similar but less severe. Based upon the calculated data, the following observations were made:

- Leading-edge Krueger flaps had more than enough deflection (δ_K) to eliminate all pressure peaks on the upper surface. The extra margin in δ_K ensures safe operation at CL_{MAX} . For maximum L/D during climb, the Krueger flap should be partially retracted.
- Unlike the high-speed condition, the axial velocity increment, rather than the swirl, dominates the slipstream effect at the takeoff condition. As a consequence, the portions of the wing scrubbed by the slipstream experience large, local increases in loading.
- An engine failure at takeoff results in an asymmetric loading that appears to be well within the trim capabilities of the lateral control system for this type of airplane.

7.0 AFT-MOUNTED PROP-FAN

7.1 CONFIGURATION AND FLIGHT CONDITIONS

Paneling of the aft-mounted prop-fan configuration is shown in Figures 49 and 50. The wing was moved aft for longitudinal stability and was represented by a single vortex panel network placed over its mean surface. Accordingly, wing thickness effects were ignored in calculating the flow over the aft-body assembly and the body was partially coke-bottled in the vicinity of the empennage for improved area distribution. The vertical tail and the strut have symmetrical profiles of 12 and 10.5% thick, respectively. The strut plane of symmetry has 2.6° of pitch and 19° of dihedral and the horizontal tail has a cambered, 10.5 percent thick section.

The longitudinal, cross sectional area distribution along the aft body stations has a direct bearing on the local pressure. Figure 51 shows a buildup of the cross sectional area in that region. Maximum area occurs at body station 1640 and generally corresponds to the location of minimum body pressure in Figure 52. Smoothing the cross sectional area distribution could greatly improve the flow field in the body-nacelle channel but is not readily feasible. For example, additional necking of the body is limited by structural considerations. Moving the strut-nacelle assembly forward could require large increases in body noise attenuation provisions. It should be noted that the area profile of Figure 51 is typical of T-tail, aft-mounted engine arrangements and is not necessarily objectionable or undesirable.

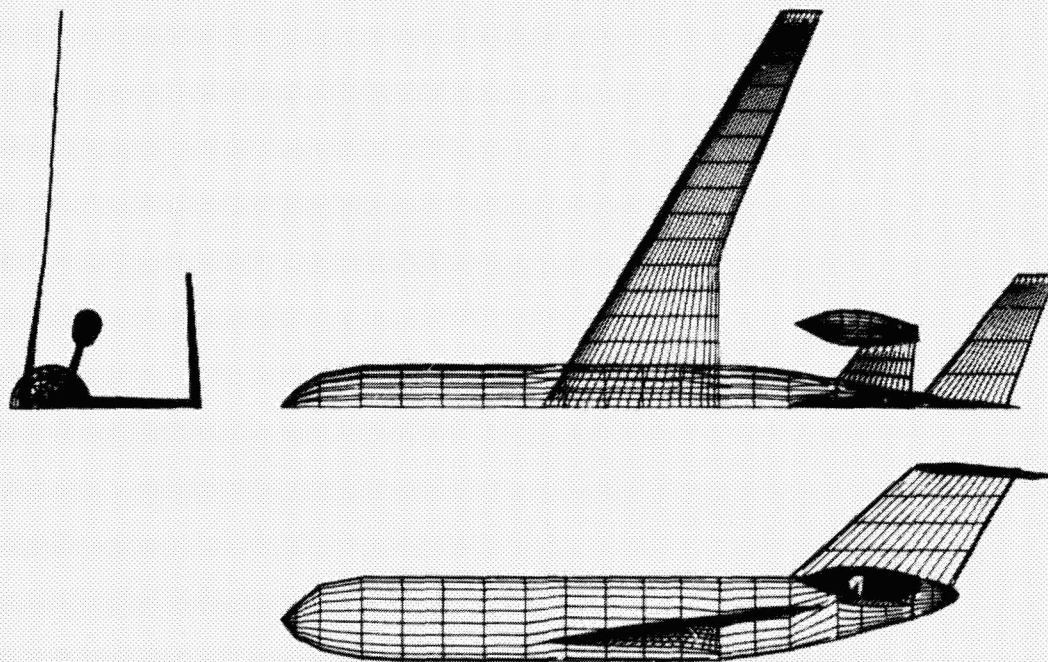


Figure 49. Paneling of Aft-Mounted Prop-Fan

ORIGINAL PAGE IS
OF POOR QUALITY

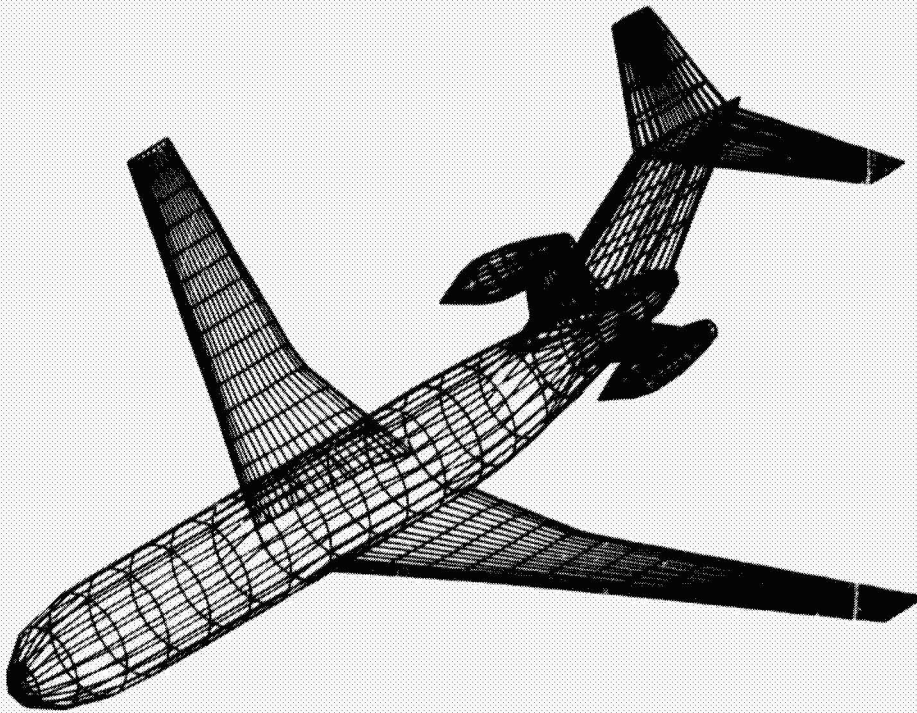


Figure 50. Aft-Mounted Prop-Fan Isometric Projection

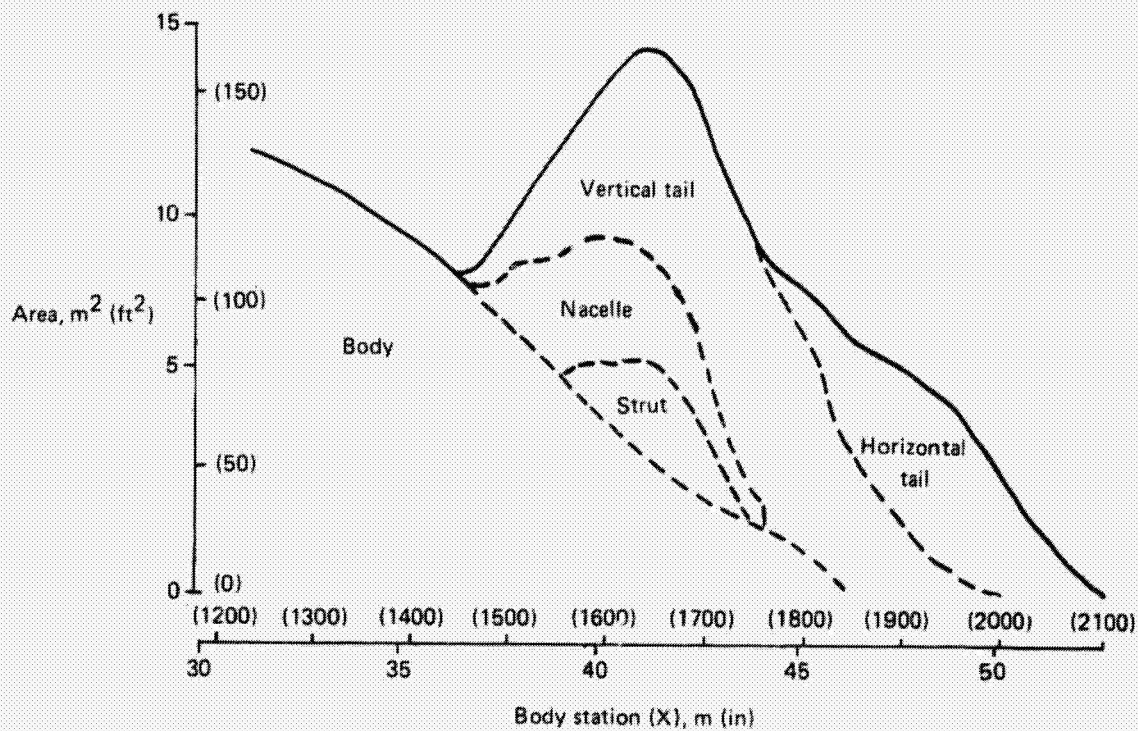


Figure 51. Aft-Mounted Prop-Fan Cross Sectional Area Distribution

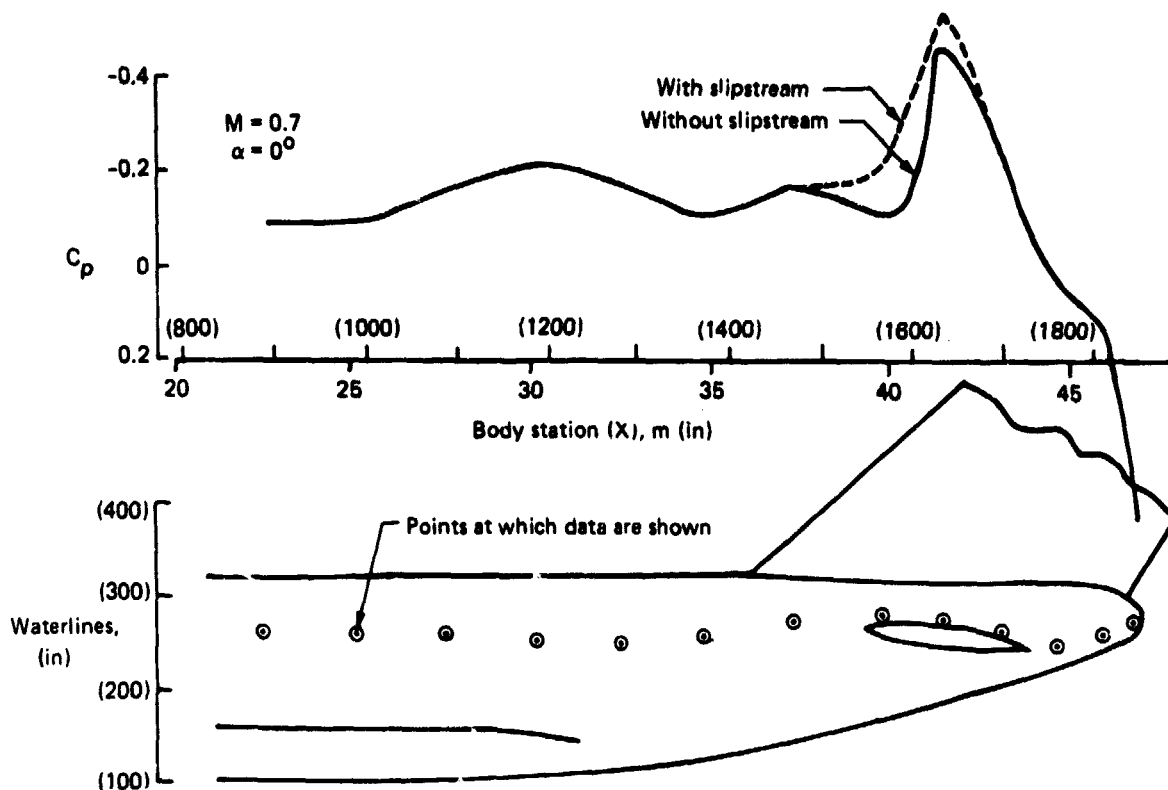


Figure 52. Aft-Mounted Prop-Fan Side-of-Body Pressure Profile

The configuration was analyzed on potential flow program A 230 at Mach 0.7 and angles-of-attack of -2 to 5°.

7.2 SLIPSTREAM CHARACTERISTICS

Radial distribution of swirl angle and total pressure ratio aft of the propeller corresponds to the cruise condition defined in Figure 13 for the wing-mounted prop-fan. Only the strut, in the present case, is washed by the propeller slipstream. However, the effect of the slipstream extends to the body and the vertical tail because of its impact on the channel cross sectional area distribution.

7.3 PRESSURE DISTRIBUTION AND SPAN LOADING

The pressure distribution along the side of the body is shown in Figure 52. The pressure is most critical at about 50% chord of the strut-body intersection on the upper side of the strut. This condition is further aggravated by the propeller slipstream, in spite of the fact

that the latter does not impinge on the body. From the point of minimum pressure, the pressure recovery occurs over a relatively short distance, increasing the danger of separation over the tail end of the body and possibly increasing drag by one or two counts.

Strut pressure profiles showing the effect of the slipstream are presented in Figures 53 through 55. In the absence of the slipstream, the strut is influenced by the downwash from the wing and suction peaks are in evidence on its lower surface. The chordwise load distribution exhibits two loops of opposite signs that integrate to produce a strut C_L close to zero. The propeller slipstream produces a strong upwash counteracting the downwash from the wing and it causes a collapse of the negative pressure loop on the strut leading edge, generally increasing the total load on the strut. This effect is particularly pronounced on strip 2 because, as shown in the figure inserts, strip 3 is close to the axis of the propeller and strip 1 is out of its range. Vertical-tail pressure profiles are presented in Figures 56 through 59 and show that the influence of the propeller slipstream clearly extends to the vertical tail and that this effect is more pronounced on the lower parts of the vertical tail and diminishes toward the tip.

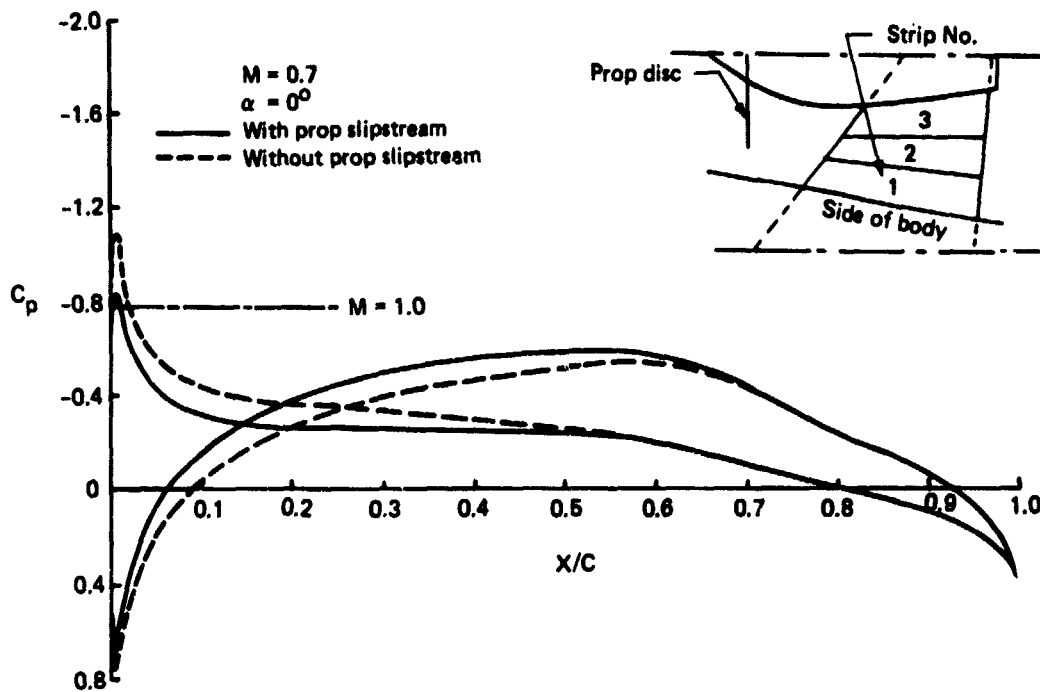


Figure 53. Aft-Mounted Prop-Fan Strut Pressure Profiles: Strip 1

ORIGINAL PAGE IS
OF POOR QUALITY

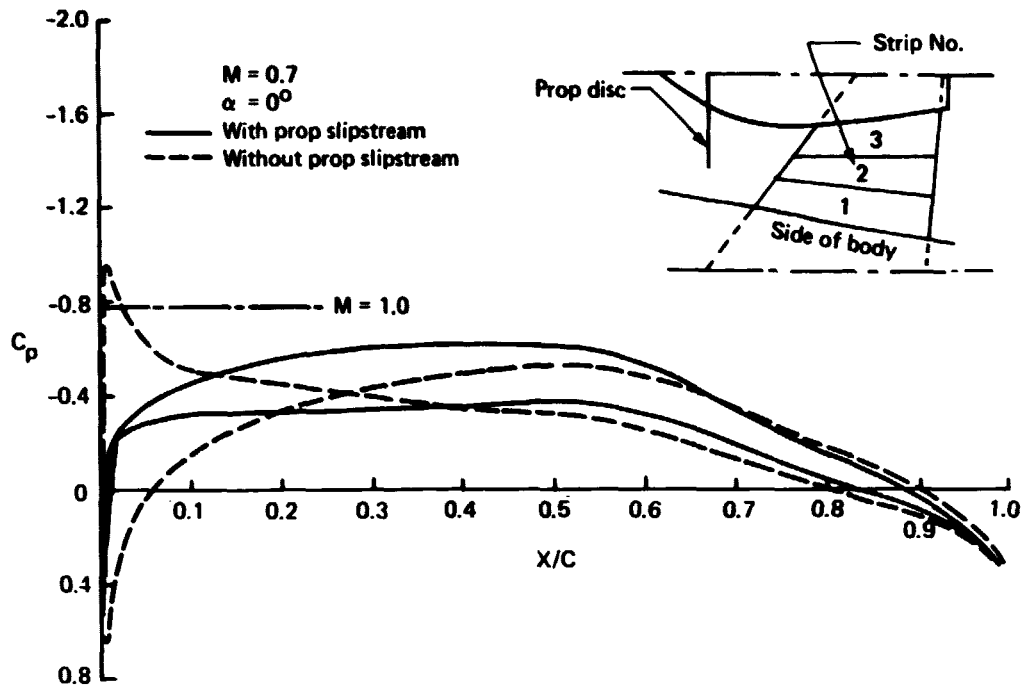


Figure 54. Aft-Mounted Prop-Fan Strut Pressure Profiles: Strip 2

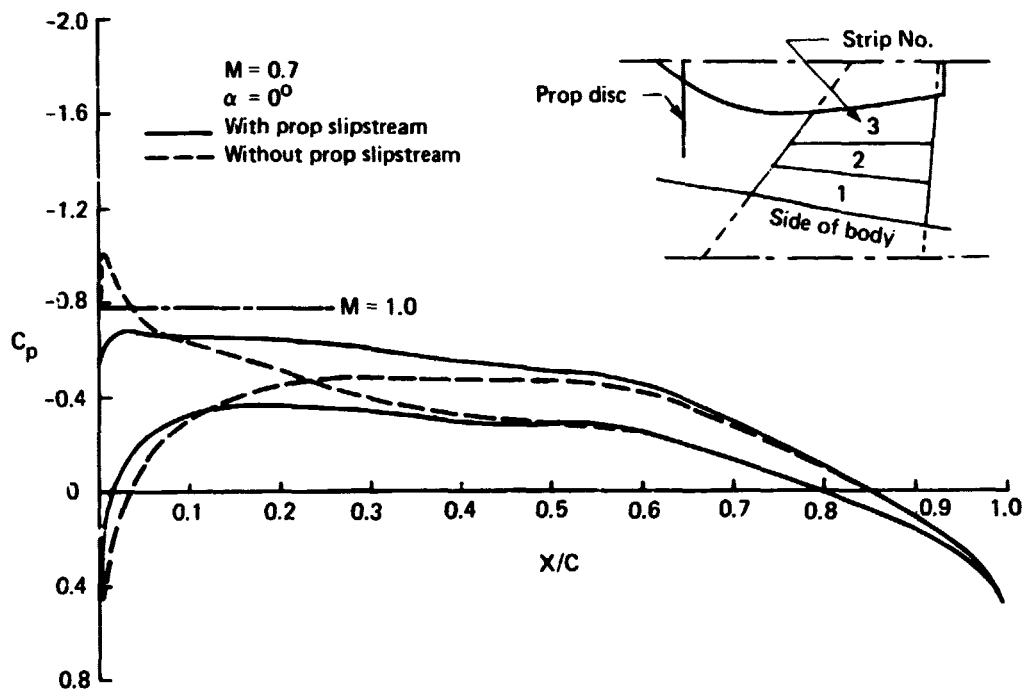


Figure 55. Aft-Mounted Prop-Fan Strut Pressure Profiles: Strip 3

ORIGINAL PAGE IS
OF POOR QUALITY

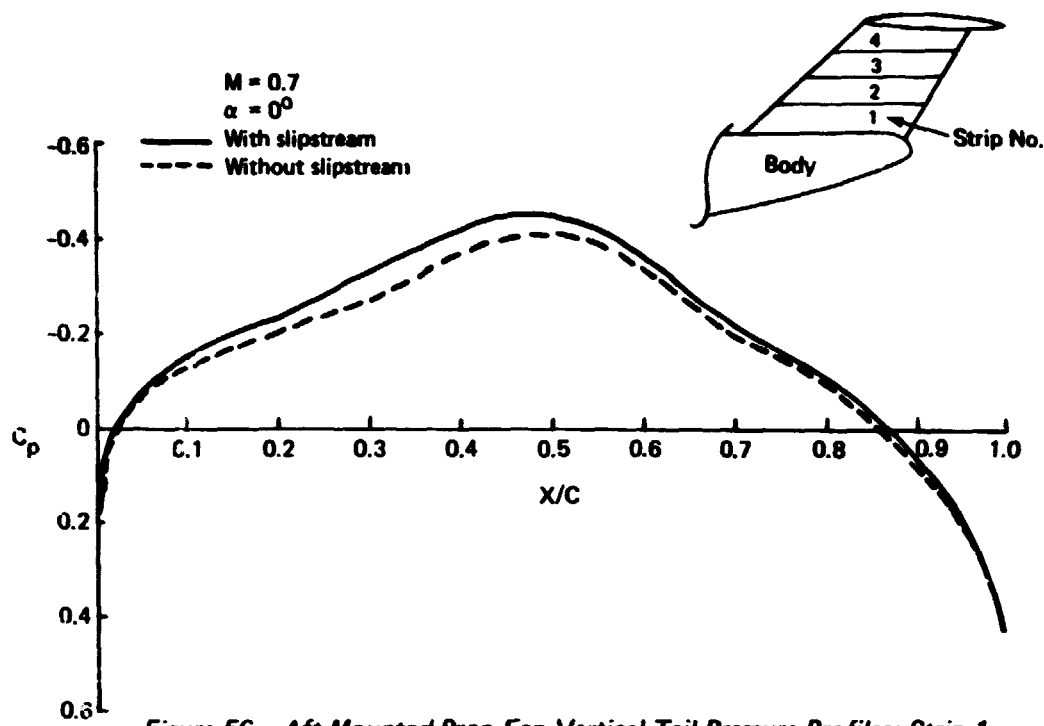


Figure 56. Aft-Mounted Prop-Fan Vertical Tail Pressure Profiles: Strip 1

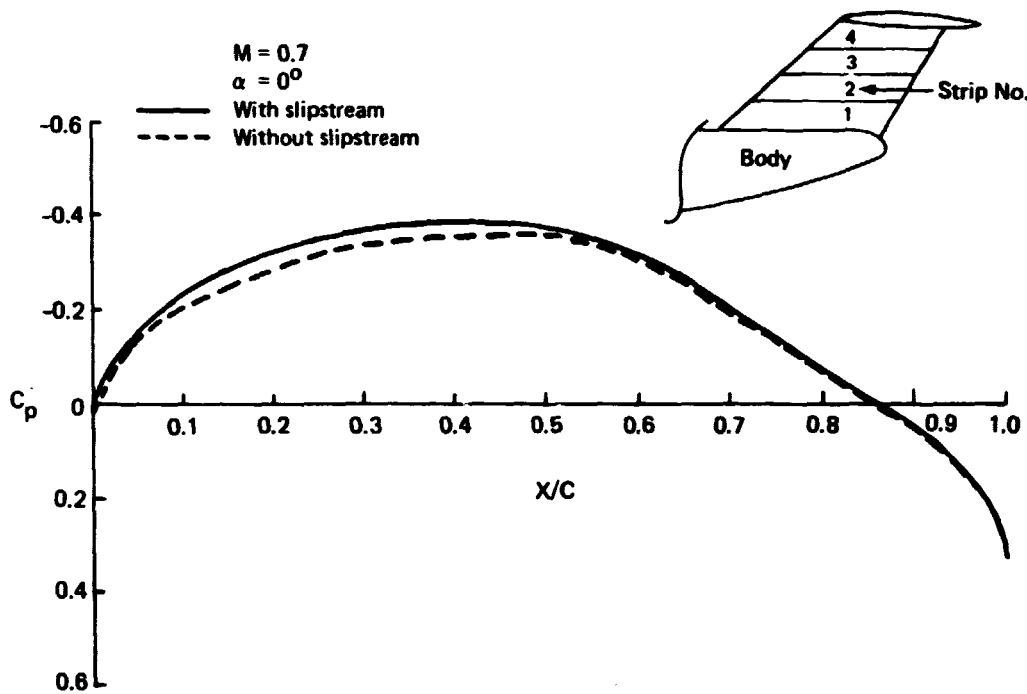


Figure 57. Aft-Mounted Prop-Fan Vertical Tail Pressure Profiles: Strip 2

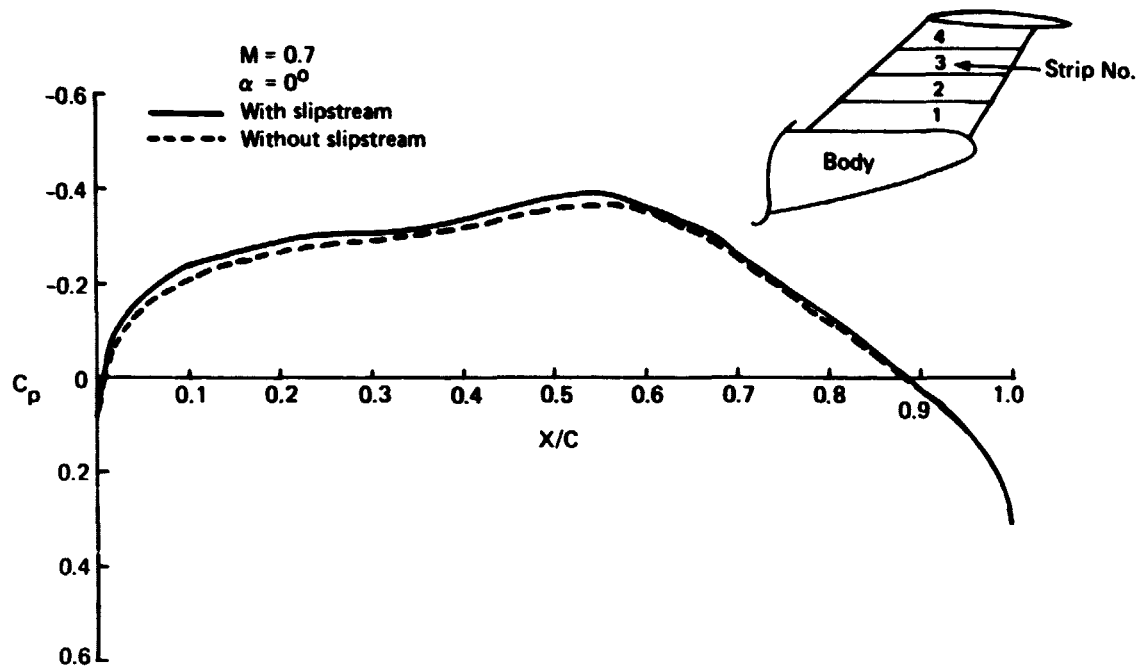


Figure 58. Aft-Mounted Prop-Fan Vertical Tail Pressure Profiles: Strip 3

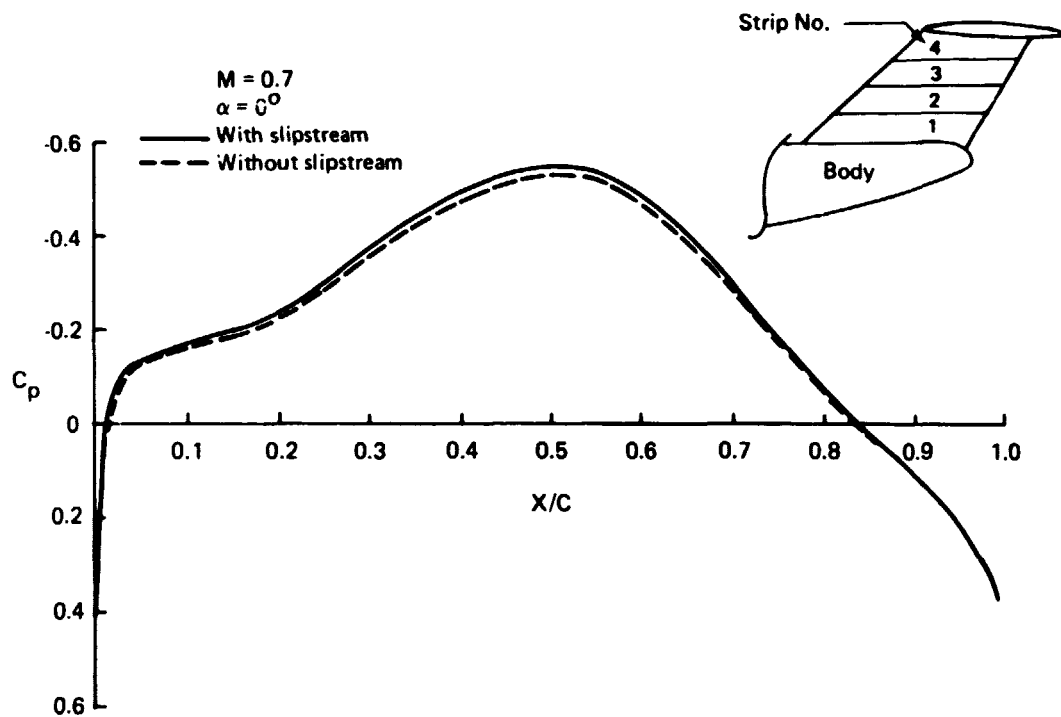


Figure 59. Aft-Mounted Prop-Fan Vertical Tail Pressure Profiles: Strip 4

Figure 60, strut spanwise load distribution, shows that the propeller slipstream clearly increases the upward load on the strut, which, to some extent, contributes to thrust recovery. This force, however, is very small due to the limited strut area. Because loading the strut serves no useful purpose, the strut could be twisted and pitched down to uniformly eliminate the span load in the presence of the slipstream. The load increment of the slipstream would probably remain unaffected as would the thrust recovery and the strut drag would be reduced.

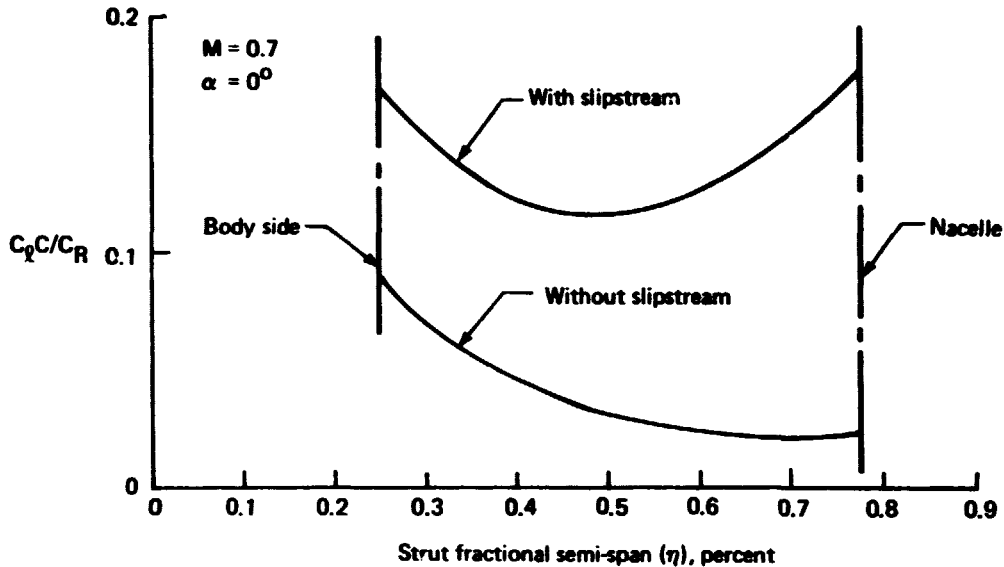


Figure 60. Aft-Mounted Prop-Fan Effect of Slipstream on Strut Loading

7.4 DRAG AND THRUST RECOVERY

Figure 61 shows a plot of induced drag of the clean wing versus C_L . The lift and drag increments due to the slipstream were calculated by integration of the surface pressures and are shown as a thrust recovery vector. Computed at $\alpha = 0^\circ$, this vector is

$$\begin{aligned}\Delta C_L &= 0.017 \\ \Delta C_D &= 0.8 \text{ drag counts.}\end{aligned}$$

Considered at constant C_L , an equivalent three counts of drag reduction could be interpreted as thrust recovery. However, the uncertainties in the above calculations are sufficient to offset any gain attributed to thrust recovery.

ORIGINAL PAGE 18
OF POOR QUALITY

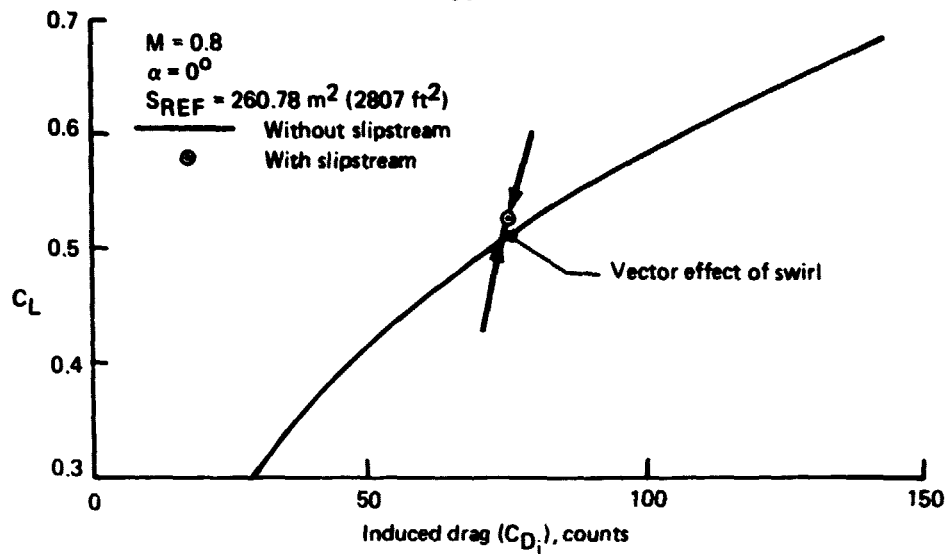


Figure 51. Aft-Mounted Prop-Fan Effect of Slipstream on Induced Drag

7.5 ASSESSMENT

In the absence of the wing-slipstream interference problem, there is little aerodynamic difference between the aft-mounted prop-fan and an equivalent turbofan configuration. Therefore, only airplane size and power plant characteristics for a given mission determine the difference in operating economics between the two airplanes.

The aft-mounted prop-fan requires relatively long struts for the propeller to clear the side of the body, so a higher incentive exists to optimize these struts for minimum drag and maximum thrust recovery. The present analysis shows the type and extent of strut loading caused by the prop slipstream and the interference effects between the various components involved. Proper loading of the strut and careful contouring of its leading edge should enhance thrust recovery without incurring drag penalties.

8.0 REFERENCES

1. *Energy Consumption Characteristics of Transports Using the Prop-Fan Concept.* NASA CR-137937, October 1976.
2. Rubbert, P.E. et al.; *A General Method for Determining the Aerodynamic Characteristics of Fan-in-Wing Configurations.* Technical Report 67-61A, USAAVLABS, 1967.
3. Geller, E.W. and Bailey, D.C.; *TEA 236, Subsonic Wing Design and Analysis Program.* Boeing Document D6-29337, 1968.
4. Rohrback, Carl; *A Report on the Aerodynamic Design and Wind Tunnel Test of a Prop-Fan Model.* AIAA Paper No. 76-667, July 1976.
5. Lundry, J.L.; *The Calculation of Lift and Induced Drag from a Curve-Fitting of Sparse Span Loading Points.* Boeing Document D6-40274 TN, August 1972.

APPENDIX A

BASELINE AND MODIFIED WING GEOMETRY

Definitions of the baseline and modified cruise wing are given in the following pages. Figure A-1 gives the planform definition which is common to both wings. The wing has the following reference quantities:

| | |
|---|------------------|
| Area, m ² (ft ²) | 260.8 (2807) |
| Aspect ratio | 10 |
| Taper ratio | 0.353 |
| C/4 sweep, deg | 30 |
| MAC, m (in) | 5.496 (216.37) |
| Span, m (in) | 51.066 (2010.49) |

Each of the two wings is defined at 16 wing buttock lines, including one on each side of the nacelle.

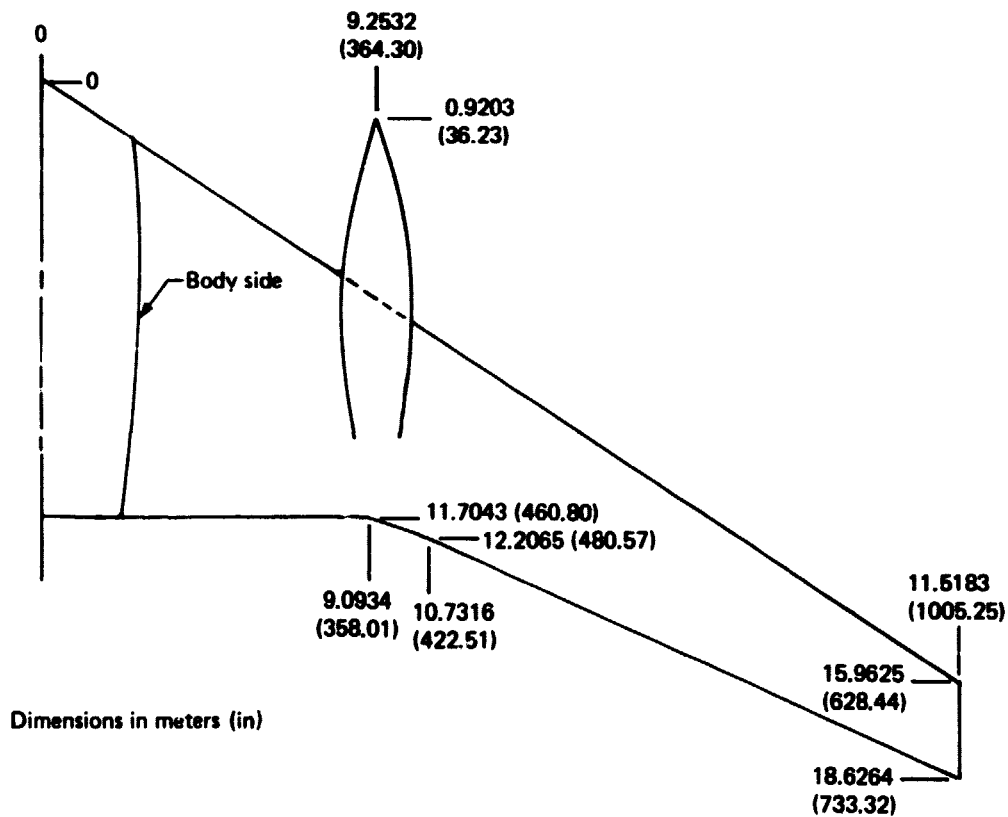


Figure A-1. Wing Planform Dimensions

ORIGINAL PAGE IS
OF POOR QUALITY

MBL: 2.7686 m (9.0833 FT)

$\eta = .1084$

(DIMENSIONS IN METERS)

| BASELINE WING | | MODIFIED WING | |
|---------------|----------|---------------|----------|
| X | Z | X | Z |
| 25,714227 | 3,057153 | 25,714227 | 3,052120 |
| 25,469491 | 3,900314 | 25,470089 | 3,099553 |
| 25,095443 | 3,960513 | 25,090084 | 3,070905 |
| 24,701952 | 4,059131 | 24,702130 | 4,040007 |
| 24,113495 | 4,177093 | 24,113693 | 4,100154 |
| 23,525058 | 4,293674 | 23,525259 | 4,271840 |
| 22,940012 | 4,400042 | 22,940711 | 4,373733 |
| 22,353173 | 4,490513 | 22,353273 | 4,408338 |
| 21,764725 | 4,580399 | 21,764824 | 4,552925 |
| 21,181249 | 4,666473 | 21,181388 | 4,629994 |
| 20,590856 | 4,734540 | 20,590957 | 4,695820 |
| 20,004418 | 4,791420 | 20,004517 | 4,751019 |
| 19,415981 | 4,836274 | 19,416080 | 4,794746 |
| 18,837519 | 4,866080 | 18,837618 | 4,824557 |
| 18,234110 | 4,878393 | 18,239209 | 4,836151 |
| 17,740434 | 4,870072 | 17,740432 | 4,832204 |
| 17,241761 | 4,839530 | 17,241756 | 4,805365 |
| 16,910540 | 4,809508 | 16,910538 | 4,776215 |
| 16,615623 | 4,772312 | 16,615621 | 4,744049 |
| 16,354007 | 4,728383 | 16,359005 | 4,703003 |
| 16,134988 | 4,677306 | 16,134985 | 4,654769 |
| 15,961662 | 4,598637 | 15,961660 | 4,579422 |
| 15,832206 | 4,498833 | 15,832206 | 4,482493 |
| 15,754501 | 4,364234 | 15,759499 | 4,357342 |
| 15,745737 | 4,267303 | 15,728649 | 4,241906 |
| 15,754501 | 4,170402 | 15,784946 | 4,154094 |
| 15,832206 | 4,061628 | 15,836743 | 4,063622 |
| 15,961662 | 3,951200 | 15,961660 | 3,955436 |
| 16,134988 | 3,837074 | 16,134985 | 3,844160 |
| 16,354007 | 3,754727 | 16,354005 | 3,763510 |
| 16,615623 | 3,679629 | 16,615623 | 3,689642 |
| 16,910540 | 3,609868 | 16,910540 | 3,621156 |
| 17,241761 | 3,548555 | 17,241759 | 3,561113 |
| 17,740434 | 3,482340 | 17,740432 | 3,496236 |
| 18,234110 | 3,445673 | 18,234207 | 3,460270 |
| 18,437519 | 3,421878 | 18,837618 | 3,436483 |
| 19,415981 | 3,413376 | 19,416080 | 3,427500 |
| 20,004418 | 3,424362 | 20,004517 | 3,437537 |
| 20,590856 | 3,450429 | 20,590957 | 3,464364 |
| 21,181289 | 3,517024 | 21,181388 | 3,527263 |
| 21,764725 | 3,600455 | 21,764824 | 3,604172 |
| 22,353173 | 3,691481 | 22,353273 | 3,694281 |
| 22,940012 | 3,775761 | 22,940711 | 3,781529 |
| 23,525058 | 3,846124 | 23,525259 | 3,844435 |
| 24,113495 | 3,977739 | 24,113696 | 3,880550 |
| 24,701932 | 3,845192 | 24,702130 | 3,800060 |
| 25,0945863 | 3,866794 | 25,090084 | 3,865806 |
| 25,469491 | 3,831847 | 25,470089 | 3,826369 |
| 25,714227 | 3,797417 | 25,714227 | 3,792083 |

ORIGINAL PAGE IS
OF POOR QUALITY

WBL: 4.1786 m (13.7092 FT)

$\eta = .1637$

(DIMENSIONS IN METERS)

| BASELINE WING | | MODIFIED WING | |
|---------------|----------|---------------|----------|
| X | Z | X | Z |
| 25,714227 | 4,046922 | 25,714227 | 4,046922 |
| 25,441926 | 4,144831 | 25,441926 | 4,144831 |
| 25,150475 | 4,214737 | 25,151156 | 4,205046 |
| 24,791839 | 4,287256 | 24,792021 | 4,284871 |
| 24,255409 | 4,393529 | 24,255541 | 4,396644 |
| 23,718479 | 4,495018 | 23,714160 | 4,503843 |
| 23,186186 | 4,568094 | 23,186276 | 4,594264 |
| 22,650604 | 4,672040 | 22,650755 | 4,655564 |
| 22,118760 | 4,746030 | 22,118670 | 4,760730 |
| 21,582350 | 4,812642 | 21,582440 | 4,827375 |
| 21,044101 | 4,868466 | 21,044191 | 4,862461 |
| 20,504490 | 4,914326 | 20,504574 | 4,926796 |
| 19,973059 | 4,949525 | 19,973149 | 4,959727 |
| 19,445721 | 4,971574 | 19,445610 | 4,976775 |
| 18,900149 | 4,976265 | 18,900268 | 4,961757 |
| 18,445547 | 4,967814 | 18,445595 | 4,967492 |
| 17,940995 | 4,934235 | 17,940493 | 4,935047 |
| 17,689648 | 4,904843 | 17,689406 | 4,904411 |
| 17,420197 | 4,875165 | 17,420195 | 4,866952 |
| 17,186259 | 4,834555 | 17,186256 | 4,824311 |
| 16,980547 | 4,787566 | 16,980595 | 4,782205 |
| 16,824032 | 4,717243 | 16,824030 | 4,714651 |
| 16,700017 | 4,626593 | 16,700015 | 4,624645 |
| 16,634736 | 4,513546 | 16,634734 | 4,519141 |
| 16,627189 | 4,423656 | 16,627187 | 4,437040 |
| 16,634736 | 4,332276 | 16,634734 | 4,356769 |
| 16,700017 | 4,239877 | 16,700015 | 4,265104 |
| 16,824032 | 4,142467 | 16,824030 | 4,172775 |
| 16,980547 | 4,045156 | 16,980545 | 4,074227 |
| 17,186259 | 3,947347 | 17,186256 | 4,004864 |
| 17,420197 | 3,849924 | 17,420195 | 3,943974 |
| 17,689648 | 3,748030 | 17,689646 | 3,882575 |
| 17,940995 | 3,642214 | 17,940993 | 3,827332 |
| 18,445547 | 3,534322 | 18,445545 | 3,765547 |
| 18,940995 | 3,427049 | 18,940993 | 3,727624 |
| 19,445547 | 3,318326 | 19,445545 | 3,694664 |
| 19,973059 | 3,209447 | 19,973057 | 3,665660 |
| 20,504490 | 3,099600 | 20,504489 | 3,641151 |
| 21,044101 | 3,078625 | 21,044141 | 3,709903 |
| 21,582350 | 3,073065 | 21,582440 | 3,751476 |
| 22,118760 | 3,084872 | 22,118670 | 3,826667 |
| 22,650604 | 3,093625 | 22,650755 | 3,910133 |
| 23,186186 | 4,014073 | 23,186276 | 3,965446 |
| 23,718479 | 4,078432 | 23,714160 | 4,054070 |
| 24,255409 | 4,118412 | 24,255541 | 4,096911 |
| 24,791839 | 4,124750 | 24,792021 | 4,110167 |
| 25,150475 | 4,111710 | 25,151156 | 4,045174 |
| 25,441926 | 4,070846 | 25,442108 | 4,062052 |
| 25,714227 | 4,041990 | 25,714227 | 4,028130 |

ORIGINAL PAGE IS
OF POOR QUALITY

ORIGINAL PAGE 18
OF POOR QUALITY

MBL: 5.8169 m (19.0842 FT)

$\eta = .2278$

(DIMENSIONS IN METERS)

| BASELINE WING | | MODIFIED WING | |
|---------------|-----------|---------------|-----------|
| X | Z | X | Z |
| 25.714227 | 4.575522 | 25.714227 | 4.460104 |
| 25.517531 | 4.421977 | 25.517693 | 4.492497 |
| 25.214988 | 4.486493 | 25.215149 | 4.537716 |
| 24.690308 | 4.552327 | 24.690470 | 4.578997 |
| 24.420300 | 4.6045016 | 24.420407 | 4.630819 |
| 23.744304 | 4.751125 | 23.744465 | 4.684800 |
| 23.471529 | 4.806601 | 23.471609 | 4.731471 |
| 22.946334 | 4.873670 | 22.946414 | 4.780703 |
| 22.524307 | 4.931514 | 22.524446 | 4.793827 |
| 22.046384 | 4.982484 | 22.046444 | 4.814739 |
| 21.570748 | 5.024052 | 21.570828 | 4.826905 |
| 21.096300 | 5.057129 | 21.096439 | 4.831500 |
| 20.620352 | 5.081116 | 20.620437 | 4.827617 |
| 20.152423 | 5.094144 | 20.152502 | 4.814053 |
| 19.684354 | 5.094354 | 19.684433 | 4.787219 |
| 19.204962 | 5.081384 | 19.204900 | 4.752681 |
| 18.7201570 | 5.052920 | 18.7201569 | 4.704113 |
| 18.230308 | 5.020229 | 18.2303036 | 4.650677 |
| 17.735072 | 4.994674 | 18.235070 | 4.625064 |
| 17.240747 | 4.957921 | 17.2407485 | 4.581990 |
| 16.7470317 | 4.915550 | 16.7470315 | 4.536264 |
| 16.250064 | 4.855106 | 16.250062 | 4.475494 |
| 15.7521344 | 4.774304 | 15.7521341 | 4.401988 |
| 15.252529 | 4.681230 | 15.252527 | 4.327207 |
| 14.751396 | 4.585264 | 14.751393 | 4.270243 |
| 14.252529 | 4.533272 | 14.252527 | 4.225182 |
| 13.7521344 | 4.440705 | 13.7521341 | 4.154951 |
| 13.252004 | 4.305703 | 13.2520062 | 4.092522 |
| 12.7470317 | 4.200942 | 12.7470315 | 4.030838 |
| 12.2407487 | 4.224237 | 12.2407485 | 3.998072 |
| 11.735072 | 4.175353 | 11.735070 | 3.965083 |
| 11.230308 | 4.126720 | 11.230306 | 3.930413 |
| 10.7201570 | 4.083981 | 10.7201569 | 3.914732 |
| 10.204962 | 4.037870 | 10.204960 | 3.890684 |
| 9.684354 | 4.010904 | 9.684433 | 3.844320 |
| 9.152423 | 3.943004 | 9.152502 | 3.802815 |
| 8.620354 | 3.888501 | 8.620437 | 3.7419516 |
| 8.096300 | 3.897794 | 8.096439 | 3.648044 |
| 7.570748 | 4.023204 | 7.570828 | 3.490432 |
| 7.046334 | 4.070571 | 7.046444 | 4.052260 |
| 6.524306 | 4.137734 | 6.524446 | 4.131956 |
| 6.003334 | 4.214834 | 6.003414 | 4.220010 |
| 5.471529 | 4.290942 | 5.471609 | 4.305917 |
| 4.944304 | 4.355333 | 4.944465 | 4.380068 |
| 4.420300 | 4.349200 | 4.420407 | 4.434943 |
| 3.890308 | 4.411751 | 3.890470 | 4.481424 |
| 3.340241 | 4.340241 | 3.340241 | 4.457382 |
| 2.751524 | 4.301524 | 2.751524 | 4.435817 |
| 2.142227 | 4.320173 | 2.142227 | 4.410121 |

ORIGINAL PAGE IS
OF POOR QUALITY

WBL: 7.4552 m (24.4592 FT)

$\eta = .2920$

(DIMENSIONS IN METERS)

BASELINE WING

MODIFIED WING

| X | Z | X | Z |
|-----------|----------|-----------|----------|
| 25.714227 | 4.054121 | 25.714227 | 4.797032 |
| 25.543137 | 4.044123 | 25.543277 | 4.041005 |
| 25.274001 | 4.754050 | 25.274141 | 4.040044 |
| 25.000778 | 4.017397 | 25.000914 | 4.430349 |
| 24.505204 | 4.040502 | 24.505344 | 4.462752 |
| 24.104630 | 4.460235 | 24.104770 | 5.013414 |
| 23.750873 | 5.025109 | 23.750943 | 5.031104 |
| 23.342004 | 5.075301 | 23.342073 | 5.039005 |
| 22.929452 | 5.116944 | 22.930021 | 5.030504 |
| 22.514370 | 5.152325 | 22.514447 | 5.031043 |
| 22.047395 | 5.179430 | 22.047405 | 5.015154 |
| 21.083230 | 5.194431 | 21.083249 | 4.442209 |
| 21.207656 | 5.212711 | 21.207725 | 4.441557 |
| 20.054120 | 5.210715 | 20.054195 | 4.422474 |
| 20.430509 | 5.210424 | 20.430577 | 4.471154 |
| 20.064327 | 5.194454 | 20.064325 | 4.417400 |
| 19.732146 | 5.107605 | 19.732144 | 4.752925 |
| 19.440227 | 5.143014 | 19.440225 | 4.700474 |
| 19.204447 | 5.114103 | 19.204445 | 4.051511 |
| 19.100715 | 5.001207 | 19.100713 | 4.002103 |
| 18.454037 | 5.043005 | 18.454034 | 4.544300 |
| 18.420097 | 4.443039 | 18.420094 | 4.442310 |
| 18.730070 | 4.430143 | 18.730064 | 4.419604 |
| 18.005322 | 4.444913 | 18.005320 | 4.305402 |
| 18.075002 | 4.744471 | 18.075000 | 4.339550 |
| 18.005322 | 4.725200 | 18.005320 | 4.304907 |
| 18.730070 | 4.053001 | 18.730064 | 4.247022 |
| 18.020097 | 4.500549 | 18.020094 | 4.140710 |
| 18.454037 | 4.524720 | 18.454034 | 4.102041 |
| 19.100715 | 4.442727 | 19.100713 | 4.140742 |
| 19.204447 | 4.441701 | 19.204445 | 4.124253 |
| 19.440227 | 4.404505 | 19.440225 | 4.100421 |
| 19.732146 | 4.371744 | 19.732144 | 4.100713 |
| 20.064327 | 4.330419 | 20.064325 | 4.040074 |
| 20.430509 | 4.314030 | 20.430577 | 4.049419 |
| 20.054120 | 4.300801 | 20.054195 | 4.111107 |
| 21.207656 | 4.247605 | 21.207725 | 4.120120 |
| 21.083230 | 4.305907 | 21.083249 | 4.153404 |
| 22.047395 | 4.327944 | 22.047405 | 4.104400 |
| 22.514370 | 4.300077 | 22.514447 | 4.241044 |
| 22.929452 | 4.420505 | 22.930021 | 4.311203 |
| 23.342004 | 4.495444 | 23.342073 | 4.342510 |
| 23.750873 | 4.507440 | 23.750943 | 4.400055 |
| 24.104630 | 4.032230 | 24.104770 | 4.500410 |
| 24.505204 | 4.074041 | 24.505344 | 4.040053 |
| 25.000778 | 4.004753 | 25.000914 | 4.703440 |
| 25.274001 | 4.000672 | 25.274141 | 4.730400 |
| 25.543137 | 4.040203 | 25.543277 | 4.747200 |
| 25.714227 | 4.010350 | 25.714227 | 4.744010 |

ORIGINAL PAGE 18
OF POOR QUALITY

WBL: 8.3820 m (27.5000 FT)

$\eta = .3283$

(DIMENSIONS IN METERS)

| BASELINE WING | | MODIFIED WING | |
|---------------|----------|---------------|----------|
| X | Z | X | Z |
| 25.714227 | 4.811735 | 25.714227 | 4.853132 |
| 25.557622 | 4.855914 | 25.557752 | 4.912020 |
| 25.315215 | 4.913016 | 25.315344 | 4.966457 |
| 25.054874 | 4.967356 | 25.060008 | 5.047257 |
| 24.878443 | 5.030776 | 24.878622 | 5.115547 |
| 24.247104 | 5.099240 | 24.297234 | 5.167622 |
| 23.916304 | 5.148725 | 23.918307 | 5.205433 |
| 23.537563 | 5.184370 | 23.537626 | 5.232055 |
| 23.159408 | 5.221933 | 23.159469 | 5.246860 |
| 22.778019 | 5.246412 | 22.778082 | 5.253640 |
| 22.395337 | 5.267653 | 22.395404 | 5.251869 |
| 22.015244 | 5.280718 | 22.015308 | 5.242204 |
| 21.633856 | 5.287157 | 21.633919 | 5.224061 |
| 21.258934 | 5.286057 | 21.258995 | 5.196873 |
| 20.871081 | 5.276088 | 20.871144 | 5.159630 |
| 20.547871 | 5.259205 | 20.547868 | 5.116500 |
| 20.224801 | 5.232486 | 20.224659 | 5.062367 |
| 20.004965 | 5.208971 | 20.004963 | 5.020567 |
| 19.818840 | 5.181743 | 19.818836 | 4.973094 |
| 19.652516 | 5.151079 | 19.652513 | 4.924488 |
| 19.510563 | 5.116045 | 19.510563 | 4.871006 |
| 19.394983 | 5.071039 | 19.394480 | 4.811349 |
| 19.311076 | 5.015443 | 19.311109 | 4.743544 |
| 19.263965 | 4.943141 | 19.263965 | 4.664316 |
| 19.255034 | 4.888588 | 19.255031 | 4.648152 |
| 19.263970 | 4.837339 | 19.263970 | 4.609158 |
| 19.311193 | 4.769140 | 19.311186 | 4.568883 |
| 19.395194 | 4.713323 | 19.395188 | 4.520555 |
| 19.518902 | 4.664547 | 19.518902 | 4.464723 |
| 19.652776 | 4.625955 | 19.652776 | 4.437731 |
| 19.819046 | 4.592061 | 19.819046 | 4.413603 |
| 20.010006 | 4.561622 | 20.010013 | 4.392092 |
| 20.224861 | 4.534550 | 20.224861 | 4.372315 |
| 20.547871 | 4.505317 | 20.547871 | 4.350583 |
| 20.871081 | 4.480461 | 20.871144 | 4.336118 |
| 21.258934 | 4.474710 | 21.258995 | 4.328031 |
| 21.633856 | 4.472475 | 21.633922 | 4.324055 |
| 22.015244 | 4.480344 | 22.015306 | 4.332270 |
| 22.395337 | 4.500301 | 22.395404 | 4.351114 |
| 22.778019 | 4.530367 | 22.778082 | 4.380811 |
| 23.159408 | 4.569871 | 23.159471 | 4.441739 |
| 23.537563 | 4.654822 | 23.537626 | 4.511751 |
| 23.918304 | 4.724547 | 23.918307 | 4.590959 |
| 24.247104 | 4.786491 | 24.297234 | 4.689244 |
| 24.878443 | 4.837514 | 24.878620 | 4.739643 |
| 25.054874 | 4.854857 | 25.060008 | 4.787547 |
| 25.315215 | 4.841670 | 25.315344 | 4.805837 |
| 25.557622 | 4.807255 | 25.557752 | 4.814331 |
| 25.714227 | 4.771128 | 25.714227 | 4.811291 |

ORIGINAL PAGE IS
OF POOR QUALITY

WBL: 10.1600 m (33.3333 FT)

$\eta = .3979$

(DIMENSIONS IN METERS)

| BASELINE WING | | MODIFIED WING | |
|---------------|----------|---------------|----------|
| X | Z | X | Z |
| 20.040189 | 5.042913 | 20.040189 | 4.009940 |
| 25.404198 | 5.084456 | 25.404312 | 4.724800 |
| 25.091214 | 5.137390 | 25.091325 | 4.796340 |
| 25.400808 | 5.105809 | 25.400980 | 4.863170 |
| 25.131771 | 5.240764 | 25.131883 | 4.950396 |
| 24.790674 | 5.295342 | 24.790786 | 5.028143 |
| 24.403847 | 5.333162 | 24.403903 | 5.098324 |
| 24.129319 | 5.362242 | 24.129375 | 5.161519 |
| 23.747062 | 5.383400 | 23.747118 | 5.217443 |
| 23.401965 | 5.399959 | 23.402010 | 5.268443 |
| 23.125732 | 5.409824 | 23.125788 | 5.313142 |
| 22.791771 | 5.414594 | 22.791824 | 5.351458 |
| 22.450673 | 5.413800 | 22.450727 | 5.384840 |
| 22.127256 | 5.407172 | 22.127309 | 5.410972 |
| 21.780479 | 5.393355 | 21.780532 | 5.430830 |
| 21.502497 | 5.375275 | 21.502447 | 5.440053 |
| 21.218517 | 5.349814 | 21.218515 | 5.440644 |
| 21.024897 | 5.328001 | 21.024884 | 5.435362 |
| 20.801450 | 5.303203 | 20.801447 | 5.424500 |
| 20.715813 | 5.275600 | 20.715813 | 5.408605 |
| 20.591069 | 5.244349 | 20.591087 | 5.386015 |
| 20.484537 | 5.206573 | 20.484537 | 5.355021 |
| 20.415810 | 5.160350 | 20.415814 | 5.314635 |
| 20.374412 | 5.100470 | 20.374409 | 5.236169 |
| 20.300570 | 5.050754 | 20.300573 | 5.203274 |
| 20.374412 | 5.015367 | 20.374409 | 5.159246 |
| 20.415810 | 4.950605 | 20.415814 | 5.093713 |
| 20.484537 | 4.911908 | 20.484537 | 5.052147 |
| 20.591069 | 4.875706 | 20.591089 | 5.004554 |
| 20.715813 | 4.845764 | 20.715813 | 4.962345 |
| 20.801450 | 4.814851 | 20.801447 | 4.922041 |
| 21.024897 | 4.790830 | 21.024894 | 4.882294 |
| 21.218517 | 4.770045 | 21.218515 | 4.842807 |
| 21.502497 | 4.754923 | 21.502444 | 4.791479 |
| 21.780479 | 4.739947 | 21.780532 | 4.747133 |
| 22.127256 | 4.730830 | 22.127309 | 4.703542 |
| 22.450673 | 4.729440 | 22.450727 | 4.670621 |
| 22.791771 | 4.737204 | 22.791824 | 4.647123 |
| 23.125732 | 4.754640 | 23.125788 | 4.630170 |
| 23.401965 | 4.785553 | 23.402021 | 4.641541 |
| 23.747062 | 4.832305 | 23.747115 | 4.666671 |
| 24.129319 | 4.840945 | 24.129375 | 4.706544 |
| 24.403847 | 4.956371 | 24.403903 | 4.754405 |
| 24.790674 | 5.019093 | 24.790786 | 4.793800 |
| 25.131771 | 5.068504 | 25.131883 | 4.809860 |
| 25.400808 | 5.087422 | 25.400980 | 4.780143 |
| 25.091214 | 5.075763 | 25.091325 | 4.744725 |
| 25.404198 | 5.042215 | 25.404309 | 4.684819 |
| 20.040189 | 5.000607 | 20.040189 | 4.633227 |

ORIGINAL PAGE IS
OF POOR QUALITY

WBL: 10.7317 m (35.2088 FT)

$\eta = .4203$

(DIMENSIONS IN METERS)

| BASELINE WING | | MODIFIED WING | |
|---------------|----------|---------------|-----------|
| X | Z | X | Z |
| 20,221434 | 5,101470 | 20,221433 | 4,705010 |
| 20,003997 | 5,143212 | 20,004100 | 4,757215 |
| 25,077642 | 5,144314 | 25,077451 | 4,824307 |
| 25,000091 | 5,241149 | 25,000000 | 4,887670 |
| 25,330334 | 5,299739 | 25,330000 | 4,970644 |
| 25,011900 | 5,345000 | 25,012047 | 5,044540 |
| 24,004030 | 5,381109 | 24,004000 | 5,112242 |
| 24,300034 | 5,407904 | 24,300000 | 5,174607 |
| 24,004431 | 5,427547 | 24,004405 | 5,229037 |
| 23,720000 | 5,441655 | 23,720133 | 5,279014 |
| 23,394029 | 5,449414 | 23,394002 | 5,324753 |
| 23,071377 | 5,453110 | 23,071430 | 5,364940 |
| 22,747025 | 5,451171 | 22,747070 | 5,400000 |
| 22,420171 | 5,445557 | 22,420204 | 5,429052 |
| 22,090122 | 5,429193 | 22,090375 | 5,452041 |
| 21,423400 | 5,411052 | 21,023440 | 5,400105 |
| 21,540574 | 5,380005 | 21,540572 | 5,472320 |
| 21,300002 | 5,304604 | 21,300001 | 5,471203 |
| 21,203442 | 5,340552 | 21,203440 | 5,400400 |
| 21,001992 | 5,313729 | 21,001990 | 5,453430 |
| 20,441207 | 5,283304 | 20,441205 | 5,434310 |
| 20,042972 | 5,247123 | 20,042970 | 5,400004 |
| 20,771015 | 5,202420 | 20,771013 | 5,370544 |
| 20,731534 | 5,140193 | 20,731530 | 5,271000 |
| 20,723451 | 5,104007 | 20,723449 | 5,271147 |
| 20,731530 | 5,064735 | 20,731530 | 5,240901 |
| 20,771015 | 5,000100 | 20,771013 | 5,100000 |
| 20,042972 | 4,965771 | 20,042970 | 5,140717 |
| 20,441207 | 4,932044 | 20,441205 | 5,102102 |
| 21,001992 | 4,903944 | 21,001990 | 5,001143 |
| 21,203442 | 4,879641 | 21,203440 | 5,022050 |
| 21,300002 | 4,850234 | 21,300001 | 4,944000 |
| 21,540574 | 4,839423 | 21,540572 | 4,900004 |
| 21,023440 | 4,819210 | 21,023440 | 4,897241 |
| 22,040322 | 4,805040 | 22,040375 | 4,853449 |
| 22,420171 | 4,790509 | 22,420224 | 4,810020 |
| 22,747025 | 4,795440 | 22,747070 | 4,770907 |
| 23,071377 | 4,803152 | 23,071430 | 4,751342 |
| 23,394029 | 4,820000 | 23,394002 | 4,730074 |
| 23,720000 | 4,849050 | 23,720133 | 4,730500 |
| 24,004431 | 4,895125 | 24,004405 | 4,753012 |
| 24,300034 | 4,952097 | 24,300000 | 4,780033 |
| 24,004030 | 5,010171 | 24,004000 | 4,821255 |
| 25,011900 | 5,070020 | 25,012047 | 4,850744 |
| 25,330334 | 5,127114 | 25,330000 | 4,850507 |
| 25,000091 | 5,140200 | 25,000000 | 4,824057 |
| 25,077642 | 5,134000 | 25,077451 | 4,765021 |
| 20,003997 | 5,101000 | 20,004100 | 4,723471 |
| 20,221434 | 5,000000 | 20,221433 | 4,0004700 |

ORIGINAL PAGE 14
OF POOR QUALITY

WBL: 12.3784 ■ (40.6050 FT)

$\eta = .4847$

(DIMENSIONS IN METERS)

| BASELINE WING | | MODIFIED WING | |
|---------------|----------|---------------|----------|
| X | Z | X | Z |
| 25.432406 | 5.220370 | 25.434804 | 4.889270 |
| 25.405744 | 5.204034 | 25.405347 | 4.431924 |
| 25.010095 | 5.312000 | 25.010998 | 4.460352 |
| 25.400182 | 5.350262 | 25.400285 | 5.037229 |
| 25.100408 | 5.410504 | 25.100510 | 5.102024 |
| 25.794033 | 5.453082 | 25.794736 | 5.157829 |
| 25.440032 | 5.495610 | 25.440983 | 5.205742 |
| 25.185076 | 5.510137 | 25.185720 | 5.247148 |
| 24.862492 | 5.527954 | 24.862543 | 5.242103 |
| 24.570718 | 5.540653 | 24.570768 | 5.312365 |
| 24.269407 | 5.547812 | 24.269950 | 5.337530 |
| 23.405109 | 5.550440 | 23.405220 | 5.350467 |
| 23.059395 | 5.548171 | 23.059445 | 5.374861 |
| 23.350803 | 5.540627 | 23.350853 | 5.386134 |
| 23.047846 | 5.520137 | 23.047890 | 5.392234 |
| 22.780715 | 5.509343 | 22.780713 | 5.392047 |
| 22.524544 | 5.485509 | 22.524582 | 5.405083 |
| 22.357469 | 5.465354 | 22.357467 | 5.377240 |
| 22.204219 | 5.442574 | 22.204217 | 5.364037 |
| 22.070870 | 5.417242 | 22.070808 | 5.349440 |
| 21.957060 | 5.388762 | 21.957058 | 5.326254 |
| 21.864395 | 5.354787 | 21.864393 | 5.298304 |
| 21.797125 | 5.313444 | 21.797123 | 5.260307 |
| 21.754343 | 5.260449 | 21.754341 | 5.211454 |
| 21.752191 | 5.221034 | 21.752189 | 5.162234 |
| 21.754344 | 5.184490 | 21.754341 | 5.102144 |
| 21.797125 | 5.131050 | 21.797123 | 5.110300 |
| 21.864395 | 5.092237 | 21.864393 | 5.075447 |
| 21.957060 | 5.060425 | 21.957058 | 5.045902 |
| 22.070870 | 5.034744 | 22.070868 | 5.012140 |
| 22.204219 | 5.012321 | 22.204217 | 4.982701 |
| 22.357469 | 4.992470 | 22.357467 | 4.954556 |
| 22.524544 | 4.975133 | 22.524582 | 4.927783 |
| 22.700715 | 4.958607 | 22.700713 | 4.904749 |
| 23.047846 | 4.943745 | 23.047890 | 4.880712 |
| 23.350803 | 4.930203 | 23.350853 | 4.861570 |
| 23.657345 | 4.930133 | 23.657445 | 4.825633 |
| 23.960109 | 4.945253 | 23.965220 | 4.812304 |
| 24.269407 | 4.959401 | 24.267958 | 4.804811 |
| 24.570718 | 4.987714 | 24.570768 | 4.818504 |
| 24.862492 | 5.030344 | 24.862543 | 4.841003 |
| 25.185076 | 5.083099 | 25.185720 | 4.874241 |
| 25.440032 | 5.144283 | 25.440983 | 4.915277 |
| 25.794033 | 5.202011 | 25.794736 | 4.945495 |
| 25.100408 | 5.249050 | 25.100510 | 4.970975 |
| 25.400182 | 5.267010 | 25.400285 | 4.985212 |
| 25.010095 | 5.257047 | 25.010998 | 4.934401 |
| 25.405744 | 5.220245 | 25.405347 | 4.896230 |
| 25.432406 | 5.193542 | 25.434804 | 4.855510 |

ORIGINAL PAGE IS
OF POOR QUALITY

MBL: 14.0211 m (46.0008 FT)

$\eta = .5491$

(DIMENSIONS IN METERS)

| BASELINE WING | | MODIFIED WING | |
|---------------|----------|---------------|----------|
| X | Z | X | Z |
| 27.040140 | 5.350769 | 27.040139 | 5.056805 |
| 27.520440 | 5.380640 | 27.520542 | 5.094979 |
| 27.343904 | 5.431011 | 27.344001 | 5.134937 |
| 27.151627 | 5.471359 | 27.151724 | 5.181456 |
| 26.864428 | 5.521343 | 26.864525 | 5.233642 |
| 26.577230 | 5.560357 | 26.577320 | 5.274901 |
| 26.291476 | 5.590025 | 26.292026 | 5.306901 |
| 26.005207 | 5.612290 | 26.005314 | 5.331558 |
| 25.720502 | 5.628354 | 25.720550 | 5.349807 |
| 25.433303 | 5.639640 | 25.433351 | 5.363160 |
| 25.145131 | 5.645803 | 25.145179 | 5.371322 |
| 24.855900 | 5.647709 | 24.856950 | 5.375027 |
| 24.571708 | 5.645105 | 24.571755 | 5.374039 |
| 24.289377 | 5.637642 | 24.289424 | 5.368637 |
| 23.997310 | 5.624770 | 23.997356 | 5.355645 |
| 23.753922 | 5.607728 | 23.753920 | 5.340400 |
| 23.510533 | 5.585127 | 23.510532 | 5.318814 |
| 23.348875 | 5.560037 | 23.348873 | 5.300302 |
| 23.204935 | 5.544540 | 23.204933 | 5.279180 |
| 23.079007 | 5.520850 | 23.079005 | 5.255901 |
| 22.972790 | 5.494108 | 22.972769 | 5.228305 |
| 22.885755 | 5.462441 | 22.885753 | 5.193907 |
| 22.8022571 | 5.423950 | 22.8022569 | 5.157138 |
| 22.727085 | 5.374690 | 22.727083 | 5.120820 |
| 22.6501307 | 5.338003 | 22.6501305 | 5.077289 |
| 22.5767060 | 5.304230 | 22.5767053 | 5.046532 |
| 22.5022571 | 5.255120 | 22.5022564 | 5.003603 |
| 22.4285755 | 5.215645 | 22.4285753 | 4.960305 |
| 22.3572790 | 5.164755 | 22.3572769 | 4.935077 |
| 23.079087 | 5.105630 | 23.079085 | 4.907940 |
| 23.204935 | 5.144942 | 23.204933 | 4.885078 |
| 23.348875 | 5.120710 | 23.348873 | 4.866510 |
| 23.510533 | 5.110835 | 23.510532 | 4.844351 |
| 23.753922 | 5.093989 | 23.753920 | 4.830732 |
| 23.997310 | 5.082465 | 23.997356 | 4.817002 |
| 24.204937 | 5.075970 | 24.204924 | 4.809830 |
| 24.571708 | 5.076207 | 24.571755 | 4.808213 |
| 24.855900 | 5.083300 | 24.856950 | 4.811740 |
| 25.145131 | 5.098854 | 25.145179 | 4.827645 |
| 25.433303 | 5.125503 | 25.433351 | 4.852410 |
| 25.720502 | 5.165555 | 25.720550 | 4.890138 |
| 26.005207 | 5.215693 | 26.005314 | 4.937828 |
| 26.291476 | 5.272388 | 26.292026 | 4.991402 |
| 26.577230 | 5.327107 | 26.577320 | 5.043400 |
| 26.864428 | 5.379375 | 26.864525 | 5.084883 |
| 27.151627 | 5.369025 | 27.151724 | 5.101073 |
| 27.343904 | 5.379201 | 27.344001 | 5.090135 |
| 27.520440 | 5.350594 | 27.520542 | 5.080057 |
| 27.040140 | 5.320170 | 27.040139 | 5.024801 |

ORIGINAL PAGE IS
OF POOR QUALITY

WBL: 15.6857 m (51.3967 FT)

$\eta = .6135$

(DIMENSIONS IN METERS)

| BASELINE WING | | MODIFIED WING | |
|---------------|----------|---------------|----------|
| X | Z | X | Z |
| 28.361471 | 5.475161 | 28.361470 | 5.177551 |
| 28.247647 | 5.508362 | 28.247738 | 5.210414 |
| 23.070913 | 5.540355 | 28.077003 | 5.251108 |
| 27.897072 | 5.580438 | 27.897163 | 5.288251 |
| 27.620449 | 5.632202 | 27.620540 | 5.334527 |
| 27.354827 | 5.687653 | 27.359917 | 5.370704 |
| 27.093025 | 5.694440 | 27.093070 | 5.398245 |
| 26.824858 | 5.714460 | 26.824902 | 5.419239 |
| 26.558512 | 5.726755 | 26.558556 | 5.434523 |
| 26.284889 | 5.738639 | 26.289933 | 5.445436 |
| 26.020356 | 5.743794 | 26.020400 | 5.451737 |
| 25.752643 | 5.745091 | 25.752666 | 5.454173 |
| 25.484021 | 5.742159 | 25.484065 | 5.452474 |
| 25.214951 | 5.734757 | 25.214995 | 5.446209 |
| 24.946775 | 5.721815 | 24.946819 | 5.434650 |
| 24.714129 | 5.706063 | 24.714127 | 5.420061 |
| 24.491483 | 5.684685 | 24.491481 | 5.394864 |
| 24.340280 | 5.660720 | 24.340274 | 5.382750 |
| 24.205650 | 5.640605 | 24.205648 | 5.363267 |
| 24.064503 | 5.624407 | 24.068501 | 5.341610 |
| 23.960521 | 5.594555 | 23.968519 | 5.316406 |
| 23.907114 | 5.570096 | 23.907113 | 5.285009 |
| 23.844017 | 5.534467 | 23.844016 | 5.250733 |
| 23.814627 | 5.468947 | 23.814625 | 5.212671 |
| 23.808543 | 5.454967 | 23.808542 | 5.179267 |
| 23.814828 | 5.423406 | 23.814825 | 5.151751 |
| 23.844017 | 5.376602 | 23.844016 | 5.110502 |
| 23.907114 | 5.345153 | 23.907113 | 5.070700 |
| 23.968521 | 5.318542 | 23.968519 | 5.046393 |
| 24.068503 | 5.290478 | 24.068501 | 5.024031 |
| 24.205650 | 5.277565 | 24.205648 | 5.004412 |
| 24.340280 | 5.260943 | 24.340276 | 4.987011 |
| 24.491483 | 5.246538 | 24.491481 | 4.971861 |
| 24.714129 | 5.231371 | 24.714127 | 4.955568 |
| 24.946775 | 5.221176 | 24.946819 | 4.944254 |
| 25.214951 | 5.215650 | 25.214995 | 4.937368 |
| 25.484021 | 5.210402 | 25.484065 | 4.936810 |
| 25.752643 | 5.223379 | 25.752688 | 4.942283 |
| 26.020356 | 5.238247 | 26.020400 | 4.955408 |
| 26.284889 | 5.263412 | 26.289933 | 4.978802 |
| 26.558512 | 5.300760 | 26.558556 | 5.014107 |
| 26.824858 | 5.347786 | 26.824902 | 5.059052 |
| 27.093025 | 5.400442 | 27.093070 | 5.109703 |
| 27.354827 | 5.451763 | 27.359917 | 5.159157 |
| 27.620449 | 5.492894 | 27.620540 | 5.196918 |
| 27.897072 | 5.510433 | 27.897163 | 5.215460 |
| 28.070913 | 5.501355 | 28.077003 | 5.205724 |
| 28.247647 | 5.474443 | 28.247738 | 5.178352 |
| 28.361471 | 5.446770 | 28.361470 | 5.149377 |

ORIGINAL PAGE 18
OF POOR QUALITY

WBL: 17.3104 ■ (56.7925 FT)

■ = .6780

(DIMENSIONS IN METERS)

| BASELINE WING | | MODIFIED WING | |
|---------------|----------|---------------|----------|
| X | Z | X | Z |
| 29,074801 | 5,599554 | 29,074801 | 5,213854 |
| 28,988849 | 5,630075 | 28,988938 | 5,313749 |
| 28,804921 | 5,667700 | 28,810006 | 5,311022 |
| 28,642517 | 5,701513 | 28,642801 | 5,394753 |
| 28,392470 | 5,743121 | 28,392558 | 5,438461 |
| 28,142424 | 5,774408 | 28,142508 | 5,488784 |
| 27,894072 | 5,798855 | 27,894114 | 5,493248 |
| 27,644489 | 5,816821 | 27,644491 | 5,511601 |
| 27,398521 | 5,829155 | 27,398563 | 5,524701 |
| 27,148874 | 5,837632 | 27,148516 | 5,533830 |
| 26,895580 | 5,841788 | 26,895821 | 5,538807 |
| 26,648381 | 5,842413 | 26,648422 | 5,540073 |
| 26,398338 | 5,839153 | 26,398375 | 5,537688 |
| 26,150525 | 5,831821 | 26,150588 | 5,531088 |
| 25,898240 | 5,819354 | 25,898281 | 5,519497 |
| 25,648336 | 5,804346 | 25,648335 | 5,505333 |
| 25,472432 | 5,784243 | 25,472431 | 5,485945 |
| 25,331885 | 5,767403 | 25,331888 | 5,469888 |
| 25,211885 | 5,747420 | 25,208384 | 5,451251 |
| 25,047319 | 5,727484 | 25,097318 | 5,431116 |
| 25,008251 | 5,704481 | 25,004249 | 5,407273 |
| 24,428474 | 5,677750 | 24,928473 | 5,383543 |
| 24,473488 | 5,644979 | 24,873482 | 5,351258 |
| 24,442588 | 5,603196 | 24,842587 | 5,309257 |
| 24,438720 | 5,571931 | 24,838718 | 5,279847 |
| 24,442570 | 5,543735 | 24,842587 | 5,250043 |
| 24,473482 | 5,502079 | 24,473482 | 5,212077 |
| 24,428474 | 5,471612 | 24,428473 | 5,188781 |
| 25,008251 | 5,447409 | 25,004249 | 5,159834 |
| 25,047319 | 5,427314 | 25,097318 | 5,154738 |
| 25,208384 | 5,410187 | 25,208384 | 5,119762 |
| 25,331885 | 5,395177 | 25,331884 | 5,108145 |
| 25,472432 | 5,382240 | 25,472431 | 5,090701 |
| 25,648336 | 5,368753 | 25,648335 | 5,076333 |
| 25,898240 | 5,354888 | 25,898281 | 5,068841 |
| 26,150525 | 5,355342 | 26,150588 | 5,061081 |
| 26,398338 | 5,358538 | 26,398375 | 5,061220 |
| 26,648381 | 5,383452 | 26,648422 | 5,067018 |
| 26,895580 | 5,377840 | 26,895821 | 5,080021 |
| 27,148874 | 5,401281 | 27,148516 | 5,102328 |
| 27,398521 | 5,435977 | 27,398563 | 5,135823 |
| 27,644489 | 5,479880 | 27,644491 | 5,178985 |
| 27,894072 | 5,528598 | 27,894114 | 5,225798 |
| 28,142424 | 5,578339 | 28,142508 | 5,272803 |
| 28,392470 | 5,614824 | 28,392558 | 5,310528 |
| 28,642517 | 5,631842 | 28,642801 | 5,327351 |
| 28,804921 | 5,623508 | 28,810006 | 5,318824 |
| 28,988849 | 5,599292 | 28,988938 | 5,294882 |
| 29,074801 | 5,573388 | 29,074801 | 5,267588 |

ORIGINAL PAGE IS
OF POOR QUALITY

MBL: 18.9550 m (62.1883 FT)

$\eta = .7424$

(DIMENSIONS IN METERS)

| BASELINE WING | | MODIFIED WING | |
|---------------|----------|---------------|----------|
| X | Z | X | Z |
| 24.788132 | 5.723446 | 29.788132 | 5.408466 |
| 29.690129 | 5.751769 | 29.690129 | 5.435904 |
| 29.542930 | 5.786044 | 29.543008 | 5.469805 |
| 29.387962 | 5.816590 | 29.388040 | 5.500352 |
| 29.150491 | 5.853844 | 29.150509 | 5.537764 |
| 28.925020 | 5.882164 | 28.925098 | 5.568443 |
| 28.645119 | 5.903269 | 28.695157 | 5.587954 |
| 28.404040 | 5.918782 | 28.404078 | 5.603890 |
| 28.234531 | 5.929555 | 28.234569 | 5.615138 |
| 28.003060 | 5.936524 | 28.003098 | 5.622716 |
| 27.770804 | 5.939777 | 27.770842 | 5.626422 |
| 27.540118 | 5.939736 | 27.540156 | 5.628971 |
| 27.308647 | 5.936147 | 27.308685 | 5.624015 |
| 27.081099 | 5.928866 | 27.081137 | 5.617394 |
| 26.845705 | 5.916892 | 26.845743 | 5.608095 |
| 26.604954 | 5.902732 | 26.604954 | 5.592500 |
| 26.453381 | 5.883801 | 26.453380 | 5.574297 |
| 26.323091 | 5.868686 | 26.323089 | 5.558950 |
| 26.207041 | 5.850636 | 26.207079 | 5.541756 |
| 26.100136 | 5.831522 | 26.100134 | 5.523025 |
| 26.014981 | 5.810327 | 26.014980 | 5.500950 |
| 25.944434 | 5.785405 | 25.944433 | 5.474251 |
| 25.895910 | 5.755490 | 25.895909 | 5.448011 |
| 25.870310 | 5.717445 | 25.870308 | 5.414233 |
| 25.864896 | 5.668846 | 25.864894 | 5.384044 |
| 25.870311 | 5.603443 | 25.870310 | 5.358129 |
| 25.890910 | 5.525555 | 25.890909 | 5.324271 |
| 25.944434 | 5.596079 | 25.944433 | 5.299164 |
| 26.014981 | 5.576230 | 26.014980 | 5.274664 |
| 26.100136 | 5.556101 | 26.100134 | 5.254800 |
| 26.207081 | 5.542809 | 26.207079 | 5.239037 |
| 26.323091 | 5.529410 | 26.323089 | 5.225106 |
| 26.453381 | 5.517942 | 26.453380 | 5.213156 |
| 26.604954 | 5.506135 | 26.604954 | 5.200609 |
| 26.845705 | 5.498557 | 26.845743 | 5.192315 |
| 27.081099 | 5.495026 | 27.081137 | 5.187894 |
| 27.308647 | 5.496670 | 27.308685 | 5.186624 |
| 27.540118 | 5.503524 | 27.540156 | 5.194571 |
| 27.770804 | 5.517032 | 27.770842 | 5.207063 |
| 28.003060 | 5.539111 | 28.003098 | 5.228135 |
| 28.234531 | 5.571167 | 28.234569 | 5.259160 |
| 28.404040 | 5.611574 | 28.404078 | 5.294541 |
| 28.645119 | 5.656700 | 28.695157 | 5.342831 |
| 28.925020 | 5.700415 | 28.925098 | 5.388465 |
| 29.150491 | 5.736746 | 29.150509 | 5.422060 |
| 29.387962 | 5.753256 | 29.388040 | 5.438624 |
| 29.542930 | 5.745802 | 29.543008 | 5.431040 |
| 29.690129 | 5.723641 | 29.690129 | 5.408643 |
| 29.788132 | 5.699957 | 29.788132 | 5.384550 |

ORIGINAL PAGE 18
OF POOR QUALITY

MBL: 20.5997 m (67.5842 FT)

$\eta = .8068$

(DIMENSIONS IN METERS)

BASELINE WING

MODIFIED WING

| X | Z | X | Z |
|-----------|----------|-----------|----------|
| 30.501463 | 5.048334 | 30.501463 | 5.522442 |
| 30.411253 | 5.073503 | 30.411325 | 5.507850 |
| 30.275939 | 5.904369 | 30.270011 | 5.578442 |
| 30.133407 | 5.431660 | 30.133479 | 5.045089 |
| 29.920512 | 5.964056 | 29.920584 | 5.038805 |
| 29.707617 | 5.989454 | 29.707609 | 5.063472 |
| 29.490105 | 0.007064 | 29.490201 | 5.062544 |
| 29.283631 | 0.020444 | 29.283607 | 5.090177 |
| 29.072540 | 0.029950 | 29.072576 | 5.705500 |
| 28.859045 | 0.035017 | 28.859620 | 5.711043 |
| 28.640029 | 0.037706 | 28.640064 | 5.714302 |
| 28.433855 | 0.037050 | 28.433890 | 5.714107 |
| 28.220900 | 0.033141 | 28.220995 | 5.710730 |
| 28.011073 | 0.025950 | 28.011706 | 5.704024 |
| 27.795170 | 0.014031 | 27.795205 | 5.643120 |
| 27.614750 | 0.001007 | 27.614749 | 5.600240 |
| 27.434331 | 5.983354 | 27.434329 | 5.603131 |
| 27.314090 | 5.968769 | 27.314495 | 5.646890 |
| 27.207790 | 5.952652 | 27.207795 | 5.633040 |
| 27.114952 | 5.935074 | 27.114951 | 5.615700 |
| 27.035712 | 5.915714 | 27.035710 | 5.590200 |
| 26.971194 | 5.893060 | 26.971192 | 5.572454 |
| 26.903357 | 5.866002 | 26.924355 | 5.550409 |
| 26.840052 | 5.831694 | 26.840050 | 5.520741 |
| 26.893072 | 5.805800 | 26.843071 | 5.480947 |
| 26.849054 | 5.783231 | 26.849050 | 5.460205 |
| 26.924357 | 5.749031 | 26.924355 | 5.430271 |
| 26.971194 | 5.724520 | 26.971192 | 5.410425 |
| 27.035712 | 5.705003 | 27.035710 | 5.369704 |
| 27.114952 | 5.689002 | 27.114951 | 5.372700 |
| 27.207790 | 5.675430 | 27.207795 | 5.350810 |
| 27.314090 | 5.663643 | 27.314495 | 5.340585 |
| 27.434331 | 5.653044 | 27.434329 | 5.336147 |
| 27.614750 | 5.643517 | 27.614749 | 5.325447 |
| 27.795170 | 5.637247 | 27.795205 | 5.318560 |
| 28.011073 | 5.634714 | 28.011706 | 5.315311 |
| 28.220900 | 5.636805 | 28.220995 | 5.310643 |
| 28.433855 | 5.643597 | 28.433890 | 5.322719 |
| 28.640029 | 5.656425 | 28.640064 | 5.334753 |
| 28.859045 | 5.670900 | 28.859620 | 5.354400 |
| 29.072540 | 5.700398 | 29.072576 | 5.383004 |
| 29.283631 | 5.743400 | 29.283607 | 5.414377 |
| 29.490105 | 5.784805 | 29.490201 | 5.400154 |
| 29.707617 | 5.825491 | 29.707609 | 5.500458 |
| 29.920512 | 5.858673 | 29.920584 | 5.533500 |
| 30.133407 | 5.874054 | 30.133479 | 5.544795 |
| 30.275939 | 5.867815 | 30.270011 | 5.543000 |
| 30.411253 | 5.847940 | 30.411325 | 5.522900 |
| 30.501463 | 5.826551 | 30.501463 | 5.501240 |

WBL: 22.2 3 m (72.9800 FT)

$\eta = .8712$

(DIMENSIONS IN METERS)

BASELINE WING

MODIFIED WING

| X | Z | X | Z |
|-----------|----------|-----------|----------|
| 31.214794 | 5.972731 | 31.214794 | 5.637205 |
| 31.132455 | 5.495217 | 31.132521 | 5.659592 |
| 31.008947 | 6.022755 | 31.009013 | 5.686921 |
| 30.878852 | 6.046743 | 30.879918 | 5.710946 |
| 30.684433 | 6.075477 | 30.684549 | 5.739891 |
| 30.490214 | 6.096735 | 30.490279 | 5.761438 |
| 30.297212 | 6.112099 | 30.297244 | 5.777101 |
| 30.103222 | 6.123105 | 30.103255 | 5.786494 |
| 29.910550 | 6.130356 | 29.910582 | 5.796124 |
| 29.718231 | 6.134610 | 29.718263 | 5.800779 |
| 29.521253 | 6.135760 | 29.521285 | 5.802324 |
| 29.327592 | 6.134380 | 29.327624 | 5.801369 |
| 29.133273 | 6.130135 | 29.133305 | 5.797611 |
| 28.942247 | 6.123015 | 28.942279 | 5.790955 |
| 28.744635 | 6.111970 | 28.744667 | 5.780448 |
| 28.574958 | 6.099402 | 28.574956 | 5.768328 |
| 28.415280 | 6.082917 | 28.415279 | 5.752344 |
| 28.265901 | 6.069452 | 28.265900 | 5.739190 |
| 28.123768 | 6.054667 | 28.123767 | 5.724716 |
| 28.051442 | 6.038637 | 28.051441 | 5.708952 |
| 27.992554 | 6.021100 | 27.992552 | 5.691911 |
| 27.949603 | 6.000714 | 27.949602 | 5.671029 |
| 27.925794 | 5.976513 | 27.925792 | 5.647843 |
| 27.921248 | 5.945943 | 27.921247 | 5.617681 |
| 27.925796 | 5.922825 | 27.925792 | 5.594508 |
| 27.947803 | 5.902979 | 27.947802 | 5.574549 |
| 27.992554 | 5.872507 | 27.992552 | 5.544350 |
| 28.051442 | 5.850907 | 28.051441 | 5.522722 |
| 28.123768 | 5.833890 | 28.123767 | 5.505400 |
| 28.208510 | 5.819844 | 28.208510 | 5.491334 |
| 28.305900 | 5.808052 | 28.305900 | 5.479230 |
| 28.415279 | 5.797877 | 28.415279 | 5.468757 |
| 28.579956 | 5.789346 | 28.579956 | 5.459897 |
| 28.744667 | 5.780894 | 28.744667 | 5.450945 |
| 28.942279 | 5.775936 | 28.942279 | 5.445476 |
| 29.133305 | 5.774400 | 29.133305 | 5.443316 |
| 29.327624 | 5.776439 | 29.327624 | 5.445284 |
| 29.521285 | 5.783670 | 29.521285 | 5.451367 |
| 29.718263 | 5.795818 | 29.718263 | 5.462856 |
| 29.910582 | 5.814609 | 29.910582 | 5.481154 |
| 30.103255 | 5.841609 | 30.103255 | 5.507298 |
| 30.297244 | 5.875361 | 30.297244 | 5.540461 |
| 30.490279 | 5.912909 | 30.490279 | 5.577572 |
| 30.684549 | 5.950067 | 30.684549 | 5.614513 |
| 30.879918 | 5.980591 | 30.879918 | 5.645087 |
| 31.009013 | 5.996067 | 31.009013 | 5.660866 |
| 31.132521 | 5.989669 | 31.132521 | 5.654925 |
| 31.214794 | 5.972339 | 31.214794 | 5.637149 |
| | 5.953145 | | 5.617780 |

ORIGINAL PAGE IS
OF POOR QUALITY

WBL: 23.8890 m (78.3758 FT)

$\eta = .9356$

(DIMENSIONS IN METERS)

BASELINE WING

MODIFIED WING

| X | Z | X | Z |
|-----------|----------|-----------|----------|
| 31.428125 | 6.047124 | 31.428125 | 5.751647 |
| 31.853657 | 6.116931 | 31.853717 | 5.771345 |
| 31.741956 | 6.141078 | 31.742015 | 5.795345 |
| 31.624297 | 6.161820 | 31.624357 | 5.816204 |
| 31.448554 | 6.186296 | 31.448613 | 5.840925 |
| 31.272811 | 6.204010 | 31.272870 | 5.858919 |
| 31.098259 | 6.216514 | 31.098288 | 5.871727 |
| 30.922613 | 6.225207 | 30.922643 | 5.880797 |
| 30.748560 | 6.230757 | 30.748589 | 5.886650 |
| 30.572816 | 6.233602 | 30.572845 | 5.889811 |
| 30.398477 | 6.233751 | 30.398506 | 5.890311 |
| 30.221324 | 6.231703 | 30.221358 | 5.886617 |
| 30.045586 | 6.227124 | 30.045615 | 5.884452 |
| 29.872822 | 6.220079 | 29.872850 | 5.877783 |
| 29.694100 | 6.209504 | 29.694128 | 5.867644 |
| 29.545165 | 6.197737 | 29.545163 | 5.856277 |
| 29.348229 | 6.182475 | 29.348228 | 5.841449 |
| 29.297307 | 6.170135 | 29.297306 | 5.829365 |
| 29.204227 | 6.156662 | 29.204226 | 5.816214 |
| 29.132585 | 6.142194 | 29.132584 | 5.801966 |
| 29.067172 | 6.126467 | 29.067171 | 5.786716 |
| 29.013914 | 6.108369 | 29.013912 | 5.768963 |
| 28.975250 | 6.087025 | 28.975249 | 5.747604 |
| 28.953535 | 6.060192 | 28.953534 | 5.721091 |
| 28.944425 | 6.039789 | 28.944423 | 5.700571 |
| 28.953537 | 6.022727 | 28.953534 | 5.683312 |
| 28.915256 | 5.995464 | 28.915249 | 5.658510 |
| 29.013914 | 5.977445 | 29.013912 | 5.637709 |
| 29.067172 | 5.962717 | 29.067171 | 5.622821 |
| 29.132585 | 5.950666 | 29.132584 | 5.610692 |
| 29.204227 | 5.940674 | 29.204226 | 5.600394 |
| 29.297307 | 5.932111 | 29.297306 | 5.591506 |
| 29.348229 | 5.925046 | 29.348228 | 5.584202 |
| 29.545165 | 5.918261 | 29.545163 | 5.576949 |
| 29.694100 | 5.914628 | 29.694128 | 5.572818 |
| 29.872822 | 5.914088 | 29.872850 | 5.571714 |
| 30.045586 | 5.917074 | 30.045615 | 5.574173 |
| 30.221329 | 5.923742 | 30.221358 | 5.580291 |
| 30.398477 | 5.935211 | 30.398506 | 5.591205 |
| 30.572816 | 5.952658 | 30.572845 | 5.606083 |
| 30.748560 | 5.978620 | 30.748589 | 5.631665 |
| 30.922613 | 6.007255 | 30.922643 | 5.661545 |
| 31.098259 | 6.041013 | 31.098288 | 5.695046 |
| 31.272811 | 6.074643 | 31.272870 | 5.728553 |
| 31.448554 | 6.102521 | 31.448613 | 5.756583 |
| 31.624297 | 6.117476 | 31.624357 | 5.771643 |
| 31.741956 | 6.112122 | 31.742015 | 5.760773 |
| 31.853657 | 6.096666 | 31.853717 | 5.751370 |
| 31.428125 | 6.079736 | 31.428125 | 5.734323 |

WBL: 25.5332 m (83.7705 FT)

$\eta = 1.0000$

(DIMENSIONS IN METERS)

BASELINE WING

MODIFIED WING

| X | Z | X | Z |
|-----------|----------|-----------|----------|
| 32.041301 | 0.221484 | 32.041301 | 5.806040 |
| 32.574703 | 0.238616 | 32.574757 | 5.883152 |
| 32.474806 | 0.259397 | 32.474859 | 5.903860 |
| 32.369581 | 0.276872 | 32.369634 | 5.921476 |
| 32.212410 | 0.297091 | 32.212463 | 5.941972 |
| 32.055238 | 0.311263 | 32.055291 | 5.956345 |
| 31.849132 | 0.320900 | 31.849159 | 5.966321 |
| 31.742227 | 0.327400 | 31.742254 | 5.973098 |
| 31.586388 | 0.331135 | 31.586414 | 5.977102 |
| 31.429216 | 0.332574 | 31.429242 | 5.978633 |
| 31.271512 | 0.331721 | 31.271538 | 5.974279 |
| 31.114874 | 0.329004 | 31.114899 | 5.975868 |
| 30.957702 | 0.324102 | 30.957728 | 5.971294 |
| 30.803194 | 0.317122 | 30.803220 | 5.964640 |
| 30.643359 | 0.307026 | 30.643385 | 5.954882 |
| 30.510163 | 0.290051 | 30.510162 | 5.944245 |
| 30.376967 | 0.282012 | 30.376966 | 5.930571 |
| 30.286498 | 0.270797 | 30.286497 | 5.919574 |
| 30.204726 | 0.258676 | 30.204725 | 5.907736 |
| 30.141183 | 0.245724 | 30.141182 | 5.895037 |
| 30.082683 | 0.231850 | 30.082682 | 5.881568 |
| 30.035052 | 0.216800 | 30.035051 | 5.868083 |
| 30.000475 | 0.197512 | 30.000473 | 5.847546 |
| 29.981055 | 0.174416 | 29.981053 | 5.824656 |
| 29.971378 | 0.156728 | 29.971377 | 5.806821 |
| 29.961057 | 0.142444 | 29.961053 | 5.792265 |
| 30.000475 | 0.119433 | 30.000473 | 5.768937 |
| 30.035052 | 0.103876 | 30.035051 | 5.752972 |
| 30.062683 | 0.091515 | 30.062682 | 5.740425 |
| 30.141183 | 0.081494 | 30.141182 | 5.730292 |
| 30.204726 | 0.073268 | 30.204725 | 5.721733 |
| 30.286498 | 0.066315 | 30.286497 | 5.714479 |
| 30.376967 | 0.060721 | 30.376966 | 5.708613 |
| 30.510163 | 0.055633 | 30.510162 | 5.703040 |
| 30.643359 | 0.053284 | 30.643385 | 5.700221 |
| 30.803194 | 0.053742 | 30.803220 | 5.700163 |
| 30.957702 | 0.057178 | 30.957728 | 5.703128 |
| 31.114874 | 0.063785 | 31.114899 | 5.709236 |
| 31.271512 | 0.074574 | 31.271538 | 5.714572 |
| 31.429216 | 0.090477 | 31.429242 | 5.735001 |
| 31.586388 | 0.112002 | 31.586414 | 5.756007 |
| 31.742227 | 0.139121 | 31.742254 | 5.782734 |
| 31.849132 | 0.169090 | 31.849159 | 5.812492 |
| 32.055238 | 0.149192 | 32.055291 | 5.842552 |
| 32.212410 | 0.224414 | 32.212463 | 5.868009 |
| 32.369581 | 0.238856 | 32.369634 | 5.882476 |
| 32.474806 | 0.234249 | 32.474859 | 5.878611 |
| 32.574703 | 0.221010 | 32.574757 | 5.865542 |
| 32.041301 | 0.206305 | 32.041301 | 5.850946 |